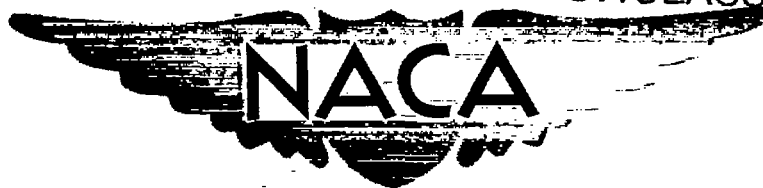


~~CONFIDENTIAL~~Copy  
6  
RM E52L16

NACA RM E52L16

OCT 3 1953

UNCLASSIFIED



# RESEARCH MEMORANDUM

COMPONENT AND OVER-ALL PERFORMANCE EVALUATION OF A  
J47-GE-25 TURBOJET ENGINE OVER A RANGE OF  
ENGINE-INLET REYNOLDS NUMBER INDICES

By Curtis L. Walker, Willis M. Braithwaite  
and David B. Fenn

Lewis Flight Propulsion Laboratory  
Cleveland, Ohio

CLASSIFICATION CHANGED

To UNCLASSIFIED

By authority of

TPL #29 Date 8/19/60  
CRG

CLASSIFIED DOCUMENT

This material contains information affecting the National Defense of the United States within the meaning of the espionage laws, Title 18, U.S.C., Secs. 793 and 794, the transmission or revelation of which in any manner to an unauthorized person is prohibited by law.

## NATIONAL ADVISORY COMMITTEE FOR AERONAUTICS

WASHINGTON  
September 29, 1953

UNCLASSIFIED

NACA LIT-1000

LANGLEY AERONAUTICAL RESEARCH LABORATORY  
Langley Field, Va.

~~CONFIDENTIAL~~

## NATIONAL ADVISORY COMMITTEE FOR AERONAUTICS

RESEARCH MEMORANDUM

## COMPONENT AND OVER-ALL PERFORMANCE EVALUATION OF A J47-GE-25 TURBOJET

## ENGINE OVER A RANGE OF ENGINE-INLET REYNOLDS NUMBER INDICES

By Curtis L. Walker, Willis M. Braithwaite, and  
David B. Fenn

## SUMMARY

An investigation was conducted in an altitude test chamber to evaluate the performance of an axial-flow turbojet engine over a range of engine-inlet Reynolds number indices. The range of Reynolds number indices investigated provided data which were applicable over a range of flight conditions, for example, altitudes from 15,000 to 55,000 feet at a flight Mach number of 0.7.

Secondary effects of exhaust-nozzle flow coefficient, air-flow leakage, and inlet temperature which should be considered before analyzing the effect of variations in engine-inlet Reynolds number index are presented. In general, the effect of reducing Reynolds number index was to lower compressor efficiency and air flow with a resultant shift in the compressor map and rematching of compressor with turbine. There was only a slight effect of Reynolds number index variation on the turbine performance.

Several minor design modifications proposed by the manufacturer (designated as a block change) did not produce any measurable improvement in engine performance.

## INTRODUCTION

Previous altitude investigations of turbojet engines made at the NACA Lewis laboratory have indicated that failure of the performance variables to generalize for all altitudes and flight Mach numbers, over the range of engine speeds where sonic flow exists in the exhaust nozzle, has been a result of either a Reynolds number effect or a variation in combustion efficiency (ref. 1). An investigation was therefore conducted in a Lewis laboratory altitude chamber to evaluate the component and over-all performance of the J47-GE-25 turbojet engine over a range of Reynolds number indices which corresponds to a wide range of altitude conditions. For example, at a flight Mach number of 0.7, the data are applicable over a range of altitudes from 15,000 to 55,000 feet. Fewer data are required by this method and departures from established generalizations may be investigated directly. The data of this investigation were presented in a preliminary data release (ref. 2). Subsequent refinements in calculation procedures have resulted in minor changes in the static sea-level thrust and in the scale thrust at high altitudes that are contained herein.

Also included in this investigation are the effects on performance of several minor design modifications to the compressor, the combustor, and the turbine shroud ring which were proposed by the engine manufacturer as a tentative block change in the production engine. The effect of inlet temperature is substantiated by additional data obtained on a J47-GE-17 engine which has a power section similar to that of the J47-GE-25.

Compressor, combustor, turbine, and over-all performance data are presented in tabular and graphical form over the range of Reynolds number indices investigated. The trends of over-all engine performance are discussed with relation to component performance variations. The effect of the block changes on performance is presented in graphical form.

2717

## APPARATUS

### Engine

A schematic sketch of the J47-GE-25 turbojet engine as it was installed in the NACA Lewis 10-foot-diameter altitude test chamber is shown in figure 1. The test chamber is described in reference 3. This engine had a 12-stage axial-flow compressor, eight tubular combustion chambers, and a single-stage turbine. The maximum diameter (turbine flange) was 37 inches and the over-all length excluding tail pipe and exhaust nozzle was 144 inches. The approximate dry weight of the engine was 2653 pounds. At rated engine speed, 7950 rpm, and rated turbine-outlet temperature, 1250° F (1710° R), the manufacturer's guaranteed sea-level static thrust was 5970 pounds. At rated engine speed and sea-level static conditions, the compressor-inlet air flow was approximately 104.5 pounds per second, the compressor pressure ratio was approximately 5.3, and a conical exhaust nozzle with an area of 2.073 square feet produced a turbine-outlet temperature of 1280° F (1740° R) based on NACA instrumentation. This exhaust nozzle had an exit to inlet area ratio of 0.87 and a half-cone angle of  $7\frac{10}{2}$ .

The fuel used in this investigation was MIL-F-5624A grade JP-4. The hydrogen-carbon ratio was 0.17 and the lower heat of combustion was 18,700 Btu per pound.

### Instrumentation

Instrumentation was located at the stations shown in figure 1. There was no instrumentation at station 2, which was a calculation station. Details of the instrumentation at each station are illustrated in figure 2, except for station 3b. There was a wall-static probe installed in each of two combustors in the plane of the cross-over tubes at station 3b.

Thrust was measured by means of balanced-diaphragm pneumatic thrust cell connected to the thrust bed, as shown schematically in figure 1.

### Engine Modifications

After calibration of the standard engine configuration was completed, modified engine parts were installed in the J47-GE-25 turbojet engine in the manner proposed by the manufacturer as a block change to the production engine. These modifications were incorporated in two additional configurations as shown in figure 3 and described in the following table:

Configuration	Engine modifications incorporated	Exhaust-nozzle area, sq ft
A (standard)	Standard engine as supplied by manufacturer with additional instrumentation installed	2.073
B	New twelfth-stage compressor seal New combustor liners, postless transition pieces Floating turbine shroud	2.106
C	New parts as installed for configuration B Shrouded fuel-spray nozzles	<sup>a</sup> 2.124

<sup>a</sup>Nozzle area for configuration C was too small to obtain rated engine speed without exceeding rated temperature.

The new twelfth-stage compressor seal (fig. 3(a)) consisted of a slant-toothed labyrinth seal instead of the V-tooth design; the minimum clearance was maintained the same but the maximum clearance was reduced by increasing the minimum dimension of diameter "D" as shown in the figure. The combustor liner was modified to induct more air into the primary combustion zone by adding three rings of air-inlet holes near the dome on the liner. The center posts in the transition pieces were removed. The location of these posts is indicated in figure 1. The proposed method of installing the floating turbine shroud ring is shown in figure 3(c). In the installation as provided, the shim extended into the space between the shroud ring and the nozzle diaphragm. Furthermore, clearances marked a, b, and c (fig. 3(b)) were not great enough to provide a free-floating shroud as evidenced by gall marks on the shim and tail cone in this area. These clearances were proposed to prevent seizing of the shroud ring on the nozzle diaphragm. For configuration C, shrouded fuel nozzles (fig. 3(c)) were installed in addition to the configuration B modifications. The purpose of the shroud around the fuel nozzle was to induct air into the combustor at the origin of the spray pattern by ejector action. These shrouded fuel nozzles are standard installation equipment on the J47-GE-17 engine.

## PROCEDURE

## Sizing Exhaust Nozzle and Determining Sea-Level Static Thrust

Prior to obtaining performance data, an attempt was made to size the exhaust nozzle to produce an exhaust-gas temperature of 1250° F (1710° R) at rated engine speed and static sea-level conditions. Since it is impossible to operate the altitude chamber at static conditions, the nozzle size was based on the extrapolation of data obtained at low altitudes and flight Mach numbers from 0.2 to 0.8. A review of the complete performance data indicated that the nozzle used in this investigation (area, 2.073 sq ft) would have actually produced an exhaust-gas temperature of about 1280° F (1740° R) based on NACA instrumentation at these conditions.

Thrust is dependent on exhaust-gas temperature and exhaust-gas temperature is a function of exhaust-nozzle area. In this investigation, the exhaust-gas temperature was measured by the engine manufacturer's four-probe and five-probe thermocouple harnesses as well as by the 25 NACA thermocouples. The readings of these different sets of instrumentation differ with the result that the sea-level static thrust would vary, depending on which temperature readings were used in sizing the exhaust nozzle. It was assumed that the NACA instrumentation (corrected for thermocouple recovery) indicated the true gas temperature, and jet thrust calculated from this temperature corresponded to scale jet thrust. Because the engine is normally rated by the manufacturer for an exhaust-gas temperature based on the thermocouple reading obtained from the four- or five-probe thermocouple harnesses, static sea-level thrust values have been included in the following table for a thermocouple reading of 1250° F (1710° R) obtained from the four- and five-probe systems with the corresponding gas temperatures included. The sea-level thrust of 6070 pounds at an exhaust-gas temperature of 1280° F (1740° R) for the exhaust nozzle used in this investigation was slightly above the manufacturer's guarantee (5970 lb) and provides a point of reference for the performance data presented herein.

Basis of performance rating	Engine speed, rpm	Engine manufacturer's exhaust-gas thermocouple reading, $T_{g,i}$ , °R		Exhaust-gas total temperature based on NACA instrumentation, $T_g$ , °R	Static sea-level thrust, lb
		Four-probe harness	Five-probe harness		
Exhaust-gas total temperature of 1740° R (obtained with exhaust nozzle used in this investigation)	7950	1684	1690	1740	6070
Exhaust-gas total temperature of 1710° R	7950	1653	1658	1710	5960
Engine manufacturer's five-probe thermocouple harness	7950	1704	1710	1760	6135
Engine manufacturer's four-probe thermocouple harness	7950	1710	1717	1766	6160

#### Obtaining Performance Data at Various Reynolds Number Indices

Engine inlet total pressure and temperature were varied to correspond to Reynolds number indices from 0.8 to 0.15. For a given set of inlet conditions, exhaust pressure was reduced to the minimum of the exhaust system with the engine operating at rated speed. The inlet temperature and pressure and the exhaust pressure were then maintained constant while data were taken over a range of engine speeds from rated speed to approximately the speed at which the exhaust nozzle became unchoked. A summary of the operating conditions covered in the investigation is given in the following table:

Reynolds number index	Inlet total temperature, °R	Inlet total pressure, lb sq ft	Ram pressure ratio
0.8	530	1740	1.70
.6	467	1108	2.14
.5	467	923	1.95
.4	467	739	1.35
.425	437	718	1.41
.4	410	620	1.70
.3	410	465	1.70
.3	410	465	1.34
.25	410	387	1.64
.2	410	315	1.48
.15	410	232	1.19

As shown in the table, three ram pressure ratios  $P_1/p_0$  were used at a Reynolds number index of 0.4 and two at 0.3 to verify the generalization with variations in ram pressure ratio. At a Reynolds number index of about 0.4, three sets of inlet conditions were used to determine whether there were any effects of temperature and pressure other than those of Reynolds number index. (The variation of the performance parameters from 0.4 to 0.425 Reynolds number index is considered small enough that they may all three be considered a Reynolds number index of about 0.4.)

All symbols are defined in appendix A, and the methods of calculation are described in appendix B.

## RESULTS AND DISCUSSION

The performance evaluation of an axial-flow turbojet engine over a range of Reynolds number indices provides data which are applicable over a range of flight conditions. However, the performance investigation of the J47-GE-25 turbojet engine has shown that several factors producing secondary performance variations should be recognized if effective use is to be made of the performance data in its application to flight conditions. These secondary effects are discussed and evaluated in the following paragraphs.

### Secondary Effects

Effect of nozzle flow coefficient. - As engine ram pressure ratio, and consequently nozzle pressure ratio, was increased at a constant corrected engine speed, the exhaust-nozzle flow coefficient  $C_d$

increased. The increase in nozzle flow coefficient with increasing pressure ratio is illustrated in figure 4(a) which, although obtained directly from reference 4, was assumed applicable to this nozzle, which has the same cone angle and area ratio. This flow coefficient was nearly constant above a nozzle pressure ratio of about 2.3, which is 25 percent higher than that required to produce sonic velocity in the exhaust nozzle. The effect of nozzle flow coefficient was typical of conical exhaust nozzles. The magnitude of this effect depends on the nozzle configuration.

During the process of sizing the nozzle, as described in PROCEDURE, the effect of varying ram pressure ratio at corrected engine speeds near rated was investigated with three different nozzle areas. The results of this investigation are presented in figure 4(b), which illustrates a decrease in corrected exhaust-gas temperature of about 40° R accompanying an increase in ram pressure ratio from 1.0 to 1.25 (which corresponds to flight Mach numbers from 0 to 0.575).

The corresponding variation in the ratio of net thrust at actual corrected exhaust-gas temperature to net thrust at constant corrected exhaust-gas temperature is shown in figure 4(c). A thrust loss of about 3 percent is incurred because of the increase in effective exhaust-nozzle flow area and accompanying decrease in corrected exhaust-gas total temperature.

Generalization of performance parameters presented in this investigation requires that there be no effect of ram pressure ratio on engine component performance. Since a nozzle pressure ratio greater than 25 percent above that required for choked flow results in a nearly constant flow coefficient, there is no effect of ram pressure ratio above a value 25 percent higher than that required to produce choked flow in the exhaust nozzle. The solid line and data points on figure 5 illustrate the relation of corrected engine speed and flight Mach number required for choked flow in the exhaust nozzle. The dashed line of figure 5 represents flight Mach numbers corresponding to ram pressure ratios 25 percent greater than those required to produce choked flow in the exhaust nozzle. However, it should be noted that if an exhaust nozzle having a smaller cone angle were used, the data would be applicable to lower flight Mach numbers. The performance data presented herein may be applied directly to flight conditions above this dashed curve. However, when the performance data are applied to lower ram pressure ratios at which the exhaust-nozzle flow coefficient varies, the trends shown in figure 4(a) should be used in conjunction with the pumping characteristics, which are presented in a following section entitled "Effect of Engine-Inlet Reynolds Number Index."

Effect of air flow leakage. - The engine as originally received had approximately 5 to 7 percent air flow leakage downstream of the inlet measuring station 1. This leakage occurred around sheet-metal parts



between station 1 and the compressor inlet, through open bolt holes at the compressor inlet, and through the gaskets on the high pressure deicing-air lines. The leakage was reduced to about 3.3 percent of station 1 air flow by using gaskets on the sheet-metal joints and sheet-metal screws instead of spring-type fasteners, plugging the open bolt holes, and using soft-aluminum gaskets on the deicing-air lines. For the performance calculations all the leakage except compressor seal leakage was assumed to occur ahead of the compressor, and compressor air flow was calculated based on measurements of gas flow at the exhaust nozzle as explained in appendix B. Both station 1 and compressor inlet (station 2) air flow are presented in table I for the data of this investigation.

In aircraft installations, the magnitude of the leakage would be a function of nacelle pressure as well as of whatever steps were taken to seal the points of leakage. The result of leakage ahead of the compressor is to increase ram drag and decrease net thrust. Therefore, in calculating net thrust, the air flow at station 1 should be used in the ram drag term.

Effect of inlet temperature. - Although a previous investigation of a similar engine (ref. 3) indicated no effect on performance of different inlet temperatures, a check was made in the present investigation at a Reynolds number index of about 0.4 for three engine-inlet temperatures from 70° to -50° F. These data (fig. 6) showed a definite, though minor, increase in the corrected jet-thrust parameter, exhaust-gas total temperature, and ideal corrected fuel-air ratio with increase in inlet temperature. (The ideal fuel-air ratio is the fuel-air ratio that would be required if combustion efficiency were 1.00.) The effect was not explainable by the conventional correction factors for a Reynolds number effect.

Examination of other variables for these conditions definitely established that the effect was not due to a change in pumping characteristics, compressor efficiency, combustor-pressure loss, or exhaust-nozzle flow coefficient. However, because of experimental scatter and possible swirl effects on the turbine-outlet total-pressure probes, it was impossible to establish whether there was a change in turbine efficiency or tail-pipe pressure losses. A study of factors likely to cause a change in turbine-outlet gas swirl indicated that a change in corrected turbine work would be required. Further examination of the engine data revealed that the corrected compressor leakage did not generalize with variations in engine-inlet temperature (corrected leakage increased with temperature increase) and a small increase in turbine work (fig. 7) and swirl with increase in inlet temperature was therefore indicated. The increased turbine-outlet gas swirl would produce a small increase in the tail-pipe pressure loss. The increased pressure loss accompanied by no change in pumping characteristics (as measured at the exhaust-nozzle inlet) results in increased corrected exhaust-gas temperature and corrected jet-thrust parameter. There was a slight increase in compressor efficiency with increases in inlet temperature, which resulted in generalization of the pumping characteristics.

A further effort to substantiate the inlet temperature effect was made by using a J47-GE-17 engine which has a power section similar to that of the J47-GE-25. Data were obtained with this engine at a Reynolds number index of 0.4 with inlet temperatures of 7° and -50° F, both with and without turbine-outlet straightening vanes.

The results of the data from this later investigation are presented in figures 8 and 9. Without straightening vanes, the corrected jet-thrust parameter (fig. 8(a)), the corrected exhaust-gas total temperature (fig. 8(b)), and the corrected ideal fuel-air ratio (fig. 8(c)) showed the same increase with increasing inlet temperature as these variables did for the J47-GE-25. However, with turbine-outlet straightening vanes installed (figs. 9(a), 9(b), and 9(c)), the trend was eliminated below a corrected engine speed of 7000 rpm and reduced at all higher engine speeds investigated.

The Reynolds number index method of investigation is still considered valid inasmuch as the effect of inlet temperature is believed to be peculiar to this engine and was of secondary importance. The effect of reducing inlet temperature from 7° to -50° F at a Reynolds number index of 0.4 was to decrease the corrected jet-thrust parameter about 2 percent, corrected exhaust-gas total temperatures about  $2\frac{1}{2}$  percent, and corrected ideal fuel-air ratio about 5 percent. When the data are applied to flight conditions, these effects can be minimized by adjusting the data by use of the trend shown in figure 6.

#### Effect of Engine-Inlet Reynolds Number Index

With the reservations discussed in the previous paragraphs, the performance data obtained over a range of engine-inlet Reynolds number indices may be applied to a wide range of flight conditions. Figure 10 is presented in order to permit the determination of Reynolds number index as a function of altitude and flight Mach number. An example of the method of obtaining performance at a given flight condition is presented in appendix C.

Compressor performance. - Compressor performance characteristics are presented in figure 11 for the range of Reynolds number indices investigated. Compressor efficiency generalized for Reynolds number indices from 0.8 to 0.4 and decreased with further reduction in Reynolds number index, as shown in figure 11(a). The peak compressor efficiency occurred at a corrected engine speed of about 7000 rpm for all Reynolds number indices investigated and decreased from about 0.835 to about 0.815 as Reynolds number index was decreased from 0.4 to 0.2. Compressor efficiency decreased approximately 0.10 from the peak value as corrected engine speed was increased to 8500 rpm.

Corrected compressor air flow is shown as a function of corrected engine speed over the range of Reynolds number indices investigated in figure 11(b). At Reynolds number indices from 0.8 to 0.3, the corrected air flow generalized below a corrected engine speed of about 7500 rpm. At a corrected engine speed of 7950 rpm (sea-level rated), the corrected compressor air flow decreased from 104 to 99 pounds per second as Reynolds number index was decreased from 0.6 to 0.15. Compressor leakage at the engine midframe was measured by means of an orifice pipe and is presented in figure 11(c) as a function of compressor-outlet total pressure. This figure is necessary in determining the air flow through the combustor.

The variation of compressor pressure ratio with corrected engine speed is presented in figure 11(d), which shows that there was no effect of Reynolds number index on this relation. The failure of the compressor operating lines (compressor pressure ratio as a function of corrected air flow) to generalize with Reynolds number index variations (fig. 11 (e)) indicates that there was a shift in the compressor map as Reynolds number index was reduced.

Combustor performance. - Variation of the total-pressure-loss ratio across the combustor with corrected engine speed is shown in figure 12(a). Over the range of engine speeds investigated the total-pressure-loss ratio showed no apparent effect of Reynolds number index. Combustion efficiency (figs. 12(b) and 12(c)) was correlated with the parameter

$\frac{(p_{3,b})^2}{W_{a,3}}$  (fig. 12(b)), which is proportional to a combustion parameter

derived in reference 5. According to this reference, correlation would be expected unless there were pronounced effects of fuel-air ratio or fuel spray pattern. At a value of the combustion parameter above 400,000, correlation was within  $\pm 0.015$  and a constant combustion efficiency of about 0.99 was indicated. At lower values of the combustion parameter, combustion efficiency dropped rapidly and the data scatter was increased to  $\pm 0.02$ . From these data it is concluded that for the Reynolds number indices and the corrected engine speeds of this investigation, the effects of fuel-air ratio and fuel spray pattern were secondary.

A more convenient method of obtaining combustion efficiency for a given engine operating condition is presented in figure 12(c). An engine operating parameter  $\delta \sqrt{\theta} (N/\sqrt{\theta})^3$  was obtained empirically, as in reference 6, from the engine operating characteristics. The correlation of combustion efficiency as a function of this engine operating parameter provides a more convenient method of obtaining combustion efficiency for given inlet conditions and a given corrected engine speed.

2717 Turbine performance. - The trends in turbine performance (fig. 13) with variations in Reynolds number index were generally obscured by data scatter. The turbine total-pressure ratio (fig. 13(a)) was approximately 2.58 over the range of corrected engine speeds investigated. Turbine efficiency, illustrated in figure 13(b), increased from about 0.81 at 6400 rpm to about 0.825 at 7800 rpm and above. The corrected turbine gas flow (fig. 13(c)) increased from about 40 to 42 pounds per second as corrected engine speed was increased from 6250 to 8800 rpm. Close inspection of the data points on the latter two curves indicates the possible existence of a slight decrease in turbine efficiency and corrected turbine gas flow with decreasing Reynolds number index, although the magnitudes of the trends are not clearly discernible because of the data scatter.

Generalized engine performance. - The effect of Reynolds number index on generalized engine performance is shown in figure 14. The corrected exhaust-gas total temperature increased as Reynolds number index was decreased (figs. 14(a) and 14(b)) because of the shift in engine operating point caused primarily by the decrease in compressor efficiency. It was necessary to present these data on separate plots for the different inlet temperatures because of the temperature effect discussed previously. For the same reason, the data obtained at a Reynolds number index of 0.8, although included in table I, were omitted from the figures showing corrected exhaust-gas temperature and corrected ideal fuel-air ratio (figs. 14(a) and 14(c)). Corrected ideal fuel-air ratio (figs. 14(c) and 14(d)) increased as a result of the required additional power to overcome loss of compressor efficiency and corresponded to the increase in exhaust-gas temperature. This parameter isolates the fuel requirement from combustion efficiency and the decrease in air flow with decreased Reynolds number. The effect of Reynolds number index on the engine pumping characteristics is shown in figure 14(e). As Reynolds number index was reduced, pumping characteristic curves shifted in the direction of increased temperature ratio for a given pressure ratio. This result would be expected as a result of the decrease in compressor efficiency. The effect of Reynolds number index on the jet-thrust parameter is presented in figures 14(f) and 14(g). At a given engine speed there was an increase in temperature ratio, a slight increase in engine pressure ratio, and a decrease in engine corrected air flow as Reynolds number index was reduced. At Reynolds number indices from 0.8 to 0.4 there was no apparent effect on the jet-thrust parameter. However, as Reynolds number index was decreased from 0.4 to 0.15 (fig. 14(g)), there was an increase in the jet-thrust parameter due to the increase in temperature ratio and pressure ratio, which offset the decrease in corrected air flow.

It can be shown from the performance data that the combined effect of reducing the Reynolds number index from 0.6 to 0.15 and the inlet temperature from 70° to -50° F resulted in a 10 percent increase in corrected fuel flow and a 2 percent increase in jet-thrust parameter at a corrected engine speed of 7950 rpm.

Net thrust and specific fuel consumption. - The conventional performance parameters such as net thrust and net-thrust specific fuel consumption may be obtained for any flight condition from the data presented. These calculations have been made for the sea-level static condition and for altitudes of 16,700, 31,400, and 51,500 feet at a flight Mach number of 0.8 and are presented in figure 15. An example of the technique used in obtaining these values is presented in appendix C.

The net thrust (fig. 15(a)) at the sea-level static condition exceeded the manufacturer's guarantee by about 100 pounds at rated engine speed. As the altitude was increased, the net thrust decreased. At an altitude of 51,500 feet and a Mach number of 0.8, the net thrust was 970 pounds for rated speed. The net-thrust specific fuel consumption for the sea-level condition was lower than the manufacturer's guarantee at rated engine speed, but was approximately the same at an engine speed of 7000 rpm which corresponds to the minimum specific fuel consumption of 0.99 pound of fuel per hour per pound of thrust at this condition. For a flight Mach number of 0.8 and the range of altitude, the engine speed which corresponds to minimum specific fuel consumption decreased from approximately 7400 rpm at an altitude of 16,700 feet to 7100 rpm at an altitude of 51,500 feet. The minimum value of the specific fuel consumption decreased over this range of altitude from approximately 1.33 pounds of fuel per hour per pound of thrust at 16,700 feet to 1.23 pounds of fuel per hour per pound of thrust at 51,500 feet. This decrease in specific fuel consumption occurred even though the corrected specific fuel consumption increased because of the decreasing inlet temperature with increasing altitude. The minimum specific fuel consumption probably occurred at about 35,000 feet.

#### Effect of Design Modifications

The effect of the design modifications proposed by the engine manufacturer as a block change is presented in figures 16 through 19 for Reynolds number indices of 0.8, 0.4, and 0.2. Data for all configurations were obtained at the same inlet temperatures. The ratio of compressor leakage air flow to inlet air flow is presented as a function of corrected compressor discharge pressure in figure 16. Figure 16 indicates that the improved twelfth-stage seal of configuration B reduced this leakage by 25 to 50 percent of its original value at the higher compressor discharge pressures. Figure 17 presents a comparison of the pumping characteristics for configuration A (standard engine) and configuration B. For a given temperature ratio, configuration B has a lower pressure ratio than configuration A. Examination of component performance at a constant corrected engine speed shows no change for the compressor and turbine pressure ratios and a very small increase in combustor total-pressure-loss ratio (less than 0.0025). However, there was a greater indicated pressure loss in the tail pipe for configuration B. The increase in pressure loss is attributed to the increased velocity in the tail pipe due to the higher air flow (caused by less compressor leakage) through the turbine and the change in area ratio caused by the larger nozzle. The change in

area ratio results in approaching critical Mach numbers at the tail-pipe instrumentation. The jet-thrust parameter (fig. 18) showed no effect from the added air flow resulting from the improved seal because of the counter effect of the greater tail-pipe pressure loss caused by the increased mass flow and velocity.

Combustion efficiency is presented in figure 19. There was no significant difference in the combustion efficiencies of configurations A and B. The addition of shrouded fuel nozzles did not change the peak efficiencies but indicated a slightly higher efficiency at lower values of the engine operating parameter. The modifications proposed by the manufacturer as a block change to the twelfth-stage compressor seal, the engine combustor, and the turbine shroud ring did not provide any significant improvement in engine performance.

#### CONCLUDING REMARKS

An investigation was conducted in an altitude test chamber to evaluate the performance of an axial-flow turbojet engine over a range of engine-inlet Reynolds number indices. The range of Reynolds number indices investigated provided data which were applicable over a range of flight conditions, for example, altitudes from 15,000 to 55,000 feet at a flight Mach number of 0.7.

This investigation indicated that secondary effects of nozzle flow coefficient and inlet temperature must be known before the effect of variations in engine-inlet Reynolds number index can be analyzed. The nozzle flow coefficient increased with increasing nozzle pressure ratio up to a value of about 2.3, which corresponds to a ram pressure ratio of about 125 percent of the ram pressure ratio required to produce choked flow in the nozzle. Consequently, below this value of ram pressure ratio there was a significant effect of ram pressure ratio on generalized performance. There was a secondary effect of inlet temperature at a constant Reynolds number index. As inlet temperature was increased at a given Reynolds number index, the corrected jet-thrust parameter, corrected exhaust-gas temperature, and corrected ideal fuel-air ratio each increased slightly. This effect was reduced when turbine-outlet straightening vanes were installed.

In general, the effect of reducing the Reynolds number index was to lower the compressor efficiency and air flow resulting in a shift in the compressor map and a rematching of the compressor and turbine. There was only a slight effect of Reynolds number index variation on the turbine performance. The combined effect of reducing the Reynolds number index from 0.6 to 0.15 and the inlet temperature from 70° to -50° F resulted in about a 10 percent increase in corrected fuel flow and about a 2 percent increase in corrected jet-thrust parameter at a corrected engine speed of 7950 rpm.

The engine modifications proposed by the manufacturer resulted in no significant improvement in engine performance. The modified twelfth-stage compressor seal reduced the leakage at the engine midframe by about 20 to 50 percent of its original value. However, the resultant increase in air flow and velocity in the tail pipe caused higher pressure loss and no improvement in thrust. The incorporation of shrouded fuel nozzles resulted in slightly higher combustion efficiency at low values of the engine operating parameter, but the effect was not discernible at high values.

Lewis Flight Propulsion Laboratory  
National Advisory Committee for Aeronautics  
Cleveland, Ohio

## APPENDIX A

## SYMBOLS

The following symbols are used in this report:

A	area, sq ft
$C_d$	exhaust-nozzle flow coefficient, ratio of effective flow area to physical flow area
$C_j$	jet-thrust coefficient, $F_{j,s}/F_{j,r}$
$C_T$	thermal expansion coefficient, ratio of hot exhaust-nozzle area to cold exhaust-nozzle area
$F_d$	thrust system scale reading, lb
$F_j$	jet thrust, lb
$F_n$	net thrust, lb
f	fuel-air ratio
g	acceleration of gravity, ft/sec <sup>2</sup>
h	enthalpy, Btu/lb
$h_f$	lower heating value of fuel, Btu/lb
M	Mach number
N	engine speed, rpm
P	total pressure, lb/sq ft
p	static pressure, lb/sq ft
R	gas constant, ft-lb/(lb)(°R)
T	total temperature, °R
t	static temperature, °R
V	velocity, ft/sec
$W_a$	air flow, lb/sec



$W_f$	fuel flow, lb/hr
$W_g$	gas flow, lb/sec
$\gamma$	ratio of specific heats
$\delta$	ratio of engine-inlet total pressure $P_1$ to NACA standard sea-level pressure, 2116 lb/sq ft
$\theta$	ratio of engine-inlet total temperature $T_1$ to NACA standard sea-level temperature, 519° R
$\theta_4$	ratio of product of $T_4$ and $\gamma_4$ to product of $T$ and $\gamma$ for NACA standard sea-level conditions, $\gamma_4 T_4 / (519)(1.4)$
$\phi$	ratio of coefficient of viscosity corresponding to $T_1$ to coefficient of viscosity corresponding to NACA standard sea-level temperature, 519° R. This ratio is a function of only temperature and is equal to $735 \theta^{1.5} / (T + 216)$ .
$\eta$	efficiency
$\frac{\delta}{\phi \sqrt{\theta}}$	Reynolds number index

## Subscripts:

a	air
b	combustor
c	compressor
cl	compressor twelfth-stage leakage air flow
i	indicated
m	fuel manifold
n	vena contracta at exhaust-nozzle outlet
r	rake
s	scale
t	turbine
tc	turbine cooling

## Station numbers:

- 0 ambient or free-stream conditions
- 0a bellmouth inlet
- 1 engine inlet
- 2 compressor inlet
- 3 compressor outlet or combustor inlet
- 3b combustor
- 4 combustor outlet or turbine inlet
- 5 turbine outlet
- 9 exhaust-nozzle inlet
- 10 exhaust-nozzle outlet

## APPENDIX B

## METHODS OF CALCULATION

Temperature. - Total temperature was determined by use of a calibrated thermocouple with an impact-recovery factor of 0.85 from the indicated temperature and the following equation:

$$T = \frac{T_1 \left( \frac{P}{p} \right)^{\frac{\gamma-1}{\gamma}}}{1 + 0.85 \left[ \left( \frac{P}{p} \right)^{\frac{\gamma-1}{\gamma}} - 1 \right]}$$

Engine air flow. - Early in the investigation, it was found that an excess of air was leaking from the engine behind the inlet measuring station 1. This air was leaking from sheet-metal joints between stations 1 and 2, from open bolt holes at the compressor inlet, and from twelfth-stage deicing-air lines. It was assumed in the calculation that all unmeasured leakage occurred between stations 1 and 2. The gas flow was determined at the exhaust-nozzle outlet from total pressure and temperature at the nozzle inlet (station 9) by the following equation with the assumption that no energy loss occurred between the nozzle inlet and outlet:

$$W_{g,n} = C_T C_d A_{10} P_n \sqrt{\frac{2\gamma_9}{\gamma_9-1} \frac{g}{RT_9} \left[ \left( \frac{P_9}{P_n} \right)^{\frac{\gamma_9-1}{\gamma_9}} - 1 \right] \left( \frac{P_9}{P_n} \right)^{\frac{\gamma_9-1}{\gamma_9}}}$$

where in the subsonic case,

$$P_n = P_0$$

and in the choked case,

$$P_n = \frac{P_9}{\left( \frac{1 + \gamma_9}{2} \right)^{\frac{\gamma_9}{\gamma_9-1}}}$$

The value of the flow coefficient  $C_d$  was determined from reference 4 using the area ratio and cone angle of the particular nozzle employed in this investigation. The magnitude of the flow coefficient is presented in figure 4(a).

The compressor-inlet air flow was then determined from the nozzle gas flow by

$$W_{a,2} = W_{g,n} - \frac{W_f}{3600} + W_{a,c1}$$

where the compressor leakage air flow  $W_{a,c1}$  was measured at two instrumented bleed ports and found to be a function of compressor-outlet pressure  $P_3$  (fig. 11(c)).

The engine-inlet air flow  $W_{a,1}$  based on pressure and temperature measurements in a bellmouth mounted on the front of the engine was determined by the same general equation as for the tail-pipe gas flow. The percentage of leakage for the section between stations 1 and 2 is

$$\frac{W_{a,1} - W_{a,2}}{W_{a,2}}$$

and after an attempt was made to plug the leaks, it was approximately 3.3 percent of the compressor-inlet air flow  $W_{a,2}$  for the range of conditions covered.

Combustor air flow  $W_{a,3}$  used in calculating fuel-air ratio was

$$W_{a,3} = W_{g,n} - W_{a,tc} - \frac{W_f}{3600} = W_{a,2} - W_{a,c1} - W_{a,tc}$$

where  $W_{a,tc}$  was the turbine cooling air flow which was found to be half of 1 percent of  $W_{a,2}$ . Therefore

$$W_{a,3} = 0.995 W_{a,2} - W_{a,c1}$$

Combustion efficiency. - Combustion efficiency was defined as the fraction of the lower heat of combustion of the liquid fuel effective in increasing the enthalpy across the combustor and was calculated from  $T_1$ ,  $T_9$ , and  $f$  based on  $W_{a,3}$  by the following formula:

$$\eta_b = \frac{h_a \left[ \frac{T_9}{T_1} + f \left( \frac{Am + B}{m + 1} \right) \right] \frac{T_9}{T_m}}{f h_f}$$

where

$$\frac{Am + B}{m + 1}$$

accounts for the difference between the enthalpy of carbon dioxide and water vapor in the burned mixture and the enthalpy of oxygen removed from the air by their formation (ref. 7), and  $T_m$  is the temperature of the fuel in the manifold (540° R).

When the ideal fuel-air ratio was calculated, the combustion efficiency was assumed the same as the ratio of fuel ideally required to the fuel actually required, which is given by

$$\frac{f_{ideal}}{f} = \frac{\eta_b h_f + \frac{Am + b}{m + 1} \left[ \frac{T_9}{T_m} \right]}{h_f + \frac{Am + b}{m + 1} \left[ \frac{T_9}{T_m} \right]}$$

The difference in the ratio  $\frac{f_{ideal}}{f}$  and  $\eta_b$  for the range of combustion efficiencies of this investigation was a maximum of 0.003.

Jet-thrust parameter. - The jet thrust as determined from the thrust system measurements was calculated from the equation

$$F_{j,s} = F_d + (A_{seal} - A_g)(P_1 - p_{seal}) + A_g(P_1 - p_0) + 0.80 \left( \frac{1}{2} \frac{W_{a,1}}{g} V_{0a} \right)$$

where  $F_d$  is equal to the thrust system scale reading adjusted for the pressure difference on the link connecting the thrust bed in the test chamber and the measuring cell outside the test chamber, and the last term  $0.8 \left( \frac{1}{2} \frac{W_{a,1}}{g} \right) V_{0a}$  is the momentum force existing at the bellmouth inlet because of failure of the bellmouth to provide the acceleration of  $W_{a,1}$  to  $V_1$ . This force was determined experimentally by instrumentation located on the surface of the bellmouth along with the instrumentation at station 1.

The jet-thrust parameter  $\frac{F_j + A_{10}P_0}{\delta}$  is used to generalize the thrust data for variations in inlet conditions and ram ratio. The value of  $A_{10}$  used in calculating this parameter was 2.073 square feet. This was the cold area of the nozzle used in this investigation and facilitates correcting the parameter to a flight condition.

Jet-thrust coefficient. - The jet-thrust velocity coefficient is defined as the ratio of scale jet thrust to rake jet thrust

$$C_j = \frac{F_{j,s}}{F_{j,r}}$$

where

$$F_{j,r} = \frac{W_{g,n}}{g} V_n + A_n (p_n - p_0)$$

The charts in reference 7 were used in the solution of the preceding equation. When all the data obtained in this investigation were employed, the jet-thrust coefficient was found to be independent of exhaust-nozzle pressure ratio and was a constant value of 0.995. The scatter in the coefficient values was approximately  $\pm 1$  percent for the range of conditions investigated.

## APPENDIX C

## CORRECTING TEST VALUES TO FLIGHT CONDITIONS

An example of the method of correcting test values to flight conditions has been given in reference 3. For a given flight condition, the value of Reynolds number index can be obtained from figure 10. Values for  $\delta$  and  $\theta$  can be readily calculated from engine-inlet total pressure and temperature. If these generalizing parameter values are known, air flow, ideal fuel-air ratio, combustion efficiency, and exhaust-gas temperature can be obtained from the various performance curves. In order to determine the net thrust, the jet-thrust parameter must be first corrected to the desired flight condition to obtain the jet thrust. Then, in order to obtain net thrust, the leakage between stations 1 and 2 must be added to the air flow for station 2, so that

$$F_n = F_j - \left( \frac{W_{a,2} + W_{a,1-2}}{g} \right) V_0$$

The values of net thrust and net-thrust specific fuel consumption presented in figure 15 were obtained in this manner. The following example is a sample calculation of one of the points.

For this calculation an altitude of 51,500 feet and a flight Mach number of 0.8 were selected. These correspond to a Reynolds number index of 0.2 (fig. 10). For the given flight condition, the inlet temperature, pressure, and correction parameters are:

$$T_1 = 443^\circ \text{ R}$$

$$P_1 = 345.1 \text{ lb/sq ft}$$

$$p_0 = 226.4 \text{ lb/sq ft}$$

$$\delta_1 = 0.1631$$

$$\theta_1 = 0.8536$$

$$t_0 = 393^\circ \text{ R}$$

From figure 14(g) a value of 11,693 pounds for the jet-thrust parameter is obtained for a corrected engine speed  $N/\sqrt{\theta} = 8652$ . The difference between the desired  $T_1$  and the  $T_1$  at which the data were obtained

was about 300°. For a difference of 60° (fig. 8(c)), a change of about 200 pounds is found in the parameter. Therefore an allowance of 100 pounds was made for the inlet temperature, making the jet-thrust parameter 11,793 pounds. This value is then reduced to jet thrust.

$$F_j = 11,793 \times 8 - p_0 A_{10} = (11,793 \times 0.1631) - (226.4 \times 2.073) = 1454 \text{ pounds}$$

For determination of the inlet momentum  $m_1 V_0$ , the mass flow is that entering the bellmouth. This is determined either from the measured values or approximately by

$$m_1 = \left( \frac{W_a \sqrt{\theta}}{8} \right)_2 \frac{8}{\sqrt{\theta} g \left( \frac{W_{a,2}}{W_{a,1}} \right)} = (105.6) \frac{0.1631}{0.9239 \times 32.2 \times 0.967} = 0.599 \text{ slug}$$

The free-stream velocity  $V_0$  can be determined from the flight Mach number

$$V_0 = M_0 \sqrt{\gamma g R t} = 0.8 \sqrt{1.4 \times 32.2 \times 53.37 \times 393} = 778 \text{ ft/sec}$$

Then the net thrust is

$$F_n = F_j - m_1 V_0 = 1454 - 0.599 \times 778 = 988 \text{ pounds}$$

The net-thrust specific fuel consumption was computed from

$$\text{sfc} = \frac{W_f}{F_n} = \frac{3600 f W_{a,3}}{F_n}$$

where

$F_n$  has been calculated equal to 988 pounds

$$f = (\eta_b f / \theta)_{\text{ideal}} \theta / \eta_b = 0.0225 \times 0.8536 / 0.967 = 0.0199 \frac{\text{lb fuel}}{\text{lb air}}$$

$\left( \frac{\eta_b f}{\theta} \right)_{\text{ideal}}$  is obtained from figure 14(d)

$\eta_b$  is obtained from figure 12(c)



$$8 \sqrt{\theta} (N/\sqrt{\theta})^3 = 9.760 \times 10^{10}$$

$$W_{a,3} = 0.995 W_{a,2} - W_{a,c1} = 0.995 \frac{105.6 \times 0.1631}{0.9239} - 0.32 = 18.23 \text{ lb/sec}$$

where  $0.995 W_{a,2}$  accounts for the air bled from the compressor discharge for turbine cooling, and where the compressor leakage at the engine midframe  $W_{c1}$  was determined from figure 11(c) for which compressor discharge total pressure was calculated by

$$P_3 = P_1 \left( \frac{P_3}{P_1} \right) = (345.1)(6.010) = 2074$$

where  $P_3/P_1$  was obtained from figure 11(e).

$$\text{Then the sfc} = \frac{3600 \times 0.0199 \times 18.23}{988} = 1.32 \frac{\text{lb fuel/hr}}{\text{lb thrust}}$$

The engine speed was obtained from the corrected speed using the equation

$$N = N/\sqrt{\theta} \times \sqrt{\theta} = 8652 \times 0.9239 = 7994 \text{ rpm}$$

#### REFERENCES

1. Fleming, William A.: Effects of Altitude on Turbojet Engine Performance. NACA RM E51J15, 1951.
2. Renas, Paul E., and Jansen, Emmert T.: Altitude Performance Characteristics of the J47-25 Turbojet Engine - Data Presentation. NACA RM E52G22. (Supersedes NACA TN 1757.)
3. Walker, Curtis L., Huntley, S. C., and Braithwaite, W. M.: Component and Over-all Performance Evaluation of an Axial-Flow Turbojet Engine over a Range of Engine-Inlet Reynolds Numbers. NACA RM E52B08, 1952.
4. Grey, Ralph E., Jr., and Wilsted, H. Dean: Performance of Conical Jet Nozzles in Terms of Flow and Velocity Coefficients. NACA Rep. 933, 1949. (Supersedes NACA TN 1757.)
5. Childs, J. Howard: Preliminary Correlation of Efficiency of Aircraft Gas-Turbine Combustors for Different Operating Conditions. NACA RM E50F15, 1950.
6. Wilsted, H. D., and Grey, R. E.: Altitude Performance Investigation of Centrifugal-Flow-Compressor Turbojet Engine. NACA RM E51B07, 1951.

7. Turner, L. Richard, and Bogart, Donald: Constant-Pressure Combustion Charts Including Effects of Diluent Addition. NACA Rep. 937, 1949. (Supersedes NACA TN's 1086 and 1655.)
8. Turner, L. Richard, Addie, Albert N., and Zimmerman, Richard H.: Charts for the Analysis of One-Dimensional Steady Compressible Flow. NACA TN 1419, 1948.

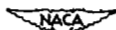


TABLE I. - PERFORMANCE

[illegible]

## AND OPERATIONAL DATA



Corrected engine speed, $\frac{N}{\sqrt{P_0}}$ , rpm	Ram pressure ratio, $\frac{P_0}{P_1}$	Compressor pressure ratio, $\frac{P_2}{P_1}$	Corrected compressor air flow, $\frac{W_{c2}}{\sqrt{P_0}}$ , lb/sec	Compressor efficiency, $\eta_c$	Compressor total pressure ratio, $\frac{P_{2s}}{P_1}$	Compressor total efficiency, $\eta_{tc}$	Engine operating parameter, $\frac{P_3}{P_2} \sqrt{\frac{T_3}{T_2}}$	Combustion chamber parameter, $\frac{P_4}{P_3} \sqrt{\frac{T_4}{T_3}}$	Turbine total pressure ratio, $\frac{P_5}{P_4}$	Corrected turbine gas flow, $\frac{W_{t2}}{\sqrt{P_0}}$ , lb/sec	Turbine efficiency, $\eta_t$	Tail-pipe pressure ratio, $\frac{P_6}{P_5}$	Engine total pressure ratio, $\frac{P_6}{P_1}$	Engine total efficiency, $\eta_{te}$	Corrected fuel flow, $\frac{W_f}{\sqrt{P_0}}$ , lb/sec	Corrected ideal fuel-air ratio, $\frac{F}{A}$	Corrected exhaust gas temperature, $\frac{T_6}{T_3}$	Corrected jet-thrust parameter, $\frac{F_j + A_1 P_0}{\sqrt{P_0}}$ , lb	R/n
7509	1.72	5.15	102.8	0.860	0.0508	0.986	4.06x10 <sup>5</sup>	84.8x10 <sup>4</sup>	2.57	41.8	0.825	0.037	1.833	3.162	5784	0.0150	1841	9.999	1
7721	1.76	5.32	103.8	0.810	0.0508	0.986	4.00	84.8	2.57	42.0	0.825	0.036	1.824	3.154	5668	0.0157	1838	9.971	2
7536	1.70	4.90	100.5	0.811	0.0481	1.004	3.77	88.8	2.57	41.8	0.830	0.039	1.747	3.002	5124	0.0148	1568	9.552	3
7587	1.74	4.90	100.5	0.815	0.0483	0.984	3.78	88.8	2.57	41.8	0.835	0.039	1.742	3.001	5124	0.0148	1568	9.552	4
7440	1.70	4.75	96.8	0.817	0.0468	0.977	3.54	84.3	2.54	41.9	0.850	0.036	1.694	2.886	4740	0.0136	1497	9.160	5
7439	1.74	4.75	96.8	0.825	0.0475	0.977	3.52	84.2	2.57	41.8	0.855	0.036	1.694	2.903	4742	0.0137	1506	9.160	6
7284	1.71	4.54	94.7	0.822	0.0449	0.986	3.32	80.0	2.58	41.3	0.825	0.039	1.619	2.790	4379	0.0129	1448	8.800	7
7283	1.74	4.54	94.8	0.833	0.0473	0.988	3.29	79.5	2.59	41.6	0.815	0.037	1.619	2.796	4381	0.0126	1450	8.863	8
7086	1.74	4.34	93.8	0.837	0.0462	0.996	3.05	75.7	2.59	41.4	0.830	0.039	1.554	2.653	3922	0.0118	1362	8.371	9
7075	1.71	4.32	93.7	0.828	0.0477	1.004	3.05	74.0	2.59	41.4	0.835	0.039	1.528	2.642	3981	0.0117	1371	8.509	10
6723	1.73	4.87	87.5	0.837	0.0514	0.994	2.58	62.1	2.60	40.8	0.810	0.041	1.353	2.564	3000	0.0097	1237	7.355	11
6702	1.70	5.06	87.5	0.835	0.0509	0.982	2.58	62.5	2.59	40.8	0.820	0.045	1.353	2.558	2987	0.0099	1224	7.345	12
6294	1.74	5.30	79.2	0.828	0.0573	0.990	2.09	48.4	2.60	40.4	0.820	0.043	1.142	2.011	2011	0.0072	1058	6.235	13
6259	1.74	5.29	79.4	0.830	0.0566	0.980	2.11	49.3	2.60	40.4	0.820	0.041	1.145	2.017	1994	0.0070	1047	6.235	14
8346	2.15	8.58	106.1	0.752	0.0456	0.996	2.98x10 <sup>5</sup>	64.7x10 <sup>4</sup>	2.58	42.0	0.825	0.034	2.023	3.628	7182	0.0191	1882	11.022	15
8341	2.14	8.58	106.4	0.751	0.0459	0.994	2.91	62.8	2.58	41.9	0.825	0.035	2.021	3.627	7157	0.0191	1883	11.003	16
8100	2.14	8.44	104.8	0.774	0.0506	0.995	2.89	61.5	2.59	41.8	0.835	0.035	1.928	3.373	6348	0.0171	1751	10.459	17
7687	2.14	8.33	104.5	0.787	0.0519	0.997	2.87	60.8	2.58	41.8	0.835	0.036	1.907	3.284	5967	0.0162	1691	10.275	18
7619	2.15	8.16	102.6	0.797	0.0510	0.999	2.39	55.5	2.60	41.7	0.845	0.036	1.817	3.146	5622	0.0153	1633	9.891	19
7560	2.14	8.02	101.2	0.813	0.0479	0.985	2.18	51.4	2.59	41.9	0.850	0.030	1.739	2.96	4908	0.0136	1539	9.35	20
7158	2.18	4.66	95.5	0.829	0.0493	1.002	1.87	45.2	2.61	41.2	0.815	0.039	1.688	2.63	3983	0.0110	1399	8.596	21
6725	2.18	4.86	87.8	0.830	0.0518	1.010	1.82	44.6	2.61	40.8	0.810	0.043	1.688	2.62	3984	0.0108	1394	8.596	22
6244	2.17	5.25	78.8	0.821	0.0505	0.987	1.25	28.3	2.63	40.5	0.835	0.042	1.114	1.988	1912	0.0067	1052	6.011	23
8358	1.95	5.72	105.4	0.744	0.0483	0.981	2.45x10 <sup>5</sup>	58.5x10 <sup>4</sup>	2.58	41.8	0.820	0.037	2.029	3.430	7306	0.0196	1915	11.055	24
8354	1.94	5.66	105.1	0.744	0.0486	0.980	2.44	55.0	2.57	41.9	0.820	0.039	2.014	3.456	7253	0.0195	1897	11.000	25
8351	1.95	5.66	105.3	0.748	0.0485	0.975	2.47	55.0	2.58	41.3	0.820	0.035	2.011	3.433	7163	0.0196	1880	10.974	26
8159	1.94	5.47	104.8	0.787	0.0508	0.994	2.27	51.8	2.59	41.8	0.830	0.037	1.937	3.126	6447	0.017	1778	10.52	27
8119	1.95	5.45	104.2	0.786	0.0505	0.995	2.24	51.2	2.59	41.8	0.835	0.037	1.927	3.118	6111	0.017	1715	10.516	28
7959	1.98	5.29	103.0	0.782	0.0512	1.001	2.14	49.3	2.59	41.7	0.830	0.039	1.847	3.077	5835	0.0163	1671	10.229	29
7865	1.98	5.06	102.1	0.789	0.0518	1.000	2.00	48.2	2.54	42.3	0.855	0.043	1.808	3.139	5977	0.0152	1629	9.863	30
7574	1.95	4.91	100.0	0.810	0.0462	0.999	1.83	45.7	2.60	41.5	0.830	0.039	1.726	2.975	5101	0.014	1561	9.29	31
7155	1.98	4.67	95.2	0.824	0.0467	1.002	1.56	38.2	2.61	41.1	0.810	0.040	1.570	2.722	4056	0.0125	1412	8.58	32
6895	1.98	5.84	86.6	0.828	0.0516	0.982	1.27	30.7	2.61	40.7	0.810	0.042	1.337	2.358	294	0.0093	122	7.46	33
6249	1.95	5.25	79.0	0.825	0.0577	0.954	1.03	24.1	2.63	40.3	0.820	0.042	1.127	2.015	2036	0.0089	105	6.123	34
8394	1.35	5.75	104.4	0.741	0.0456	0.996	1.94x10 <sup>5</sup>	48.9x10 <sup>4</sup>	2.59	41.4	0.805	0.036	2.053	3.751	7425	0.0202	1917	11.067	35
8352	1.35	5.75	105.8	0.748	0.0475	0.980	1.94	45.0	2.57	41.7	0.825	0.037	2.053	3.466	7444	0.0197	1912	11.031	36
7971	1.35	5.32	102.5	0.771	0.0514	0.998	1.70	39.4	2.62	41.6	0.845	0.036	1.928	3.253	6115	0.0178	1724	10.978	37
7783	1.32	5.20	101.2	0.800	0.0511	0.984	1.56	37.9	2.59	41.1	0.850	0.040	1.827	3.181	5447	0.0156	1650	9.828	38
7817	1.35	5.00	99.8	0.828	0.0495	0.994	1.48	35.6	2.69	41.0	0.825	0.040	1.781	3.045	5172	0.015	1581	9.553	39
7187	1.34	4.60	86.3	0.827	0.0463	0.978	1.23	31.0	2.59	40.7	0.800	0.041	1.588	2.759	4172	0.0125	1432	8.610	40
6710	1.34	4.55	87.3	0.825	0.0463	0.984	1.01	25.2	2.59	40.4	0.810	0.039	1.587	2.756	4192	0.0125	1428	8.517	41
8671	1.39	5.99	107.0	0.712	0.0468	0.984	2.01x10 <sup>5</sup>	44.7x10 <sup>4</sup>	2.56	42.1	0.845	0.037	2.151	3.491	7294	0.0217	1954	11.288	42
8399	1.42	5.56	104.5	0.720	0.0464	0.984	1.96	42.3	2.58	41.6	0.835	0.036	2.014	3.476	7153	0.0213	1919	11.278	43
8153	1.41	5.56	104.4	0.740	0.0493	0.989	1.73	39.8	2.59	41.5	0.835	0.037	1.947	3.19	6851	0.0177	1804	10.696	44
8065	1.42	5.45	103.4	0.772	0.0522	0.992	1.64	38.4	2.60	41.3	0.840	0.038	1.914	3.168	6219	0.0168	1710	10.56	45
7759	1.43	5.15	100.2	0.797	0.0507	0.998	1.47	35.3	2.61	40.8	0.815	0.041	1.797	3.140	5166	0.0150	1629	9.796	46
7883	1.43	4.89	96.5	0.812	0.0493	0.988	1.41	30.8	2.59	40.9	0.810	0.041	1.653	2.952	514	0.0130	1491	8.929	47
8390	1.42	4.16	80.4	0.815	0.0472	0.972	1.05x10 <sup>5</sup>	26.8x10 <sup>4</sup>	2.59	40.6	0.809	0.040	1.72	2.571	5592	0.0136	1435	7.931	48
8517	1.42	3.95	81.2	0.827	0.0519	0.947	0.85	20.9	2.59	40.4	0.805	0.039	1.222	2.277	4716	0.0118	1382	7.416	49
8634	1.68	6.13	106.1	0.691	0.0471	0.986	1.62	40.4	2.59	41.6	0.831	0.039	2.166	3.154	6488	0.0229	1915	11.061	50
8624	1.70	6.25	105.6	0.715	0.0467	0.985	1.69	38.1	2.60	41.4	0.828	0.039	2.092	3.389	7600	0.0208	1919	11.263	51
8477	1.69	5.78	105.4	0.730	0.0474	1.000	1.61	38.3	2.59	41.5	0.831	0.039	2.04	3.730	7277	0.0196	1887	11.039	52
8296	1.69	5.56	104.1	0.743	0.0494	0.995	1.61	33.9	2.58	41.7	0.843	0.040	1.972	3.551	8708	0.0181	1815	10.73	53
8048	1.69	5.37	103.4	0.772	0.0510	0.988	1.37	31.1	2.60	41.6	0.837	0.039	1.876	3.329	6982	0.0164	1728	10.423	54
7635	1.69	4.97	100.0	0.803	0.0495	0.990	1.18	27.9	2.60	41.2	0.821	0.040	1.75	3.01	5992	0.015	1685	9.531	55
7130	1.69	4.36	97.5	0.817	0.0461	0.984	0.96	23.1	2.62	40.7	0.813	0.038	1.536	2.678	397	0.0115	1380	8.333	56
6850	1.66	3.81	86.6	0.827	0.0469	0.947	0.78	19.0	2.63	40.5	0.820	0.037	1.524	2.535	2930	0.0091	1212	7.136	57
8683	1.68	6.01	106.7	0.706	0.0472	0.981	1.29x10 <sup>5</sup>	26.8x10 <sup>4</sup>	2.58	42.0	0.827	0.040	2.151	3.019	6321	0.0218	1968	11.611	58
8498	1.71	6.03	105.2	0.728	0.0478	0.981	1.22	27.5	2.58	41.8	0.826	0.042	2.076	3.011	7551	0.0201	1970	11.348	59
8456	1.68	5.60	104.6	0.723	0.0474	0.988	1.20	27.2	2.58	41.4	0								

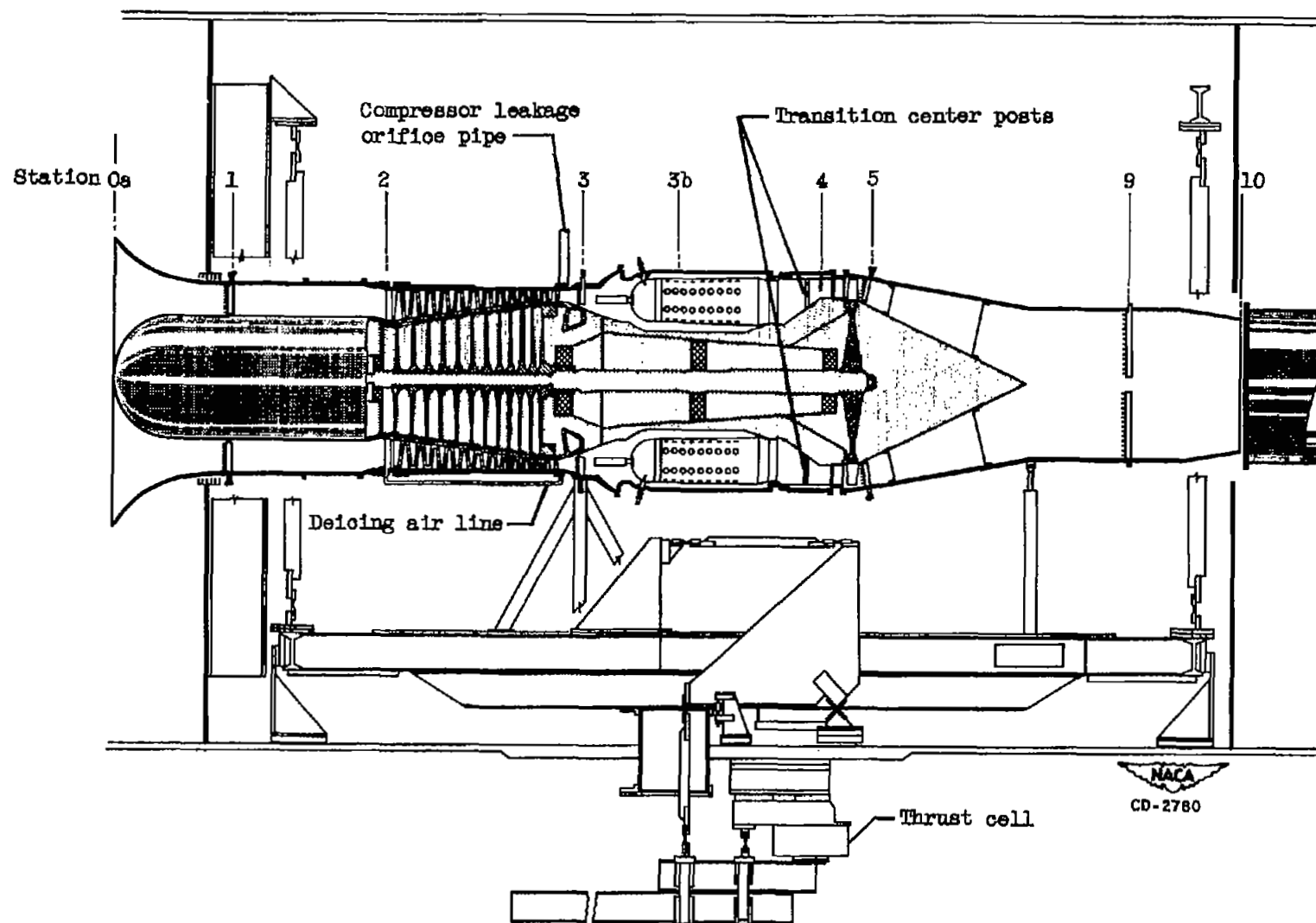
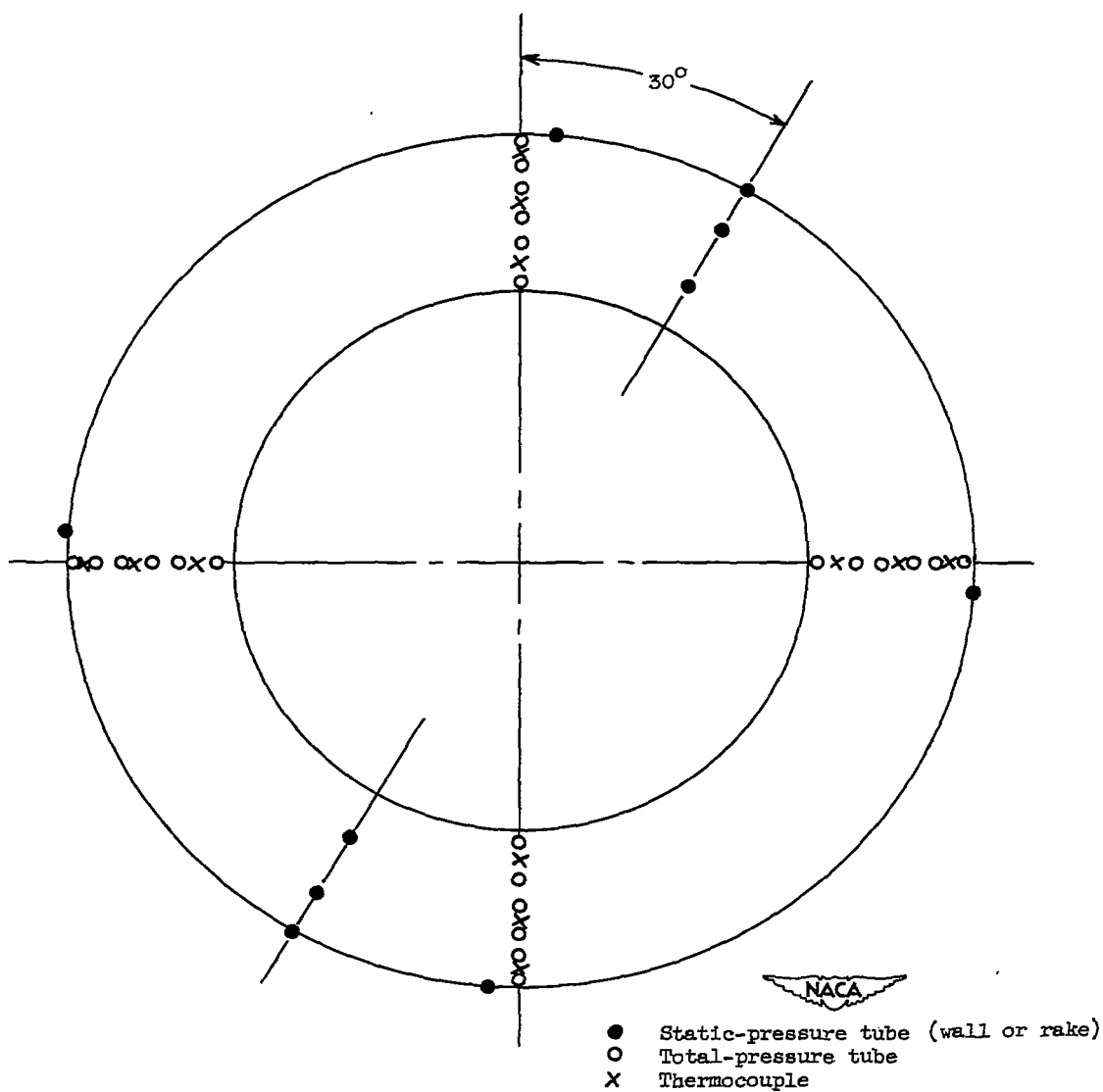
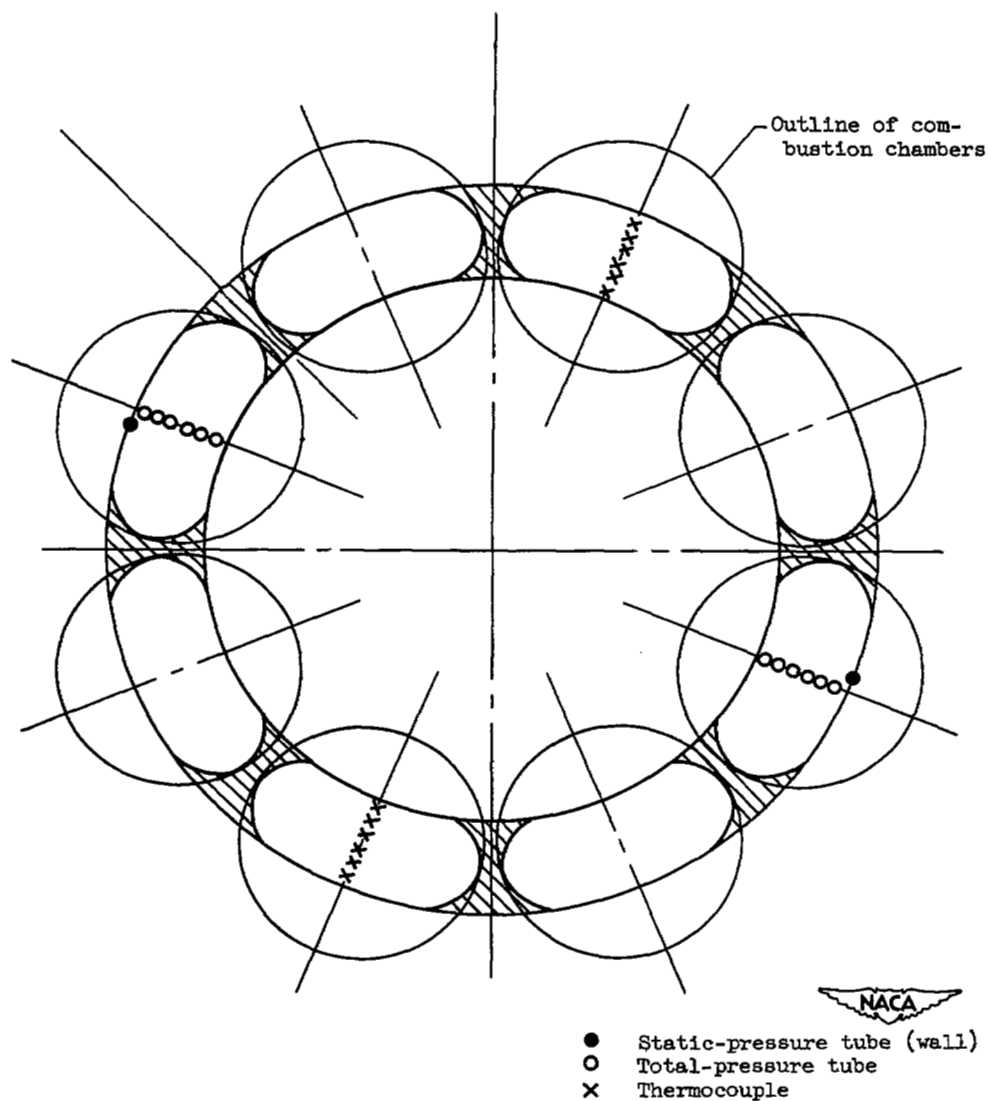


Figure 1. - Schematic diagram of engine in altitude chamber showing station locations.



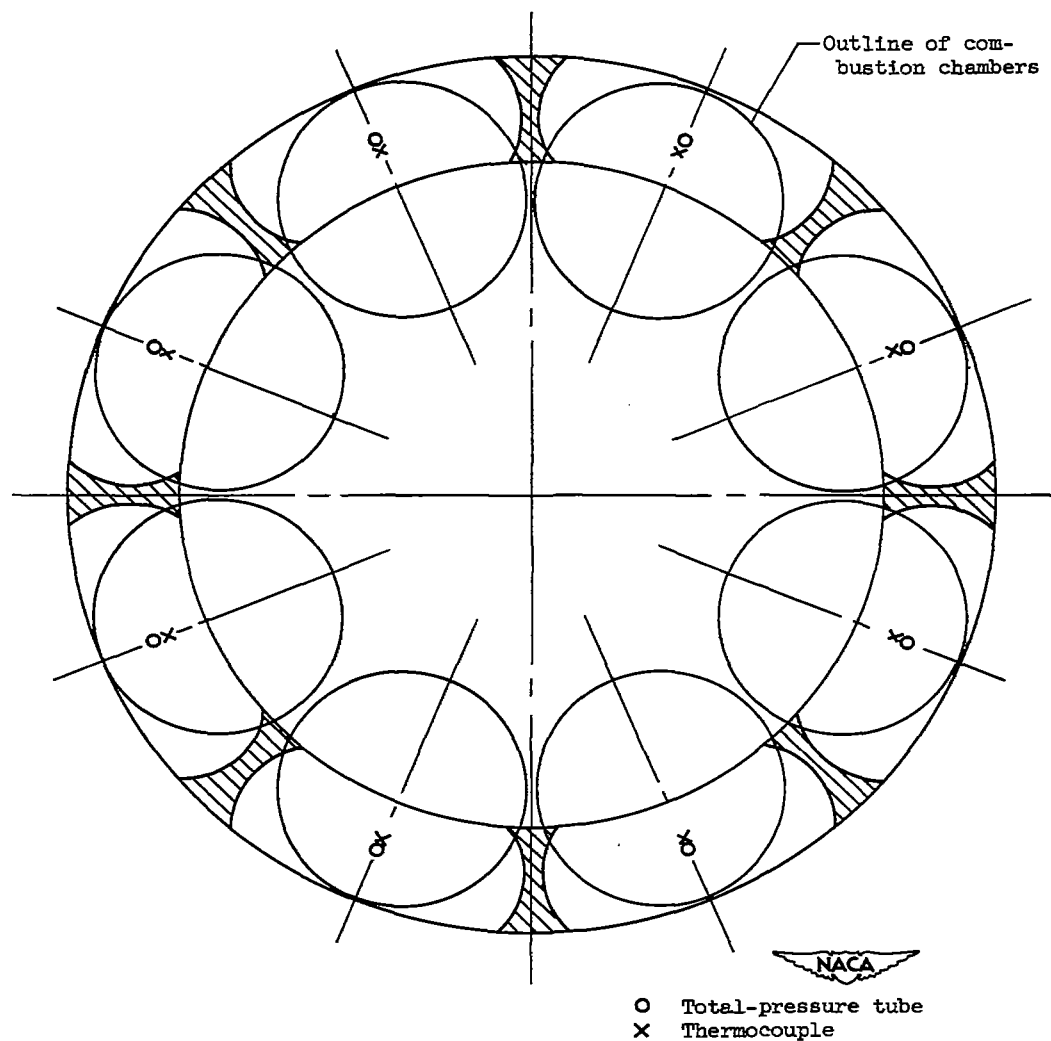
(a) Instrumentation at engine inlet, station 1, 21 inches upstream of leading edge of compressor-inlet guide vanes.

Figure 2. - Location of instrumentation at various measuring stations as viewed from upstream.



(b) Instrumentation at compressor outlet, station 3, 2 inches downstream of trailing edge of compressor-outlet guide vanes.

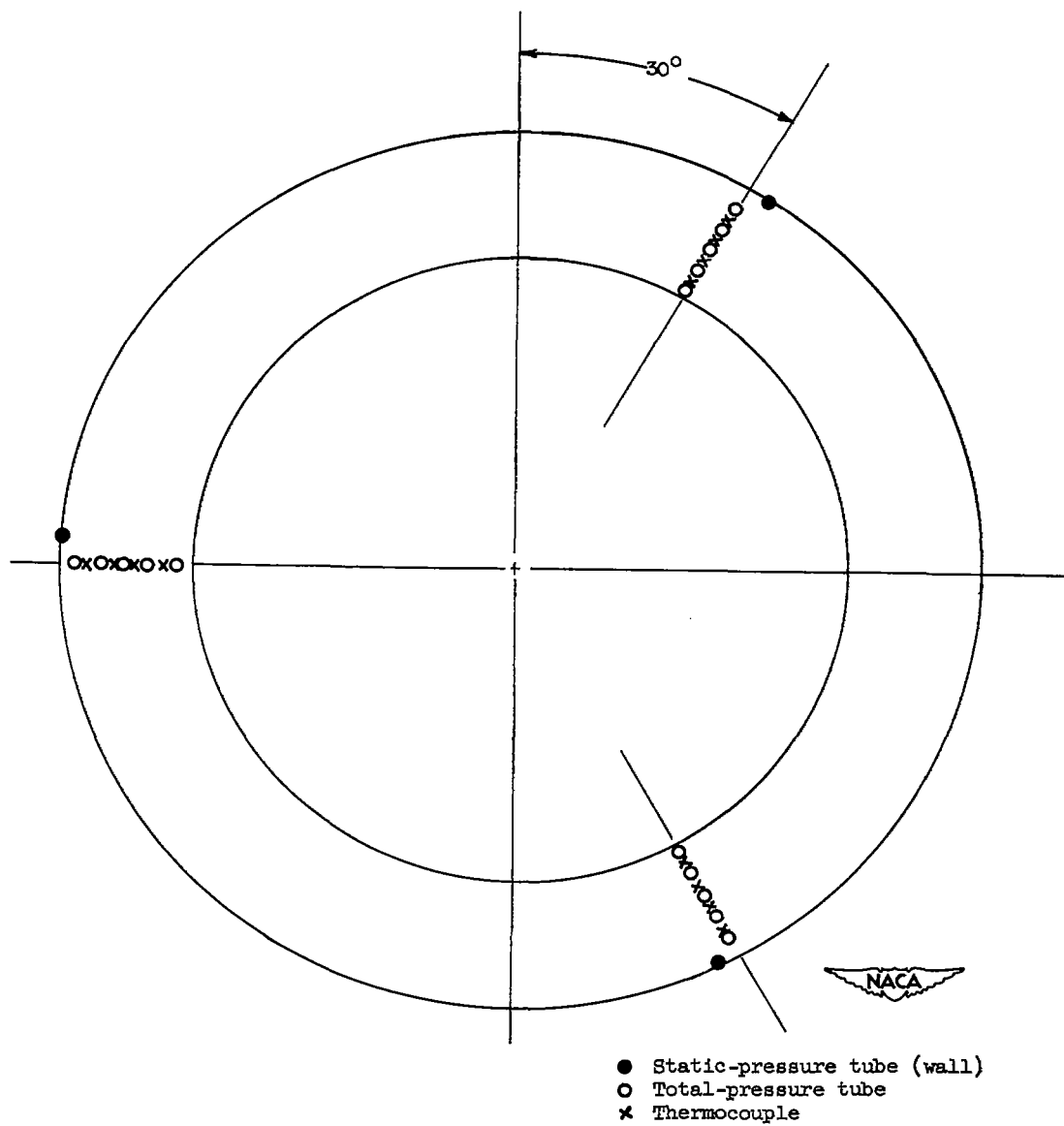
Figure 2. - Continued. Location of instrumentation at various measuring stations as viewed from upstream.



(c) Instrumentation at turbine inlet, station 4,  $1\frac{3}{4}$  inches upstream of leading edge of turbine-inlet guide vanes.

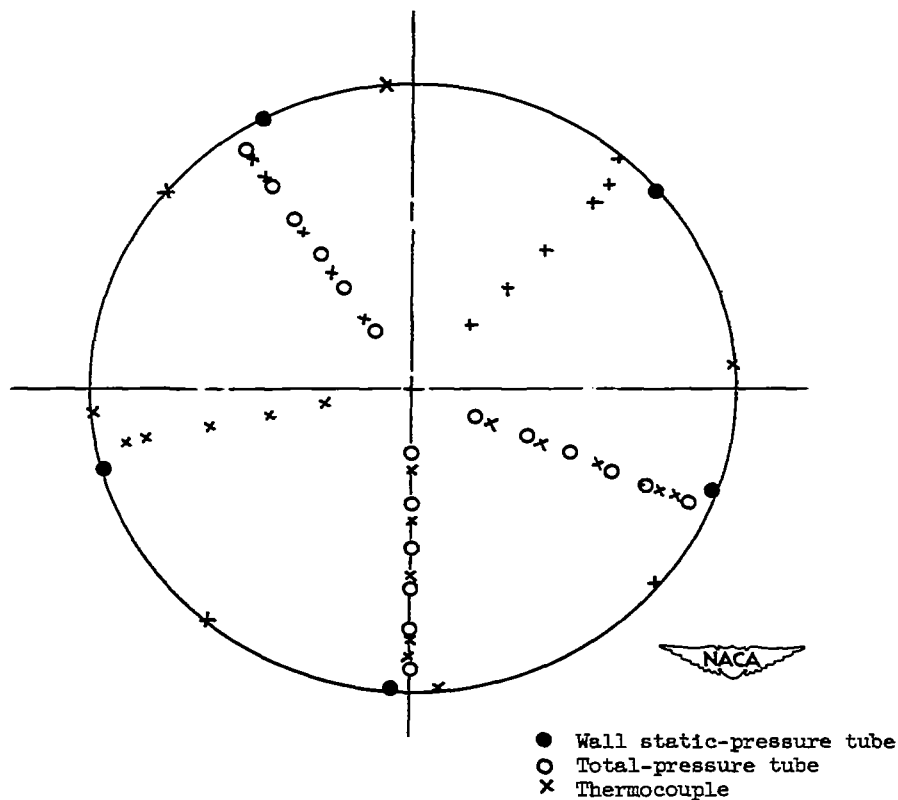
Figure 2. - Continued. Location of instrumentation at various measuring stations as viewed from upstream.





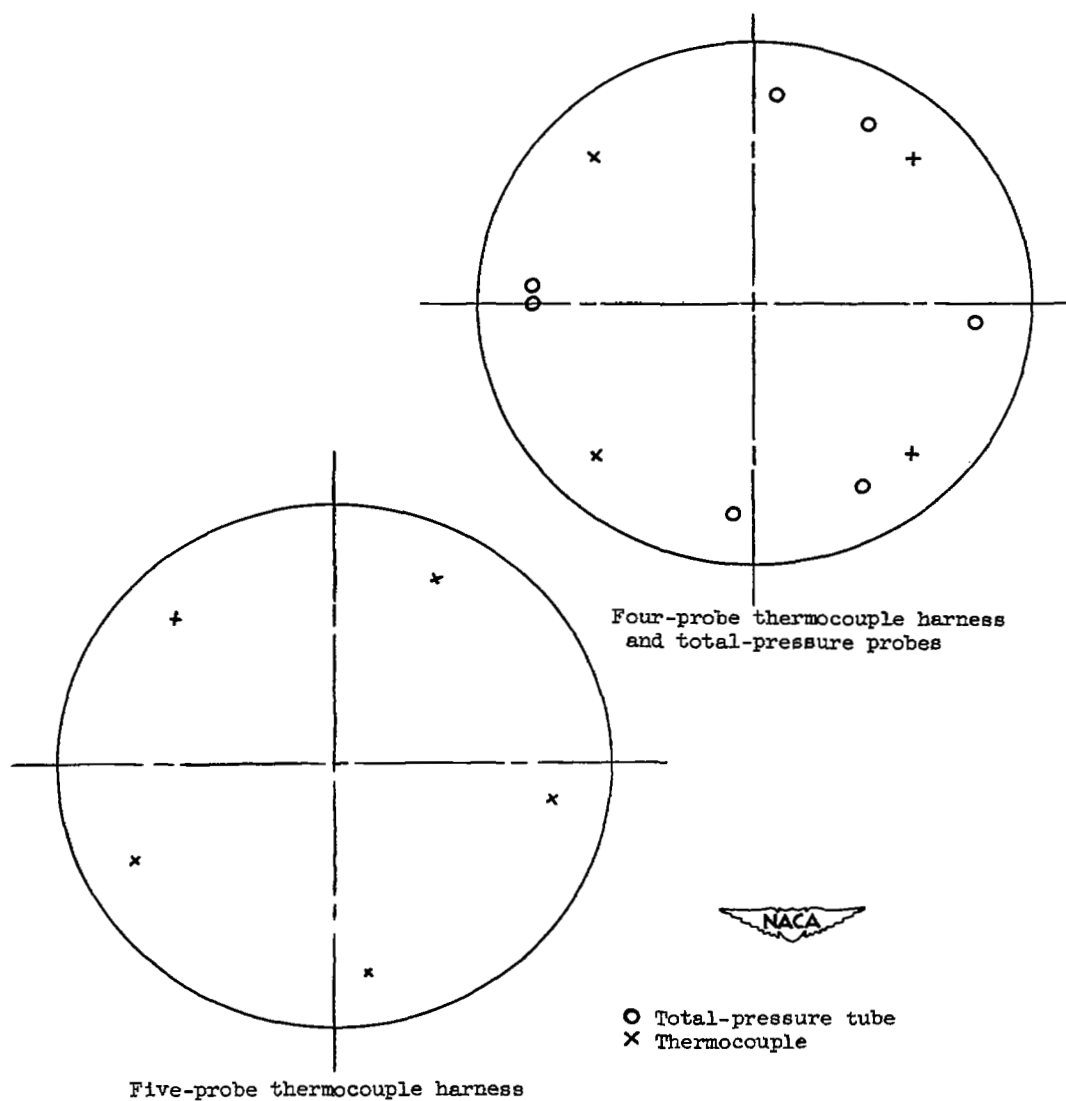
(d) Instrumentation at turbine outlet, station 5,  $4\frac{7}{8}$  inches downstream of trailing edge of turbine blades.

Figure 2. - Continued. Location of instrumentation at various measuring stations as viewed from upstream.



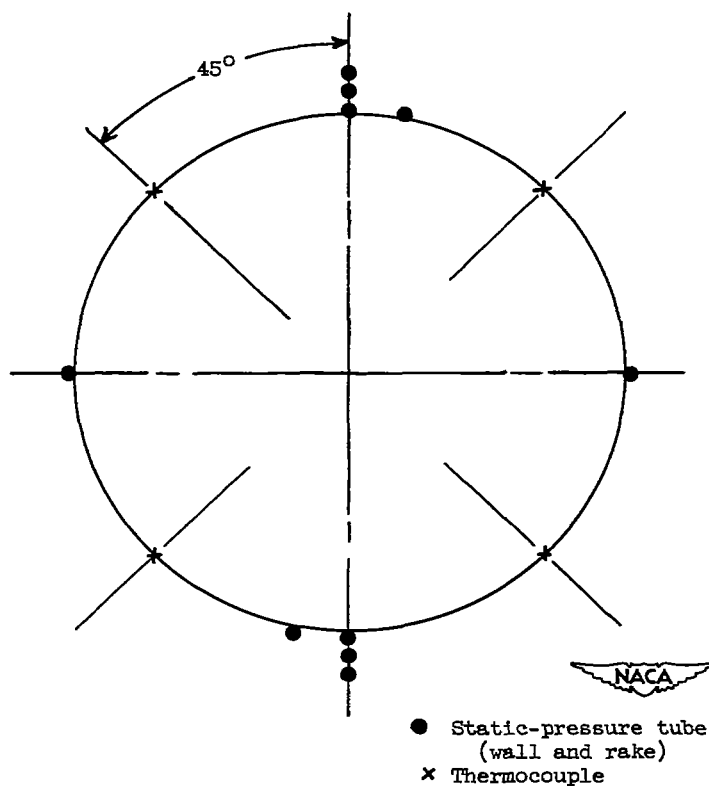
(e) NACA instrumentation at nozzle inlet, station 9,  $15\frac{1}{8}$  inches downstream of tail-cone-outlet flange.

Figure 2. - Continued. Location of instrumentation at various measuring stations as viewed from upstream.



(f) Manufacturer's instrumentation at nozzle inlet, station 9,  
 $15\frac{1}{8}$  inches downstream of tail-cone-outlet flange.

Figure 2. - Continued. Location of instrumentation at various measuring  
stations as viewed from upstream.



(g) Instrumentation at nozzle lip, station 10.

Figure 2. - Concluded. Location of instrumentation at various measuring stations as viewed from upstream.

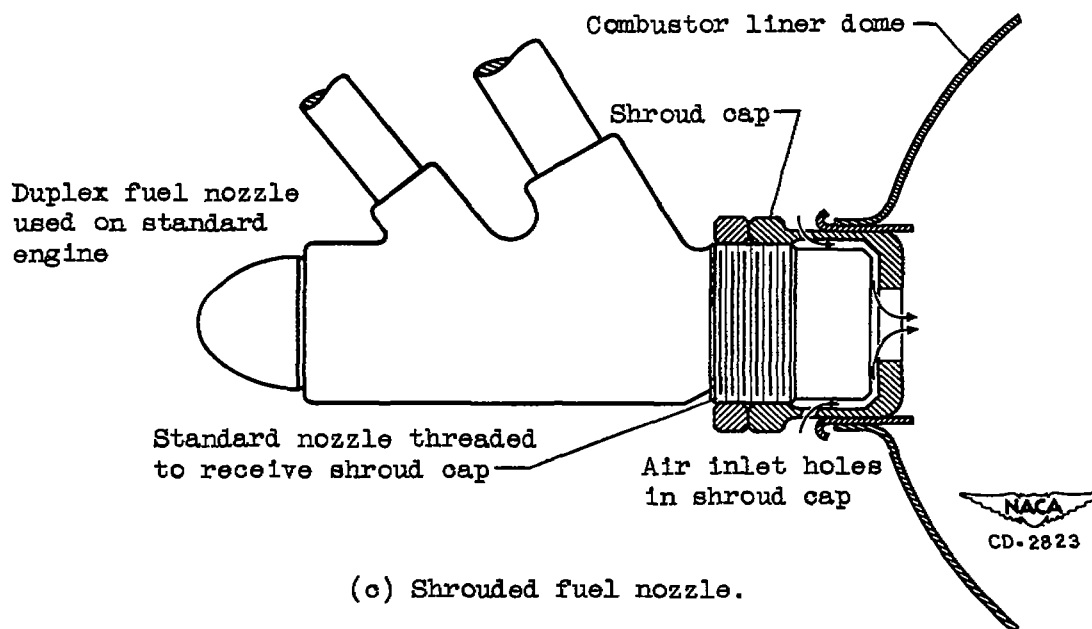
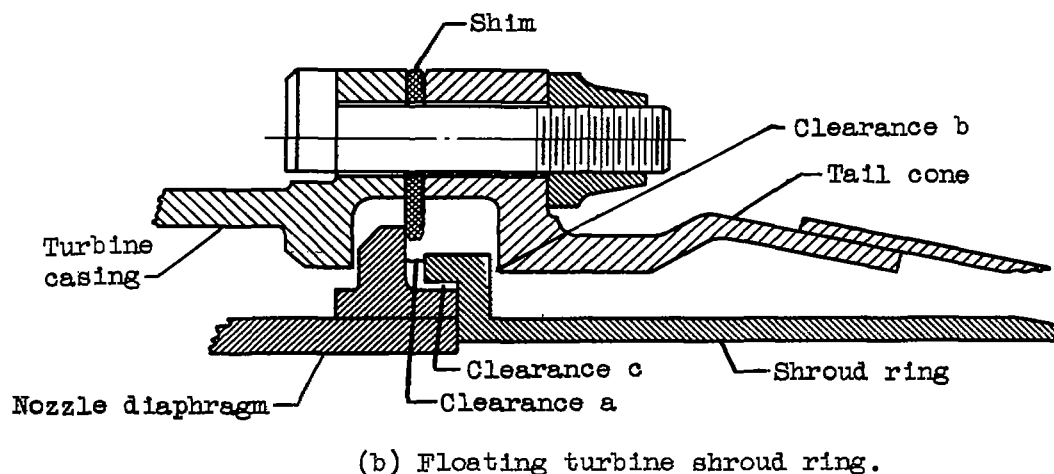
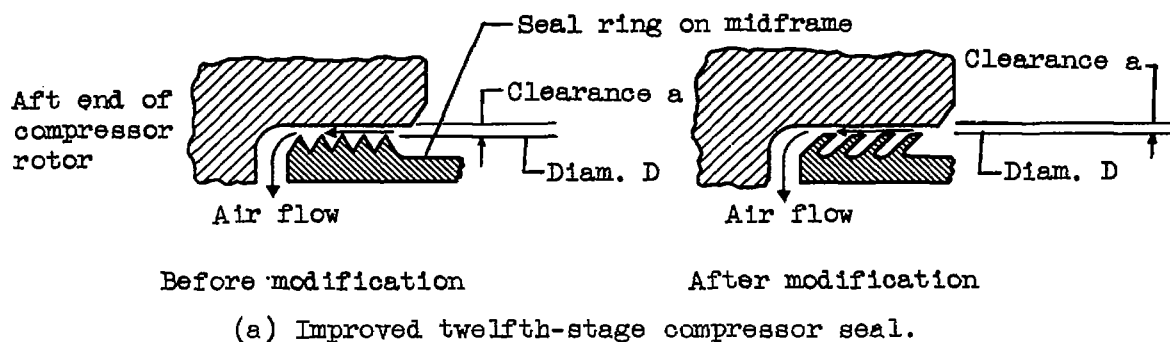
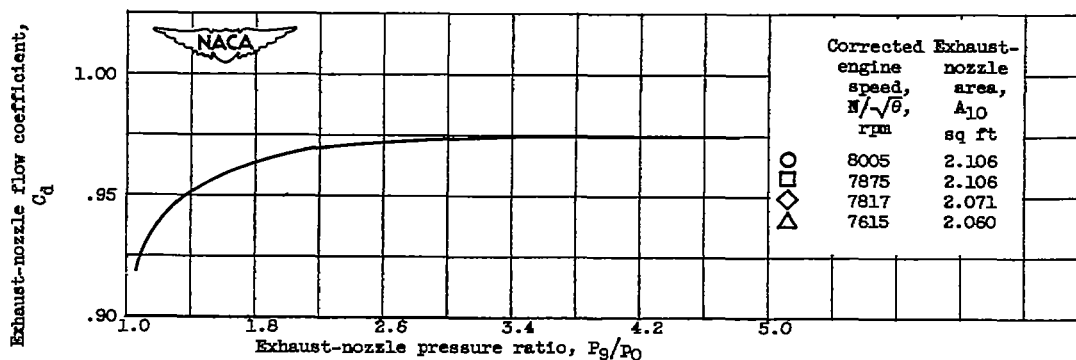
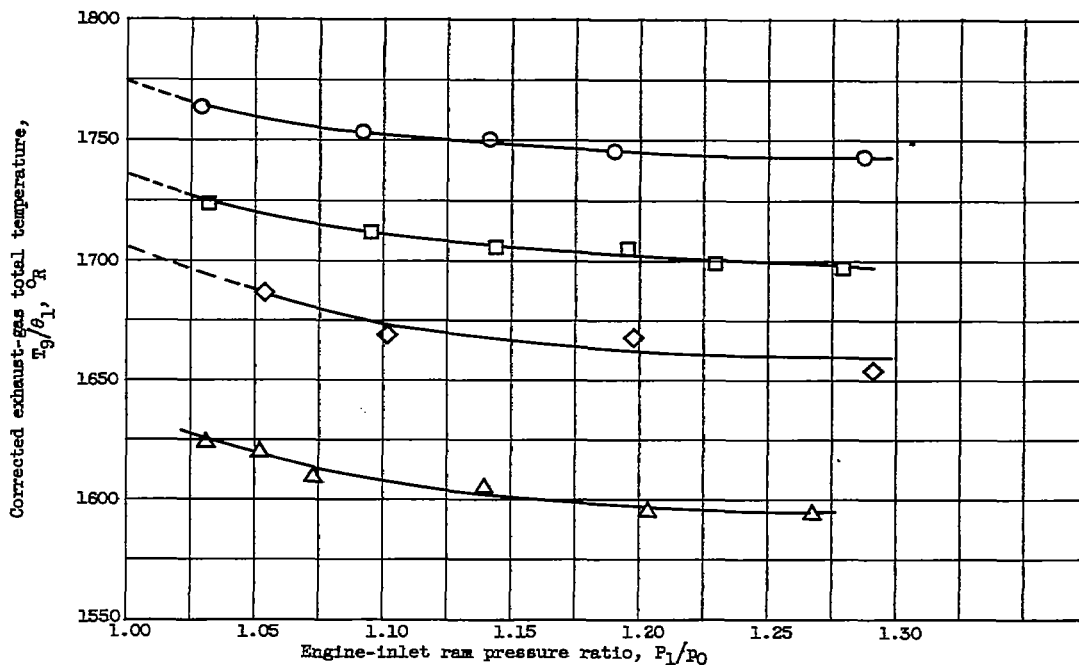


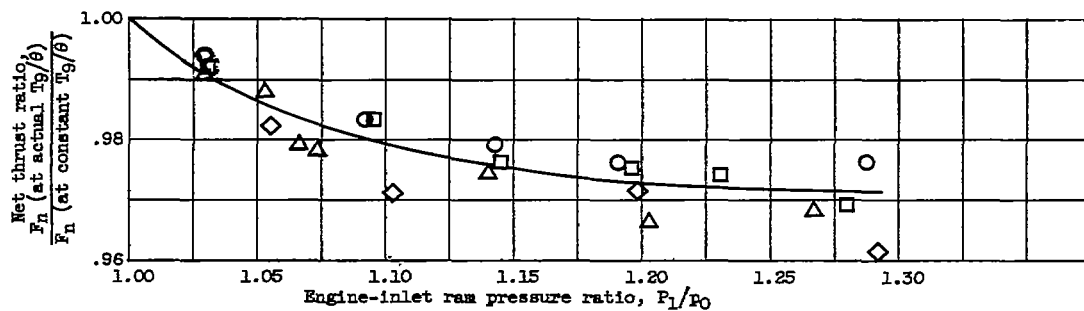
Figure 3. - Engine modifications incorporated in configurations B and C.



(a) Exhaust-nozzle flow coefficient as function of nozzle pressure ratio (ref. 4).



(b) Corrected exhaust-gas total temperature.



(c) Net thrust loss.

Figure 4. - Effect of exhaust-nozzle flow coefficient on engine performance.

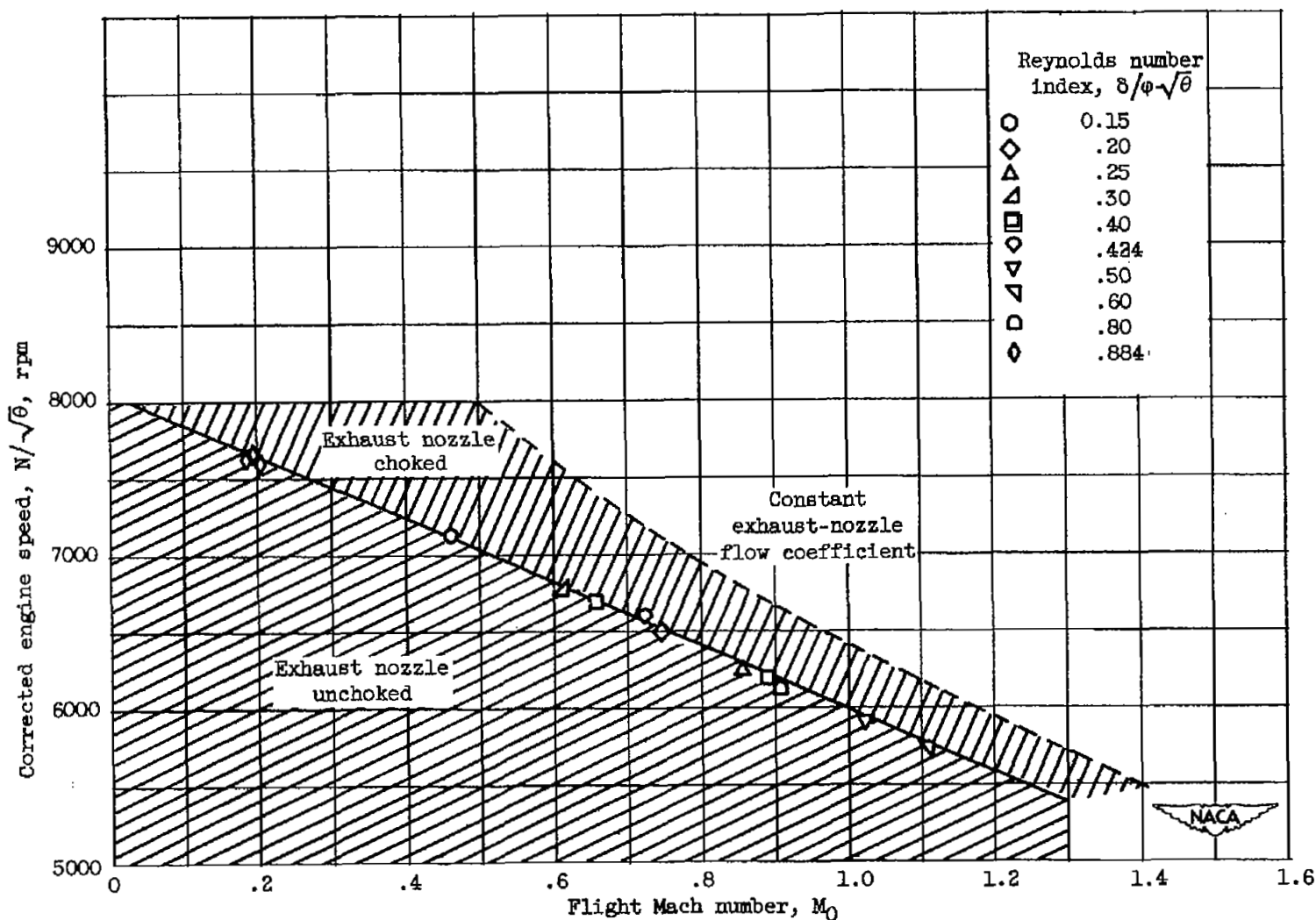
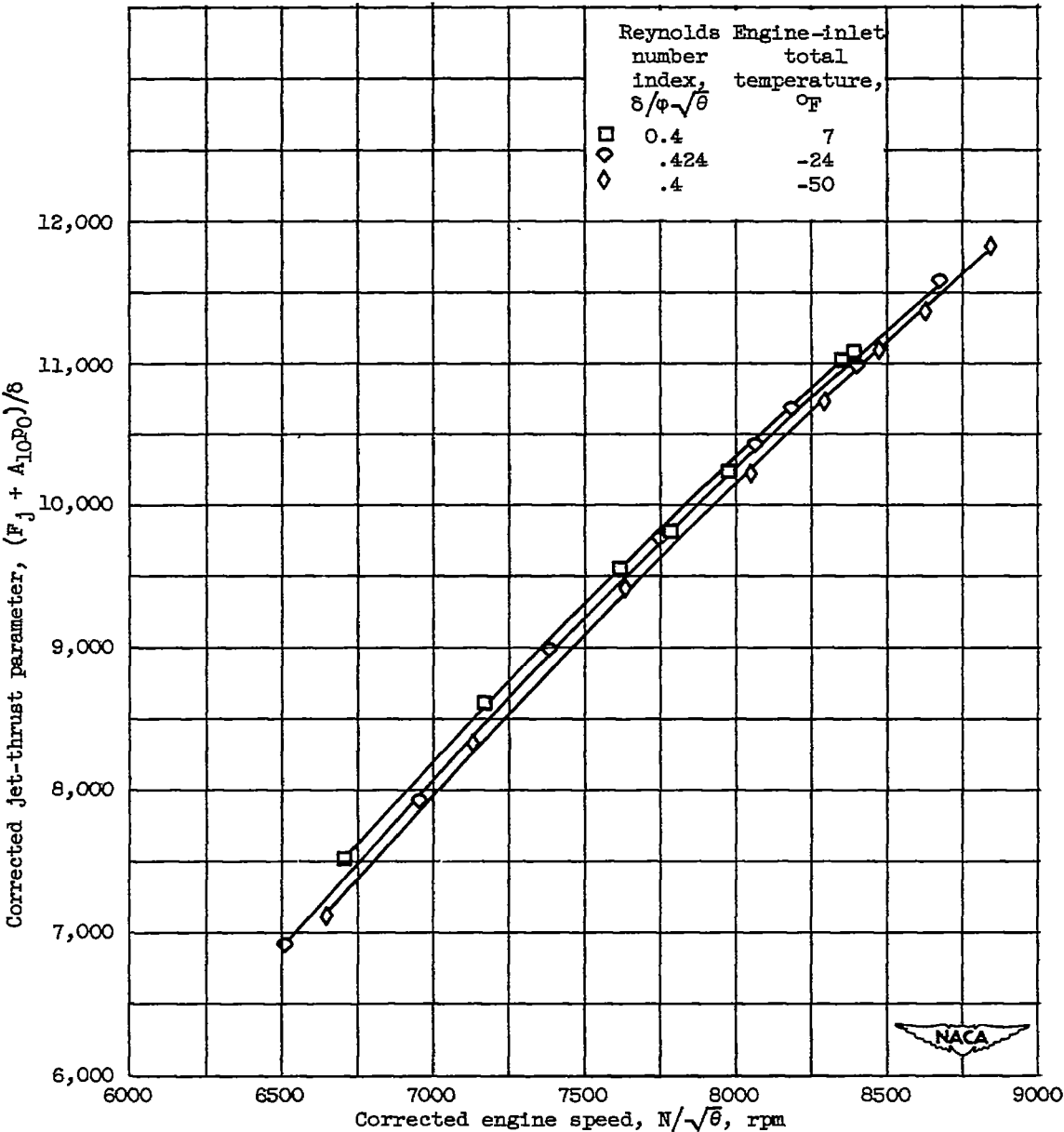


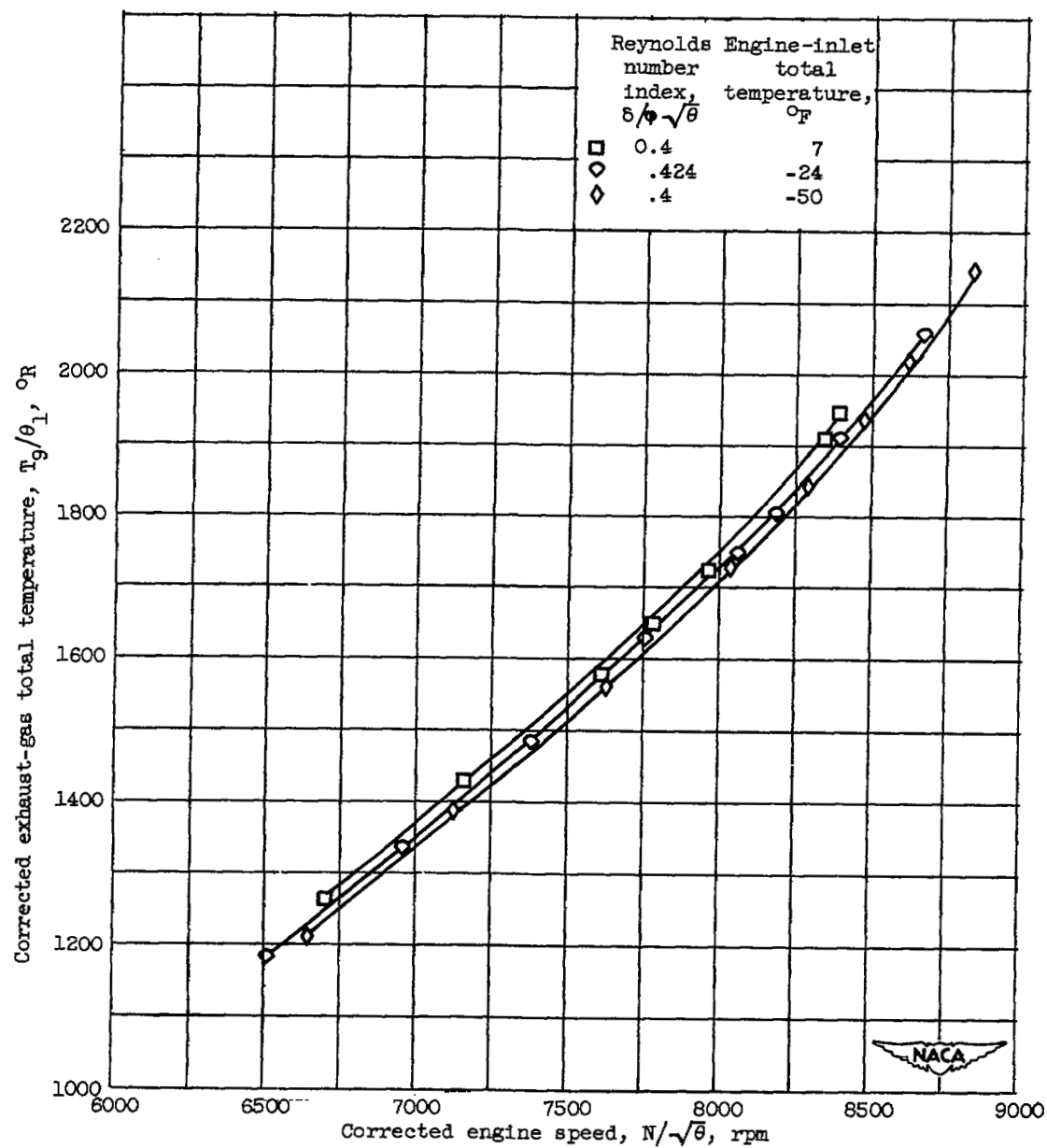
Figure 5. - Flight conditions for which varying flow coefficient corrections must be applied to performance data.



(a) Jet-thrust parameter.

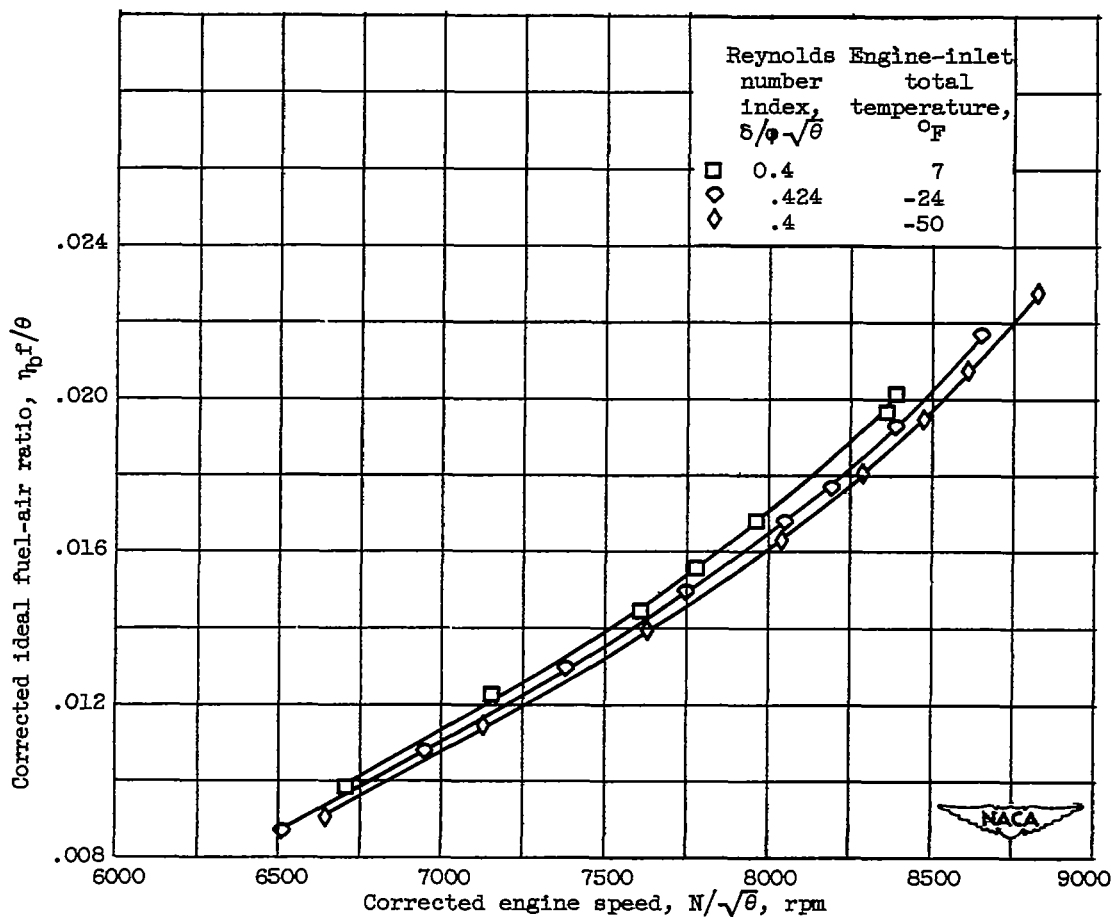
Figure 6. - Effect of engine-inlet total temperature on engine performance at constant Reynolds number index.





(b) Corrected exhaust-gas total temperature.

Figure 6. - Continued. Effect of engine-inlet total temperature on engine performance at constant Reynolds number index.



(c) Corrected ideal fuel-air ratio.

Figure 6. - Concluded. Effect of engine-inlet total temperature on engine performance at constant Reynolds number index.

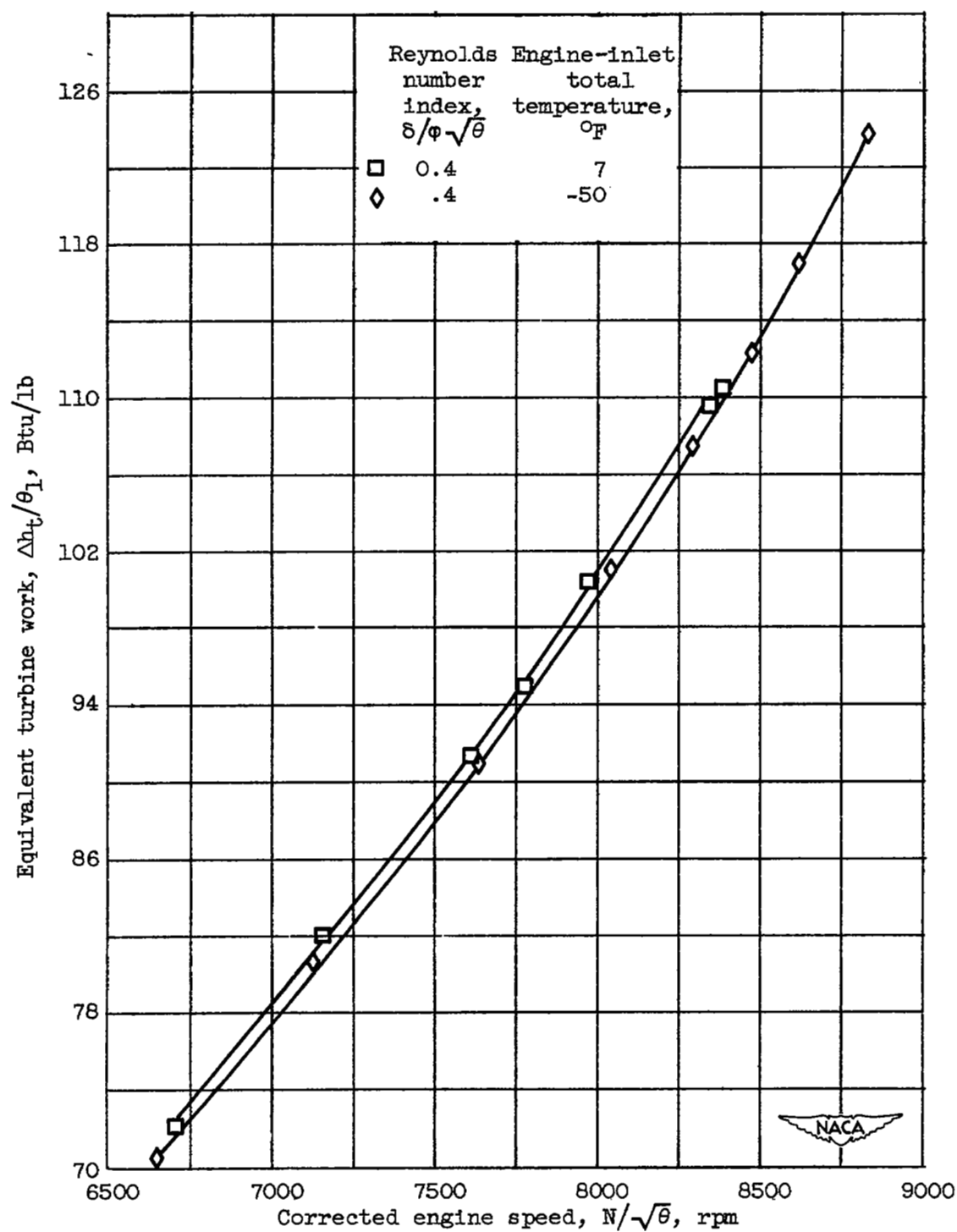
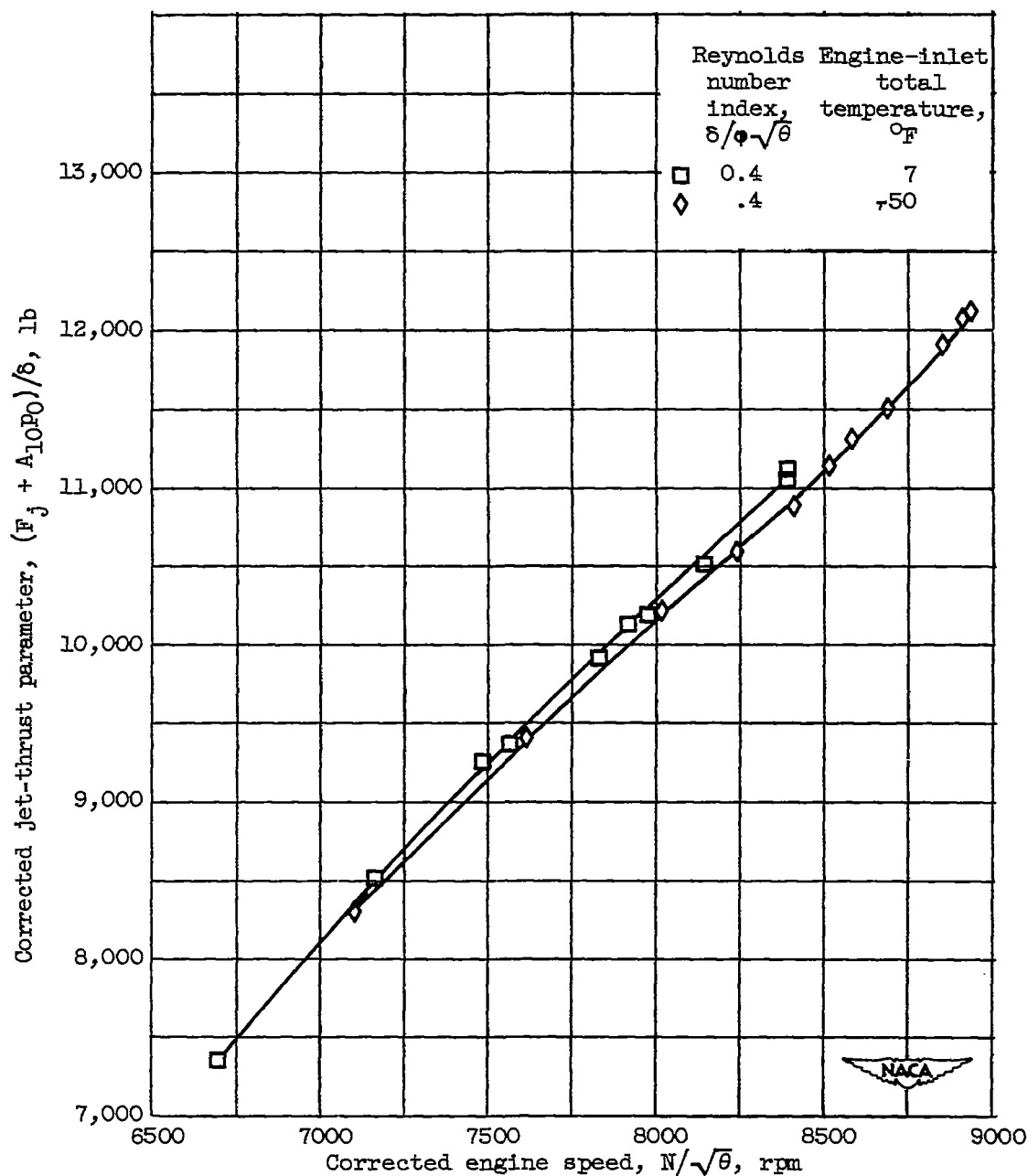
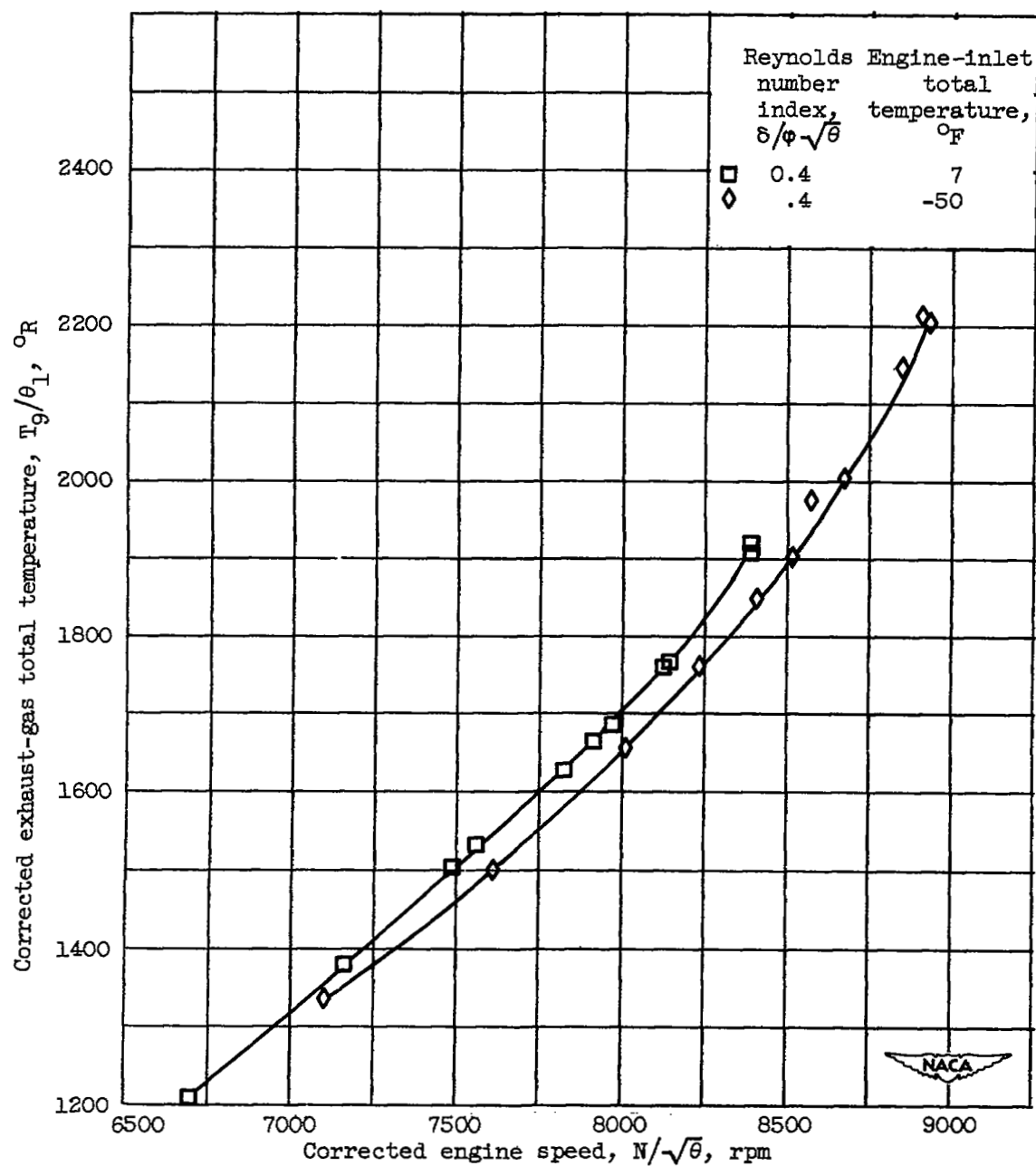


Figure 7. - Effect of engine-inlet total temperature on equivalent turbine work.



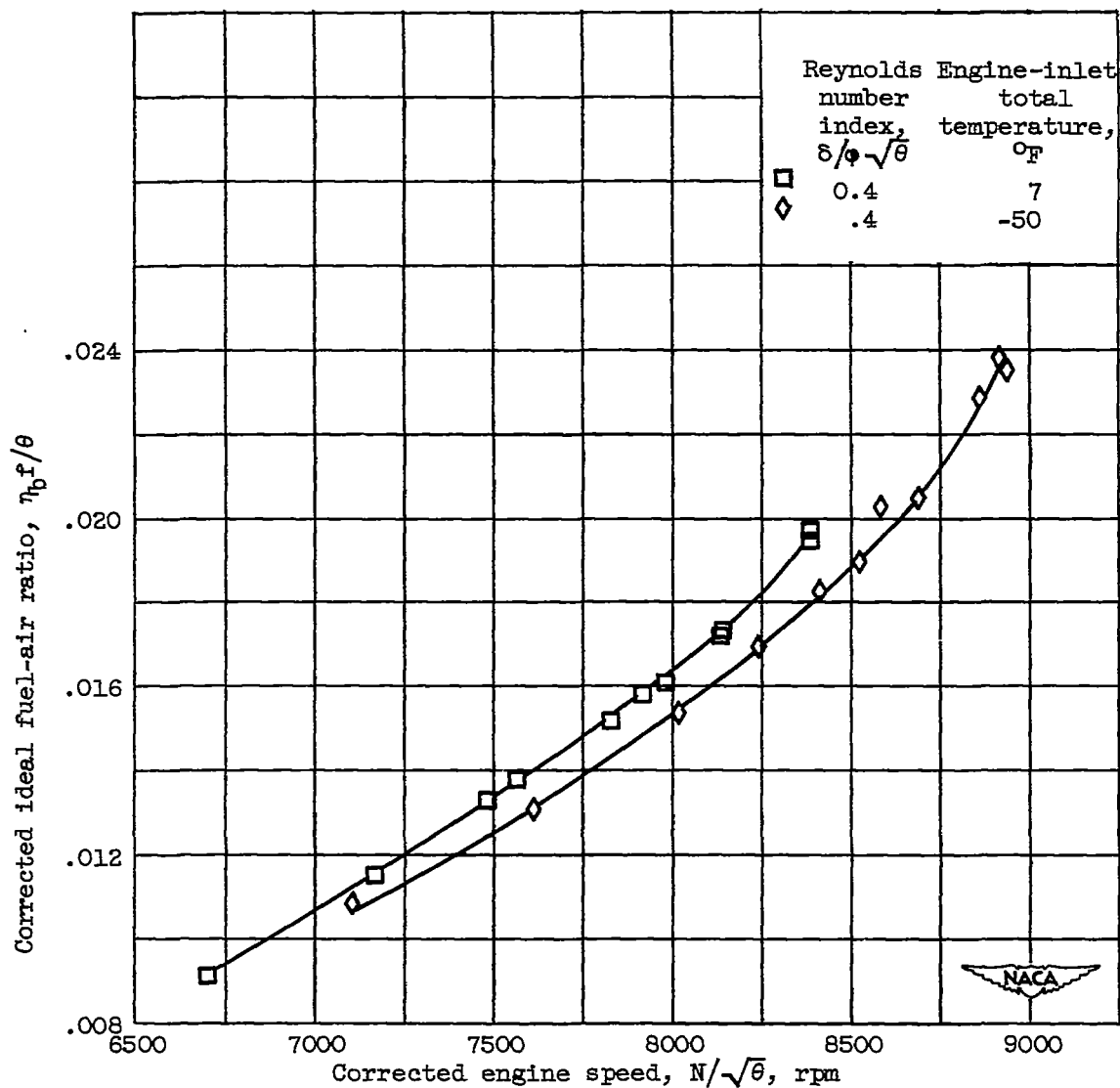
(a) Corrected jet-thrust parameter.

Figure 8. - Effect of engine-inlet total temperature on performance of J47-GE-17 engine with no turbine-outlet straightening vanes installed.



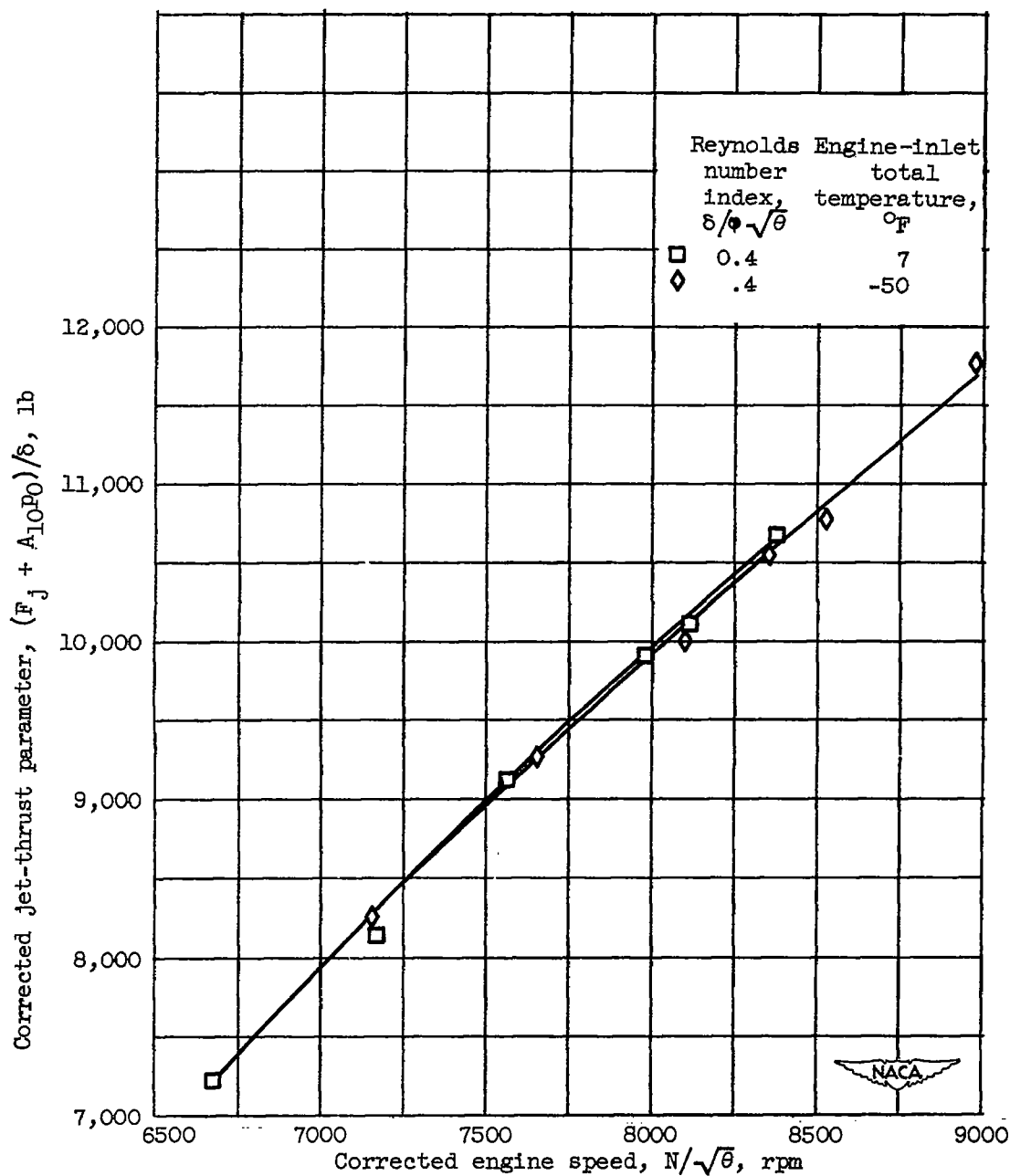
(b) Corrected exhaust-gas total temperature.

Figure 8. - Continued. Effect of engine-inlet total temperature on performance of J47-GE-17 engine with no turbine-outlet straightening vanes installed.



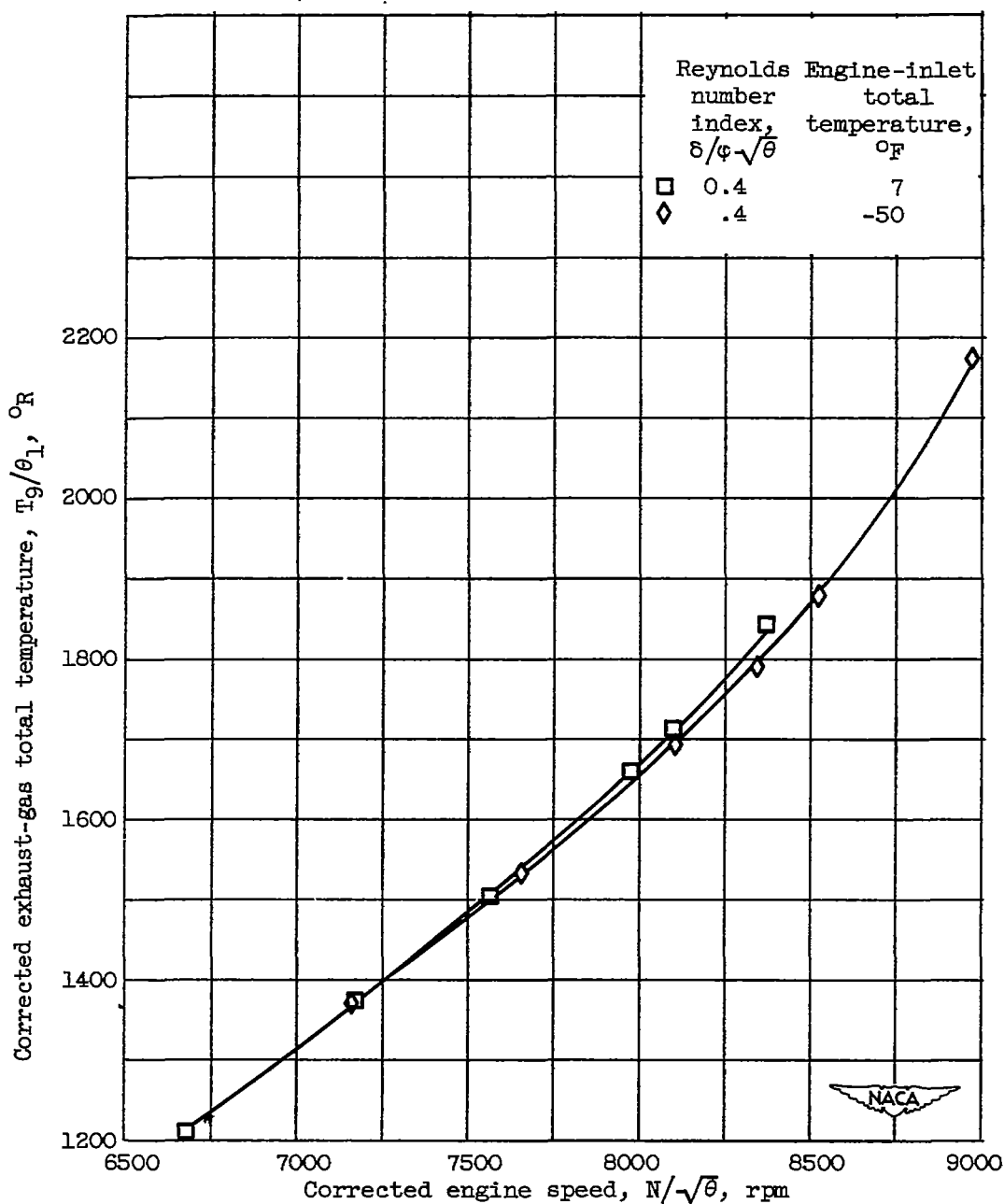
(c) Corrected ideal fuel-air ratio.

Figure 8. - Concluded. Effect of engine-inlet total temperature on performance of J47-GE-17 engine with no turbine-outlet straightening vanes installed.



(a) Corrected jet-thrust parameter.

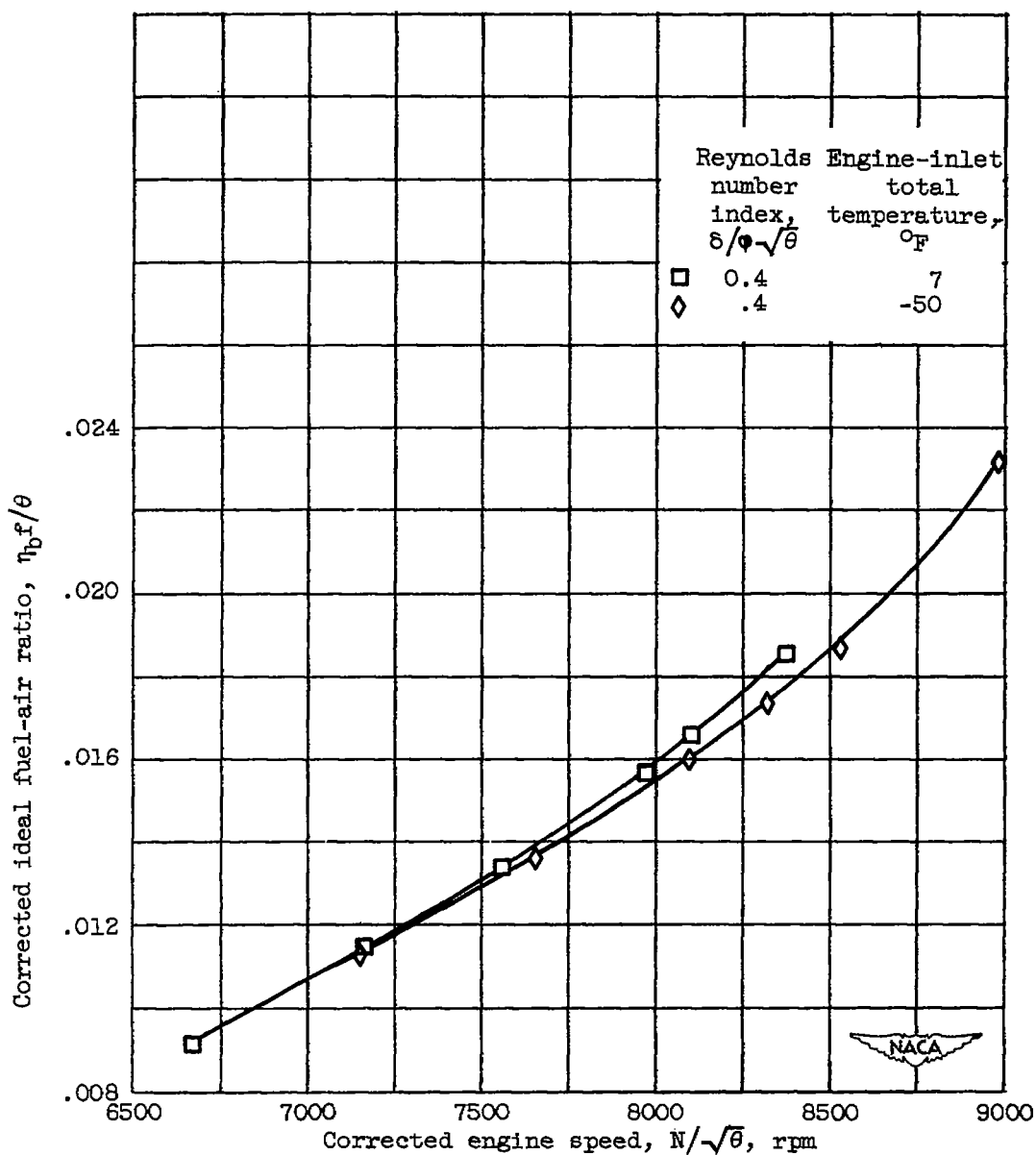
Figure 9. - Effect of engine-inlet total temperature on performance of J47-GE-17 engine with turbine-outlet straightening vanes installed.



(b) Corrected exhaust-gas total temperature.

Figure 9. - Continued. Effect of engine-inlet total temperature on performance of J47-GE-17 engine with turbine-outlet straightening vanes installed.





(c) Corrected ideal fuel-air ratio.

Figure 9. - Concluded. Effect of engine-inlet total temperature on performance of J47-GE-17 engine with turbine-outlet straightening vanes installed.

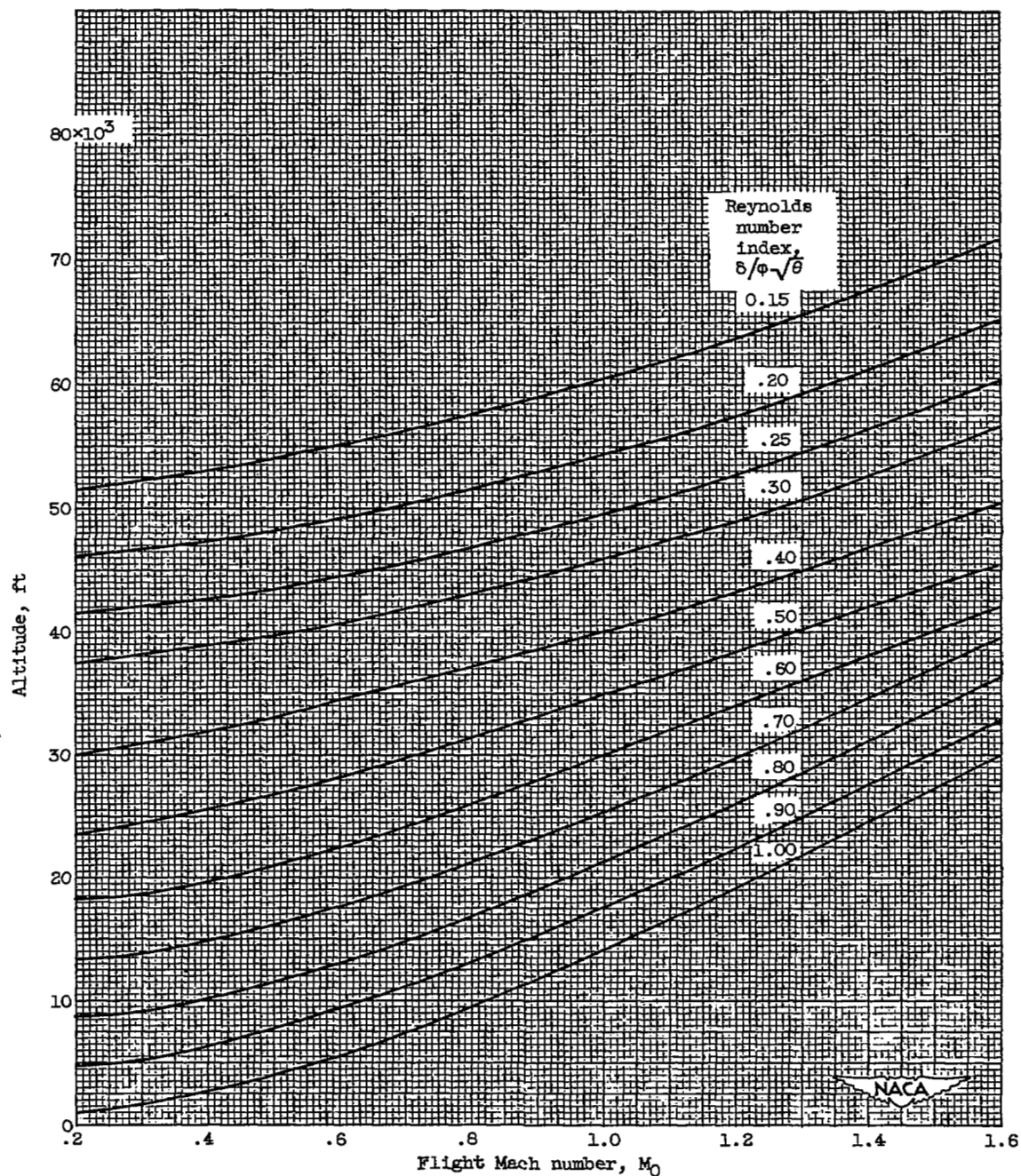
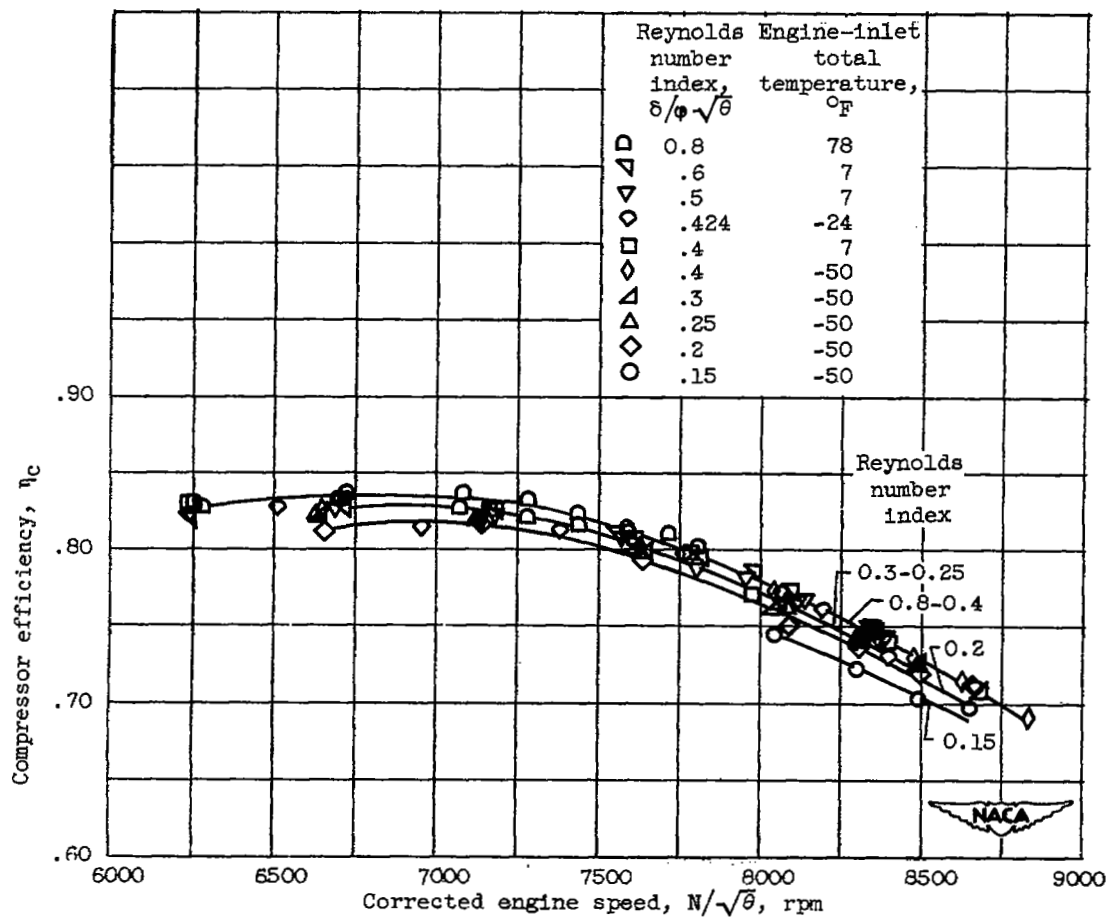
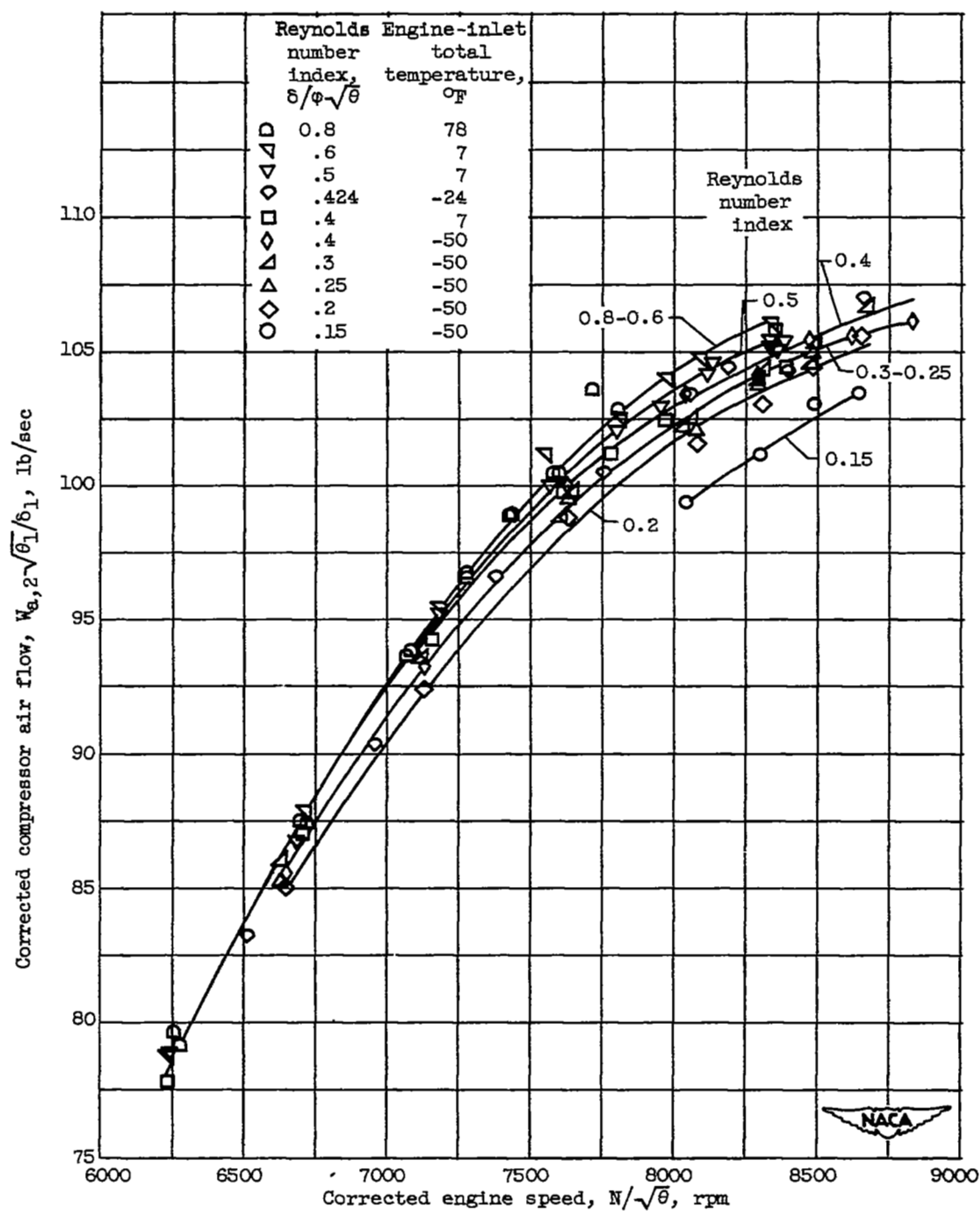


Figure 10. - Reynolds number index as a function of altitude and Mach number assuming 100 percent ram pressure recovery.



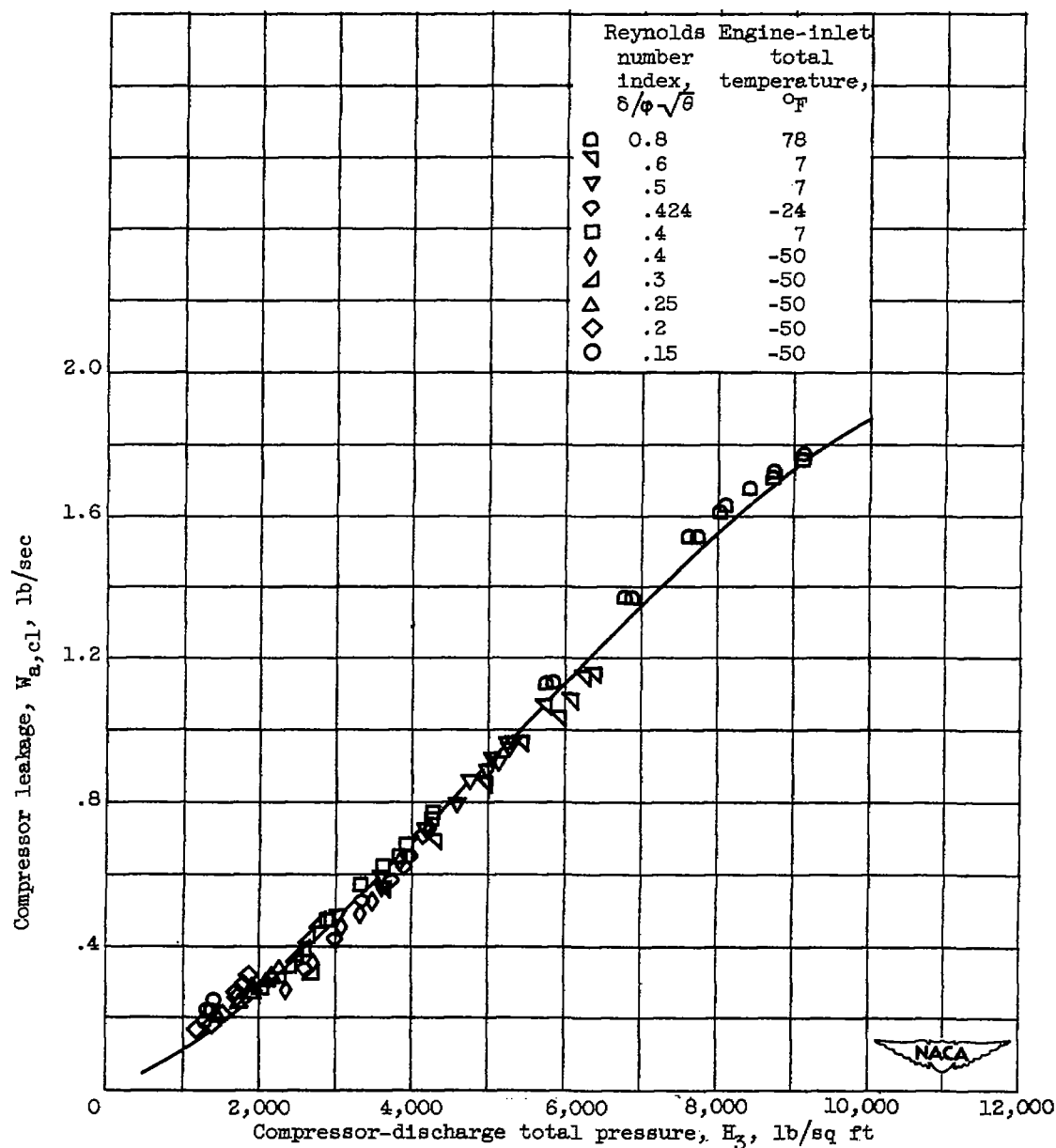
(a) Compressor efficiency.

Figure 11. - Effect of Reynolds number index on compressor performance.



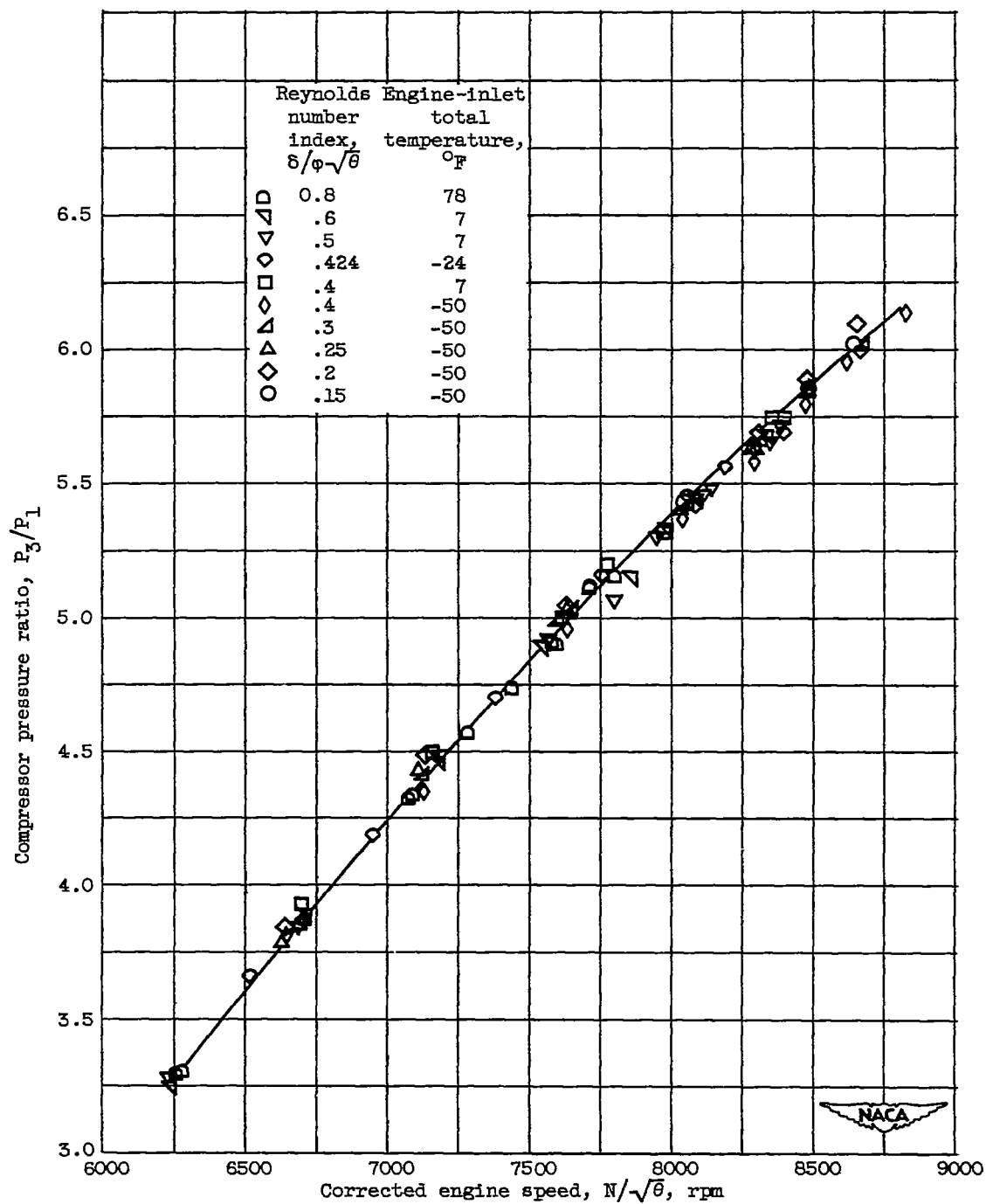
(b) Corrected compressor air flow.

Figure 11. - Continued. Effect of Reynolds number index on compressor performance.



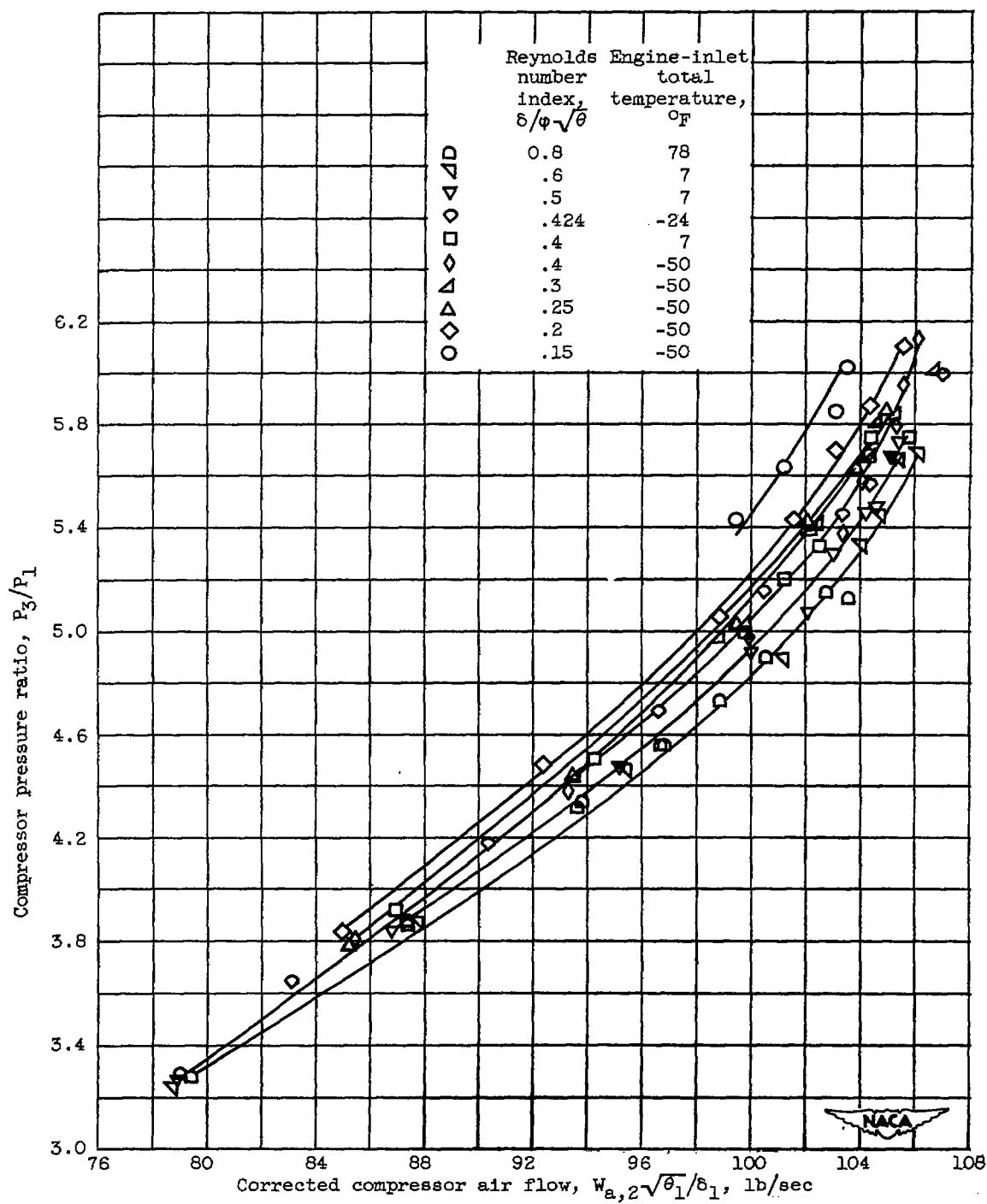
(c) Compressor leakage at engine midframe as function of compressor-discharge total pressure.

Figure 11. - Continued. Effect of Reynolds number index on compressor performance.



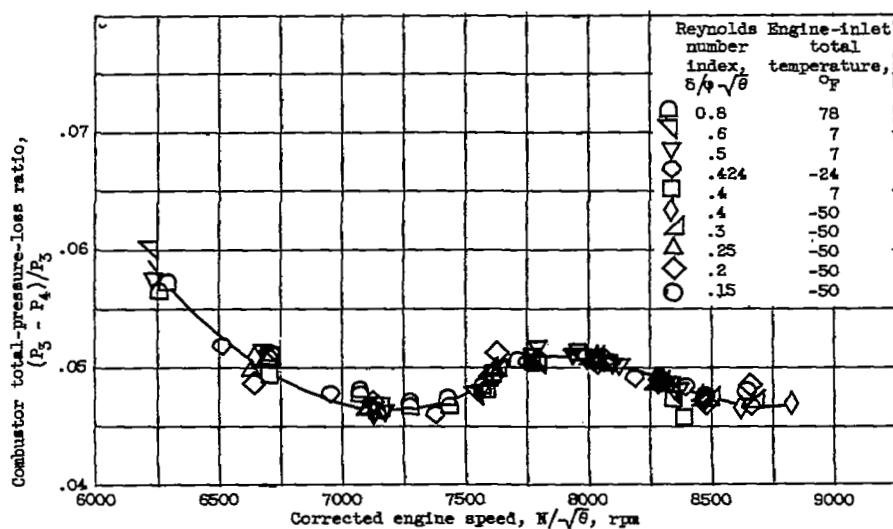
(d) Compressor pressure ratio as function of corrected engine speed.

Figure 11. - Continued. Effect of Reynolds number index on compressor performance.

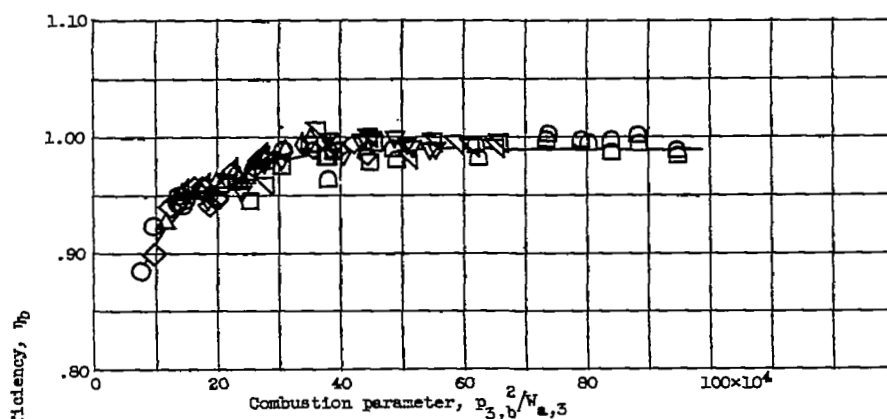


(e) Compressor pressure ratio as function of corrected compressor air flow.

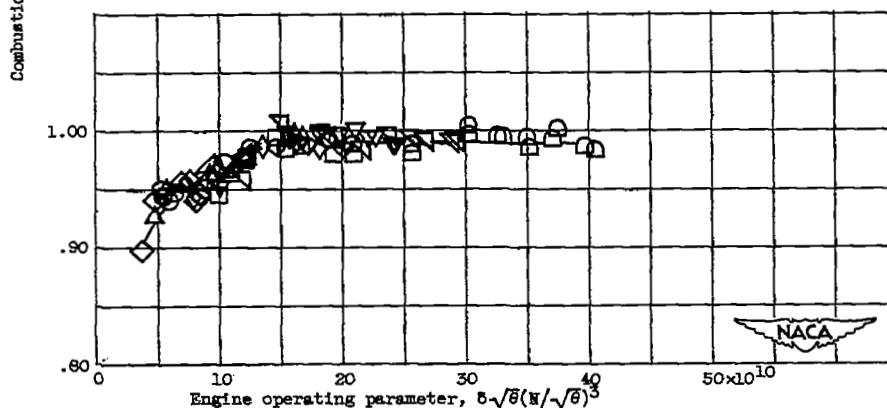
Figure 11. - Concluded. Effect of Reynolds number index on compressor performance.



(a) Combustor pressure loss ratio.



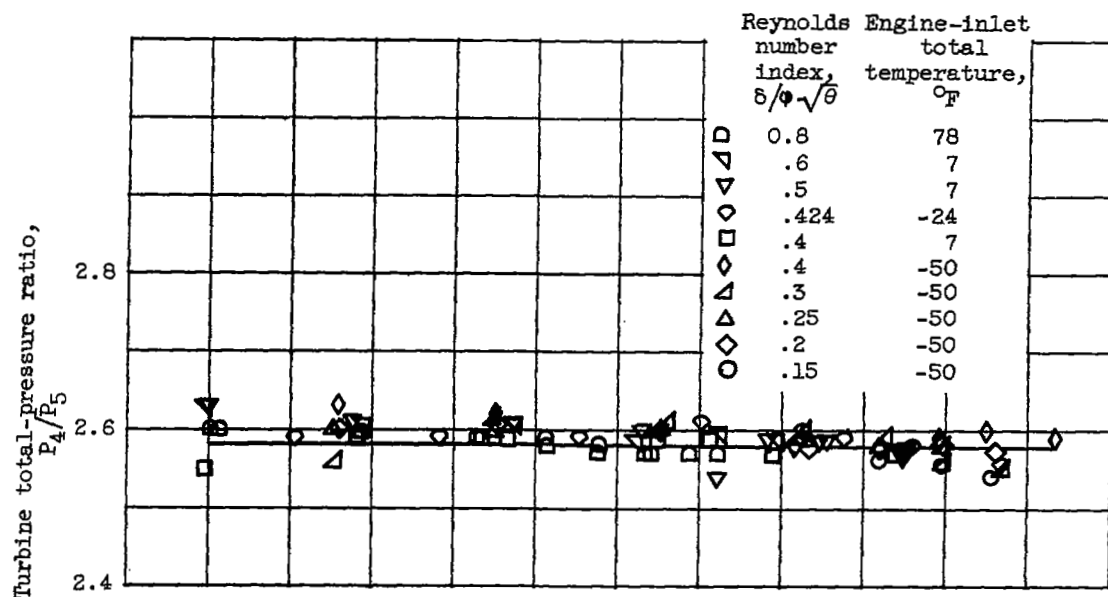
(b) Combustion efficiency.



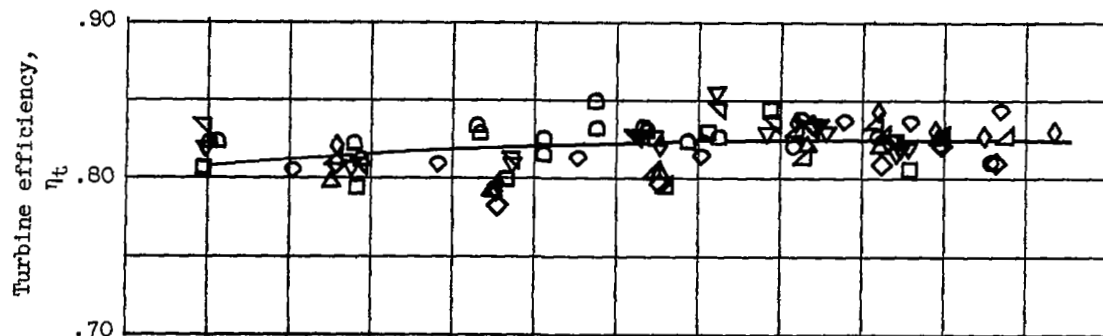
(c) Combustion efficiency as function of inlet conditions.

Figure 12. - Effect of Reynolds number index on combustor performance.

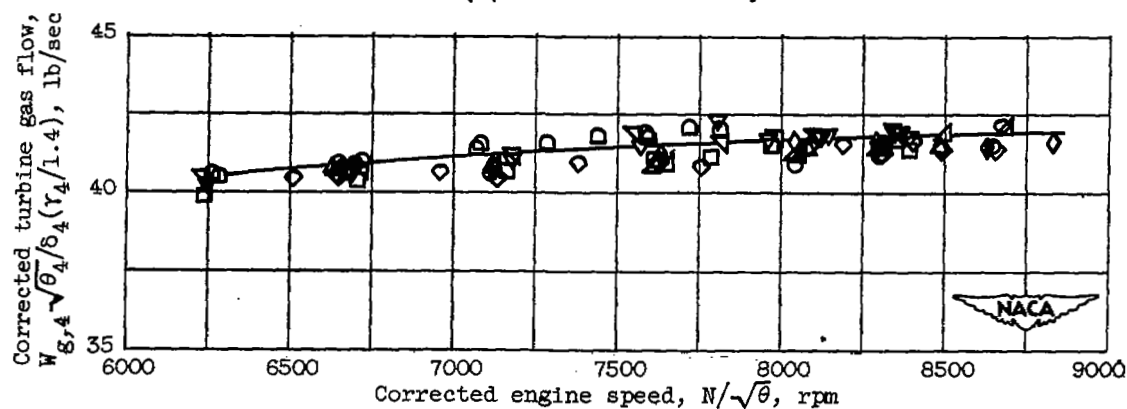




(a) Turbine pressure ratio.

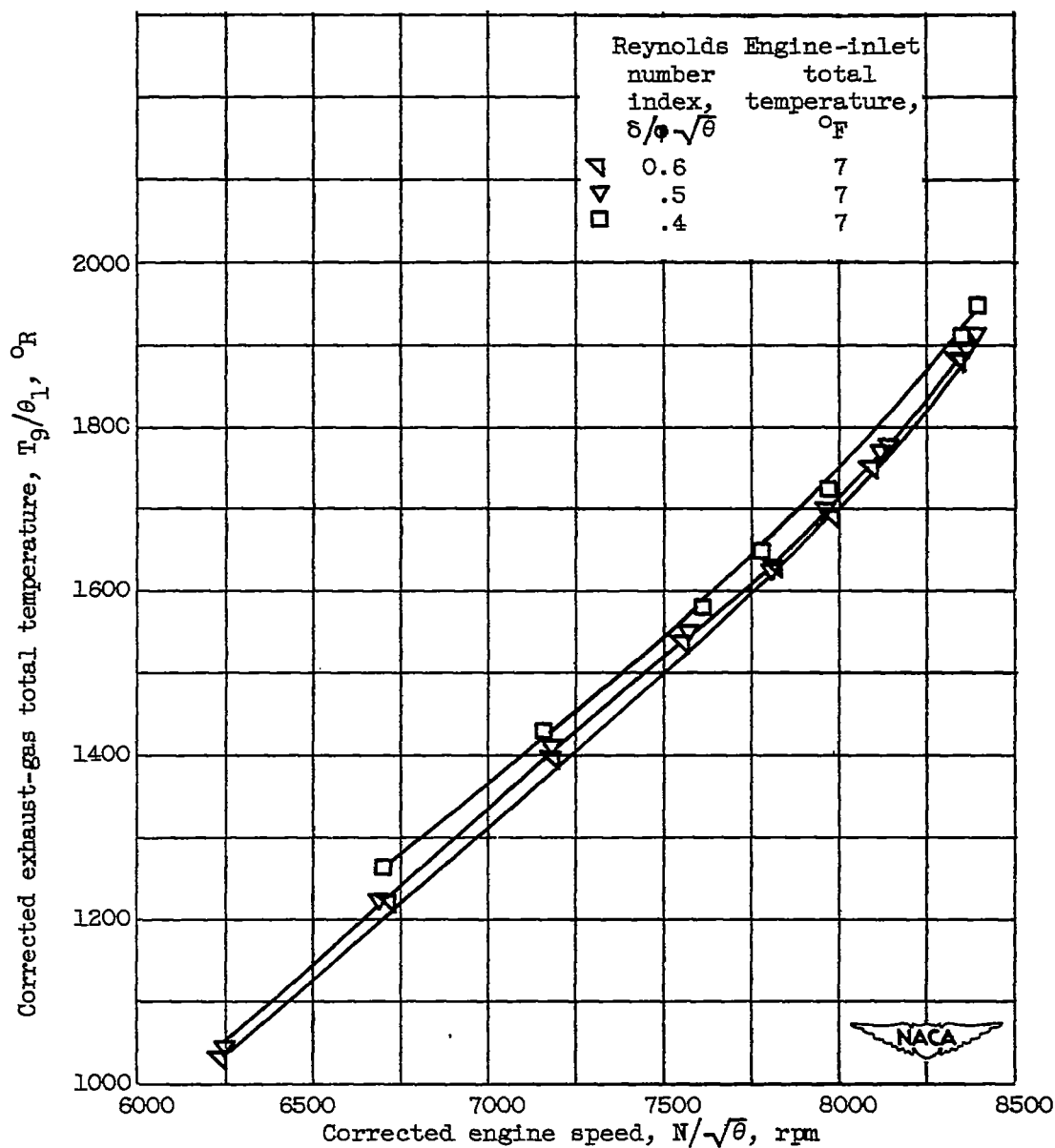


(b) Turbine efficiency.



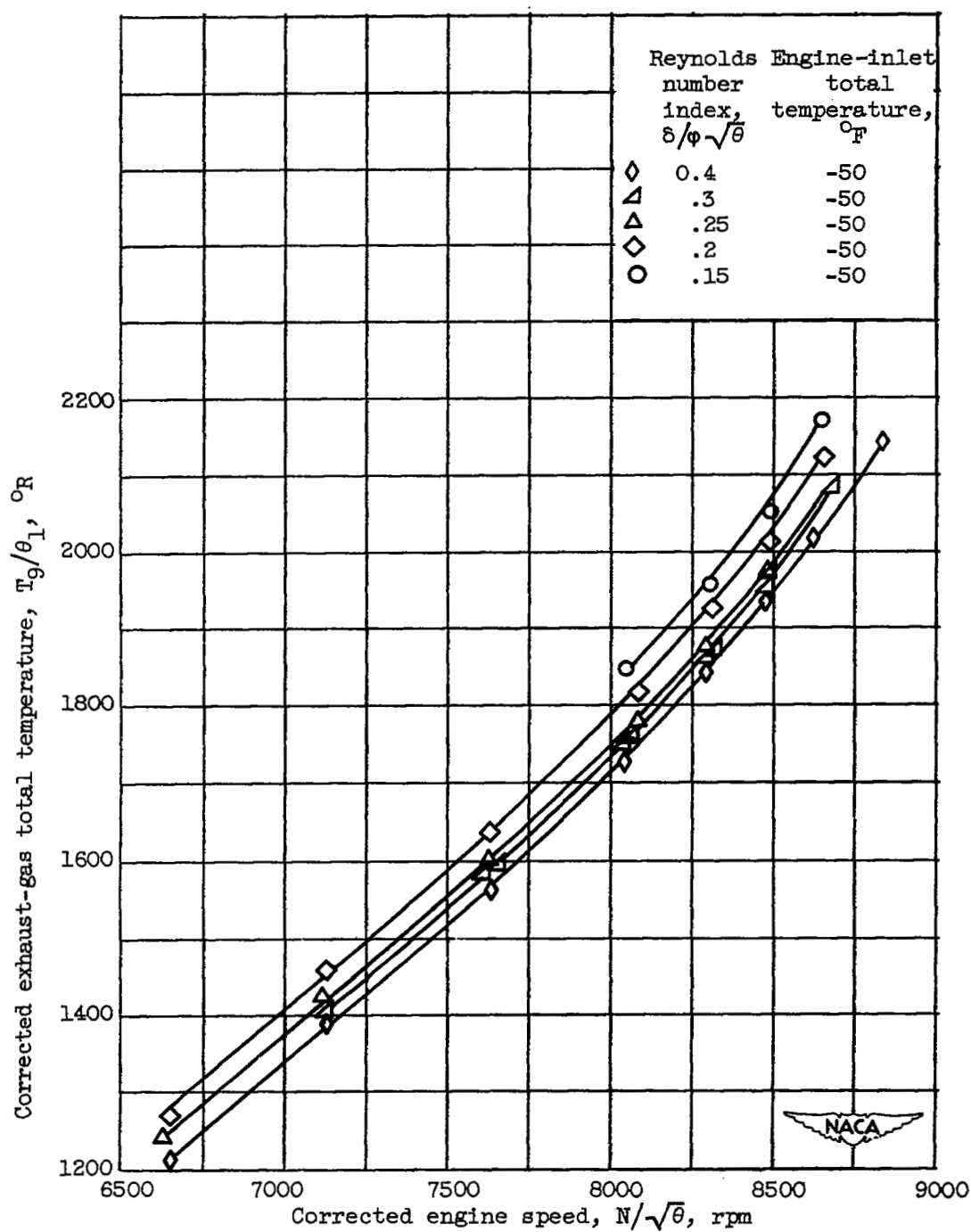
(c) Corrected turbine gas flow.

Figure 13. - Effect of Reynolds number index on turbine performance.



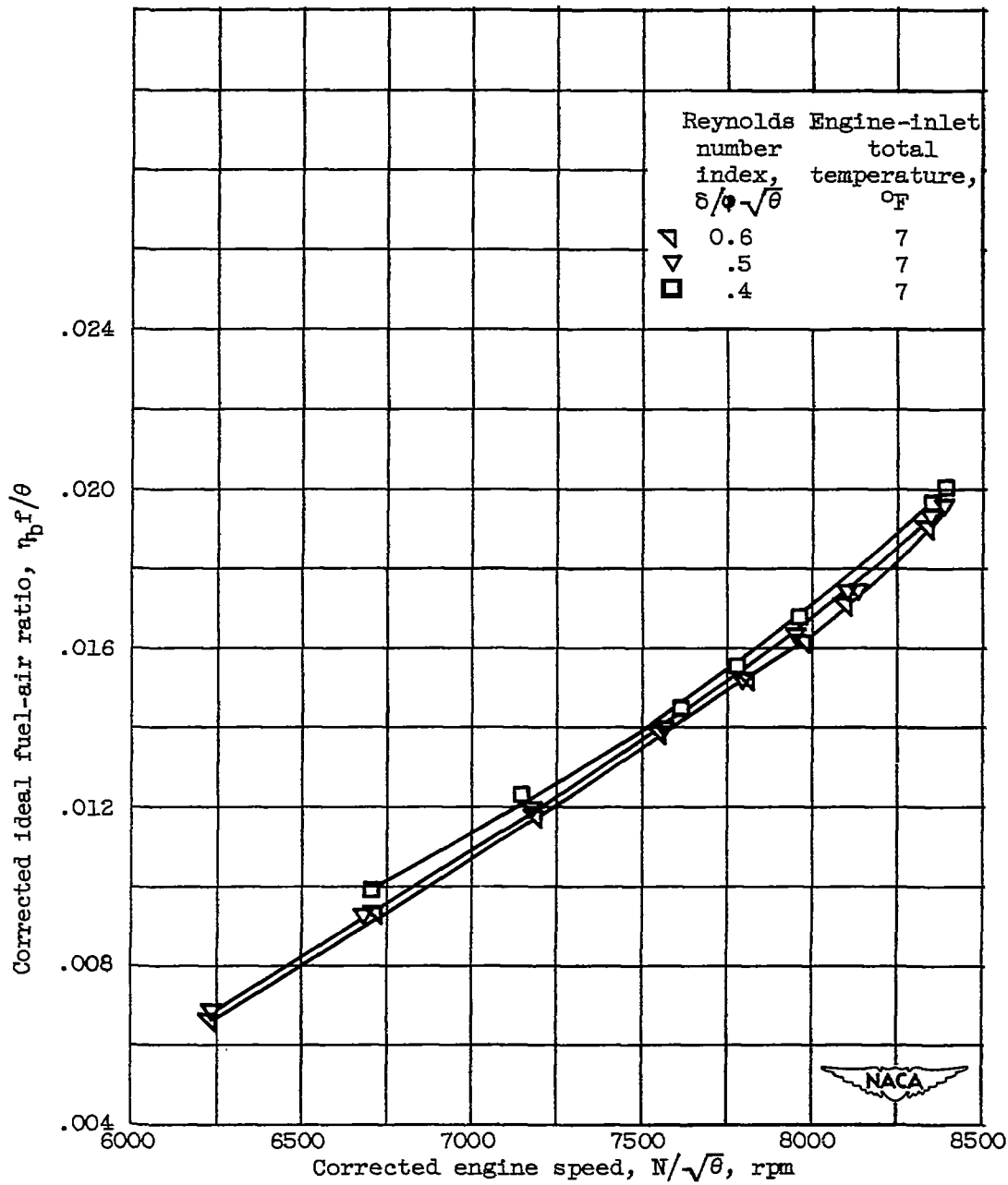
(a) Corrected exhaust-gas total temperature at inlet temperature of 7° F.

Figure 14. - Effect of Reynolds number index on over-all engine performance.



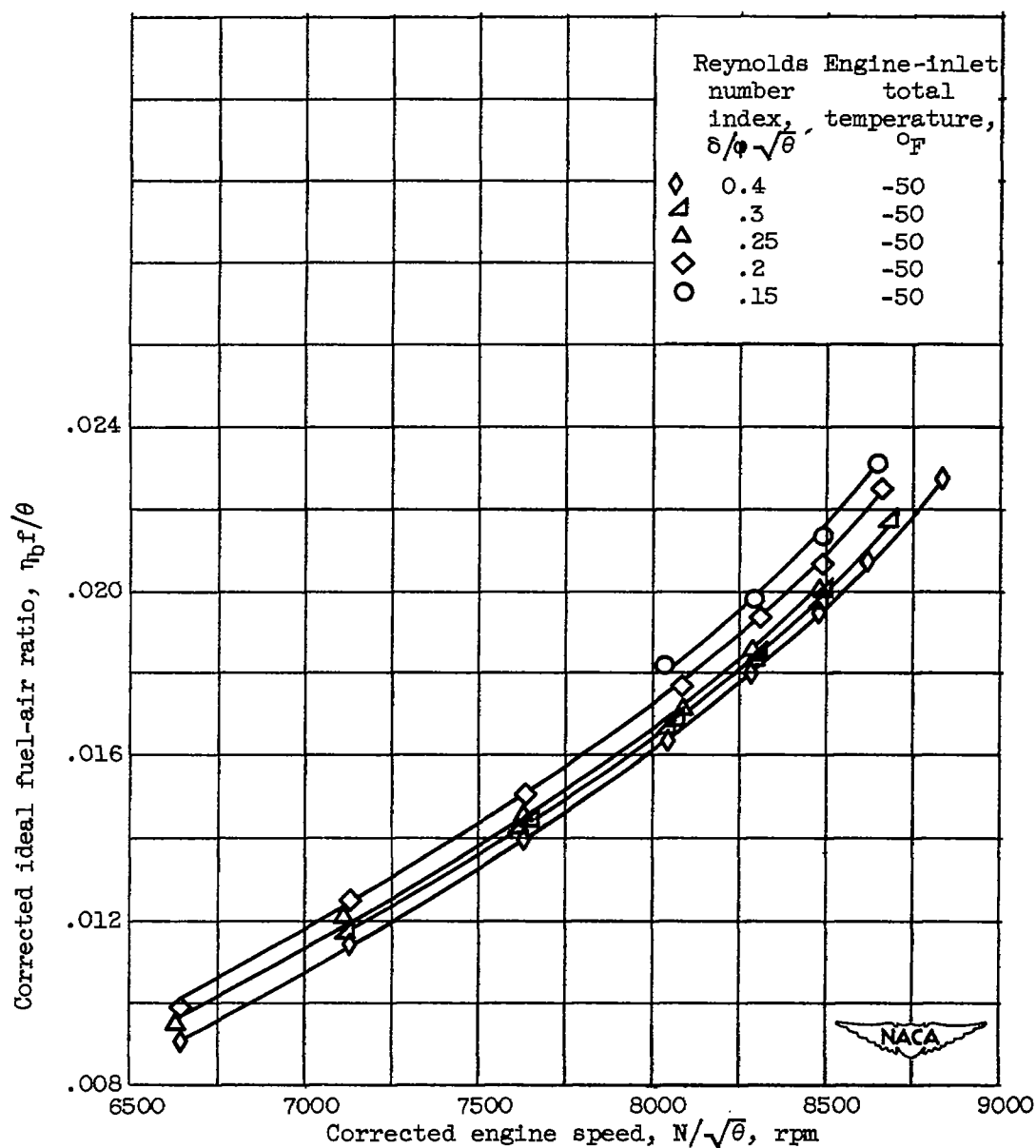
(b) Corrected exhaust-gas total temperature at inlet temperature of  $-50^{\circ}\text{F}$ .

Figure 14. - Continued. Effect of Reynolds number index on over-all engine performance.



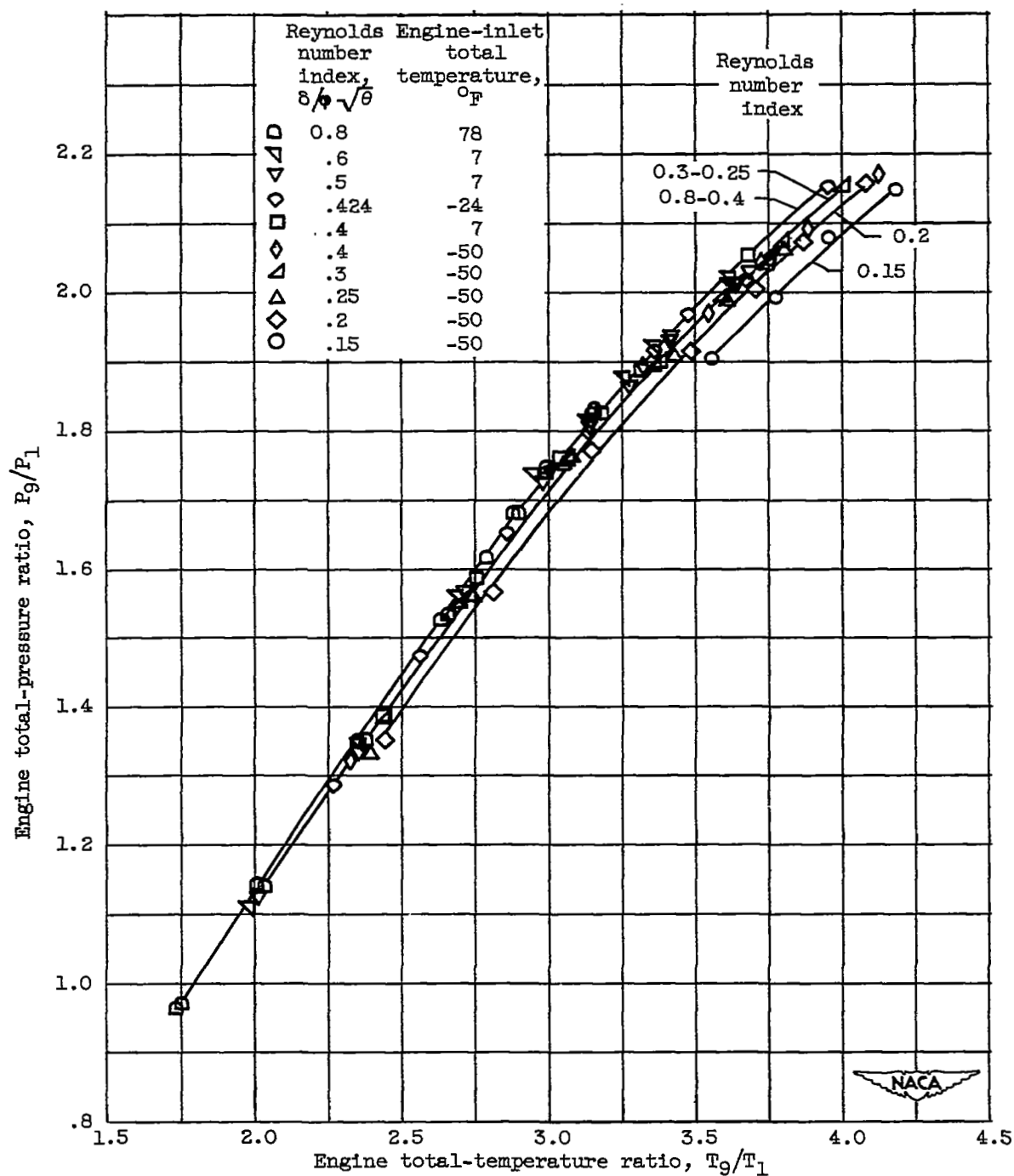
(c) Corrected ideal fuel-air ratio at inlet temperature of 7° F.

Figure 14. - Continued. Effect of Reynolds number index on over-all engine performance.



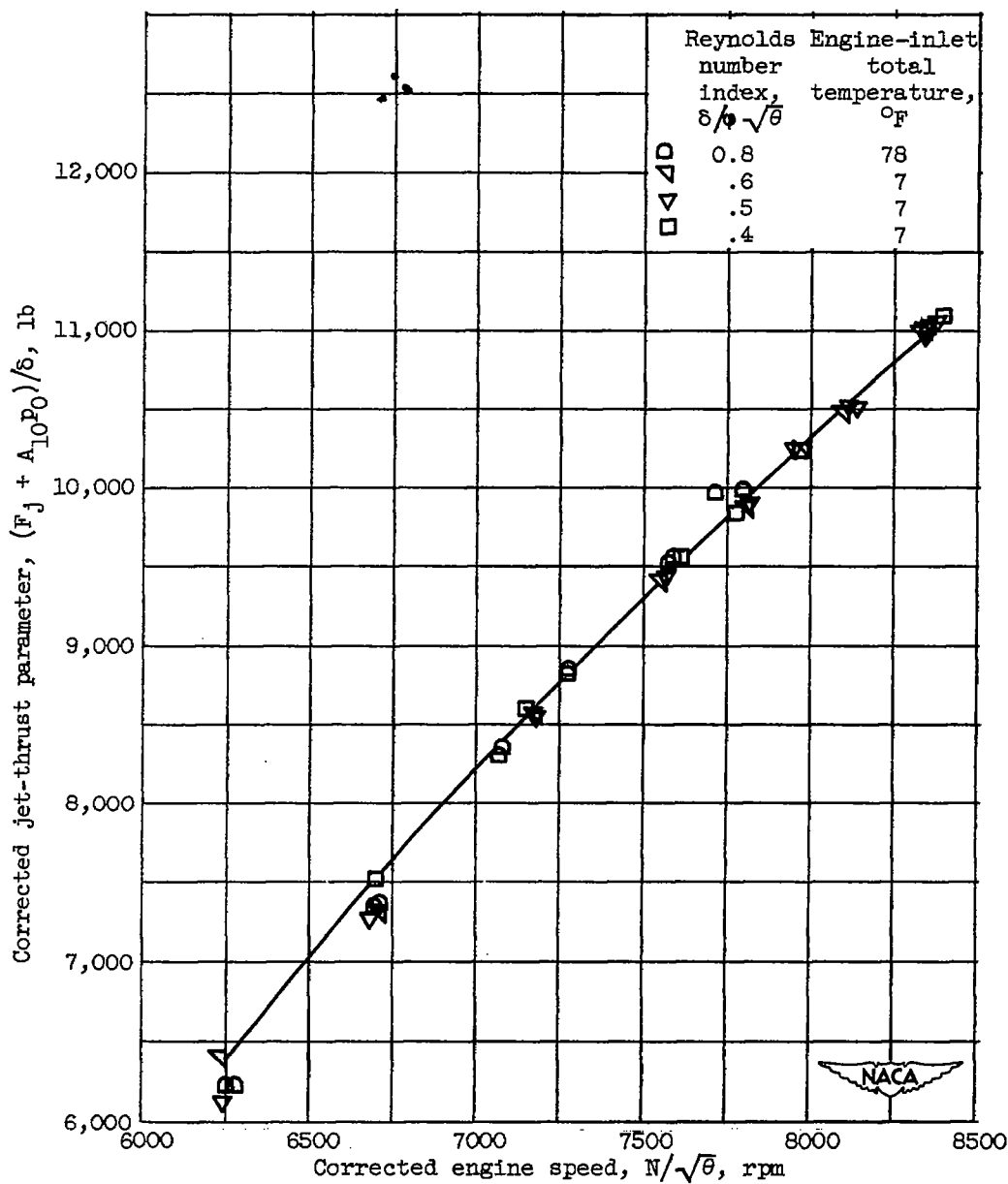
(d) Corrected ideal fuel-air ratio at inlet temperature of  $-50^{\circ}\text{F}$ .

Figure 14. - Continued. Effect of Reynolds number index on over-all engine performance.



(e) Engine pumping characteristics.

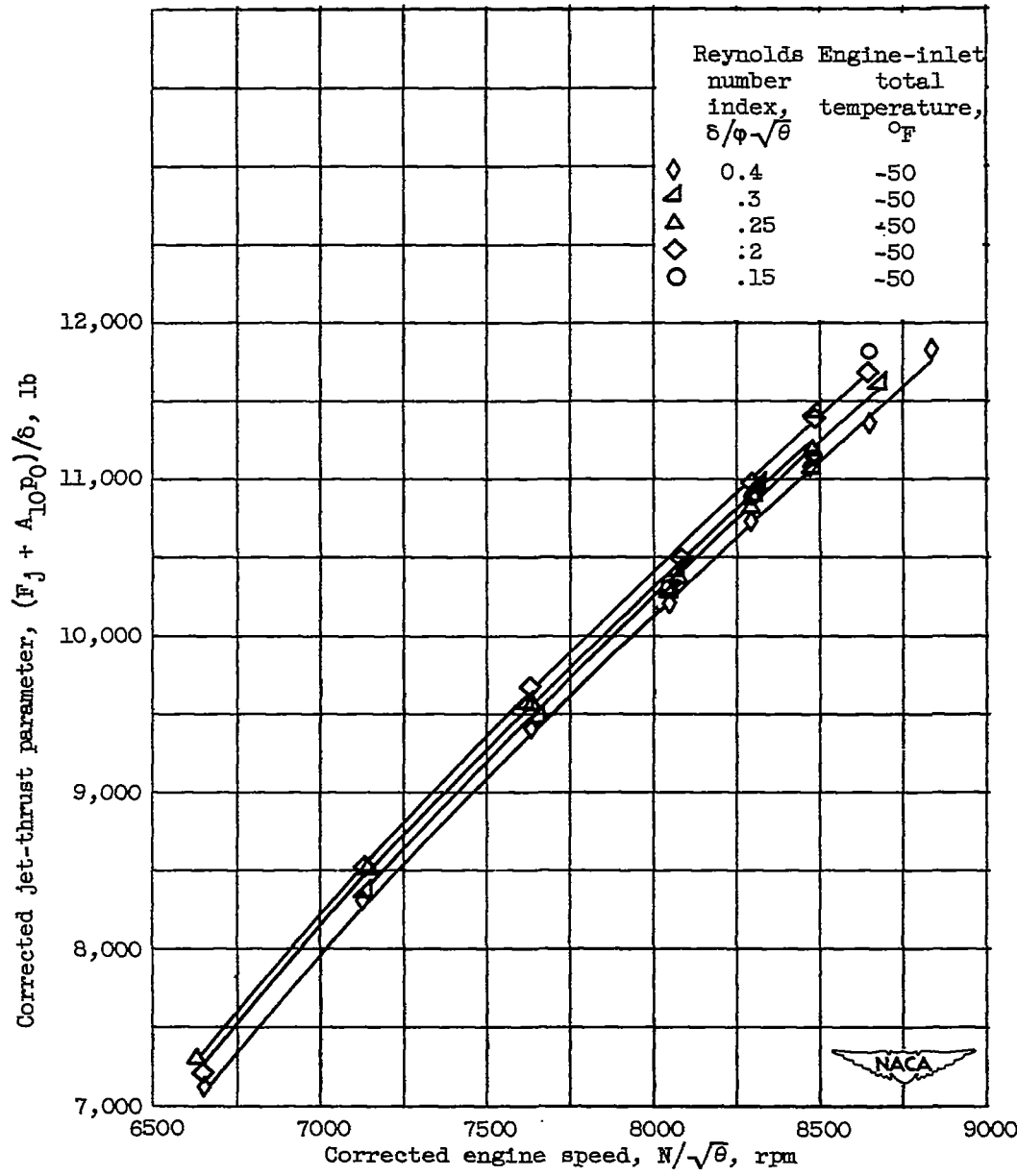
Figure 14. - Continued. Effect of Reynolds number index on over-all engine performance.



(f) Corrected jet-thrust parameter at inlet temperatures of  $7^{\circ}$  and  $78^{\circ}$  F.

Figure 14. - Continued. Effect of Reynolds number index on over-all engine performance.

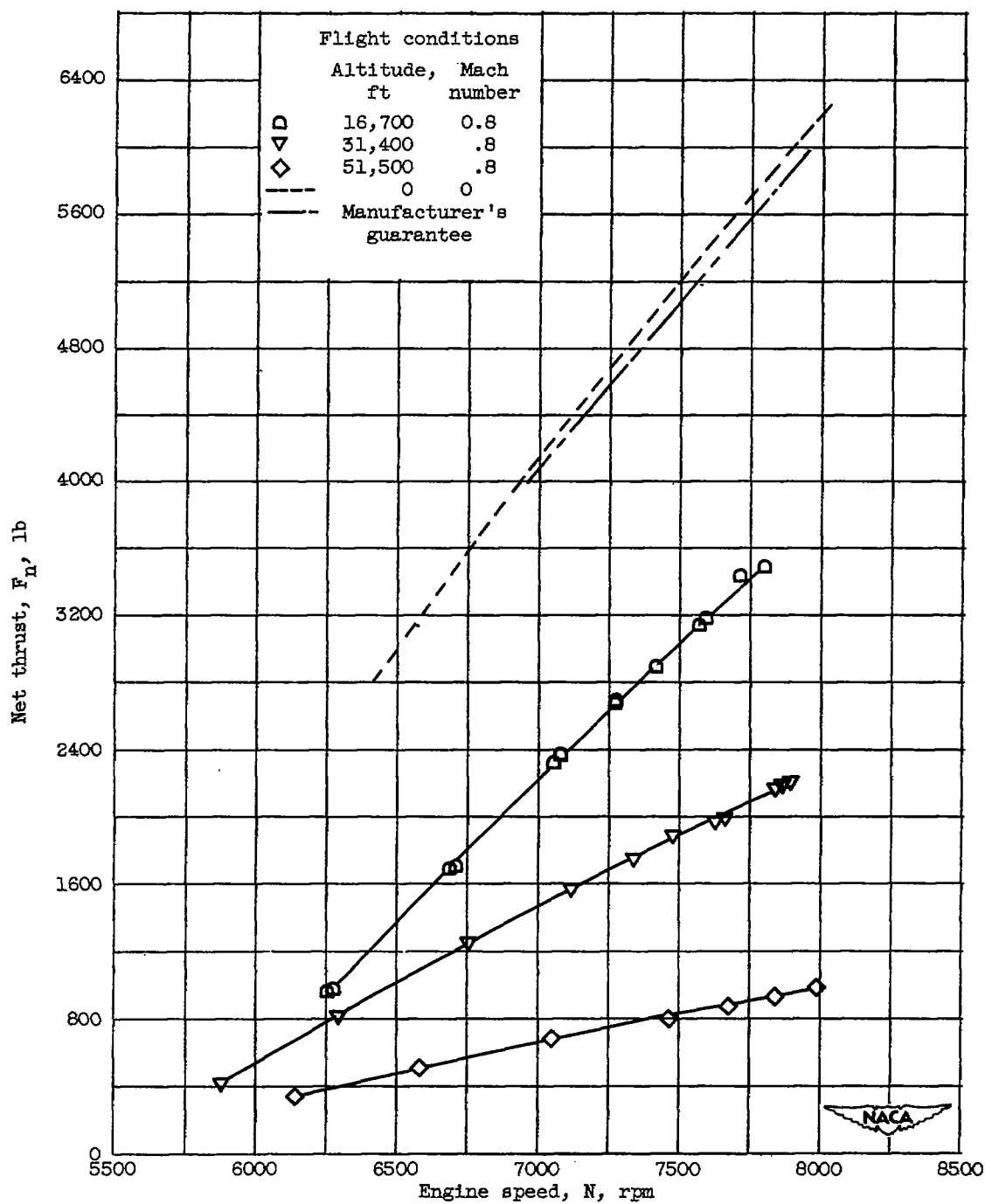
2717



(g) Corrected jet-thrust parameter at inlet temperature of -50° F.

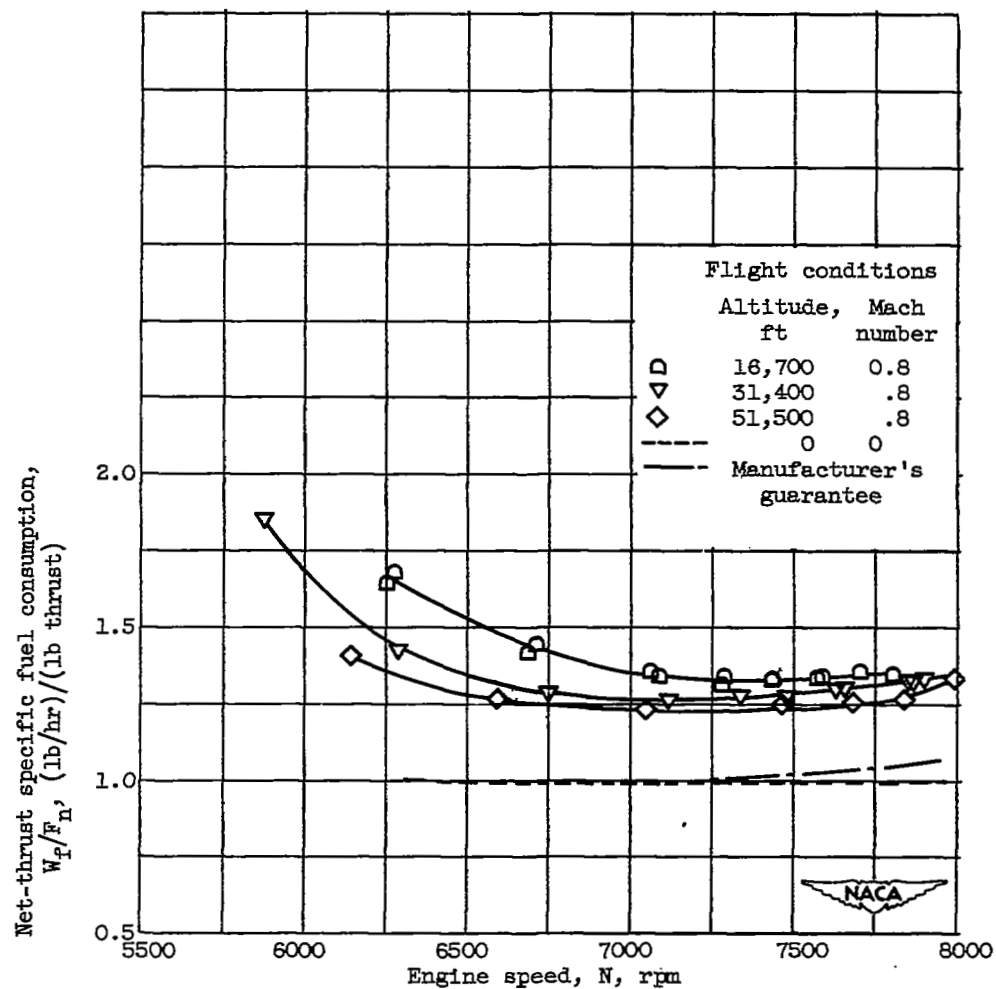
Figure 14. - Concluded. Effect of Reynolds number index on over-all engine performance.





(a) Net thrust.

Figure 15. - Effect of varying altitude on net thrust and net-thrust specific fuel consumption.



(b) Net-thrust specific fuel consumption.

Figure 15. - Concluded. Effect of varying altitude on net thrust and net-thrust specific fuel consumption.

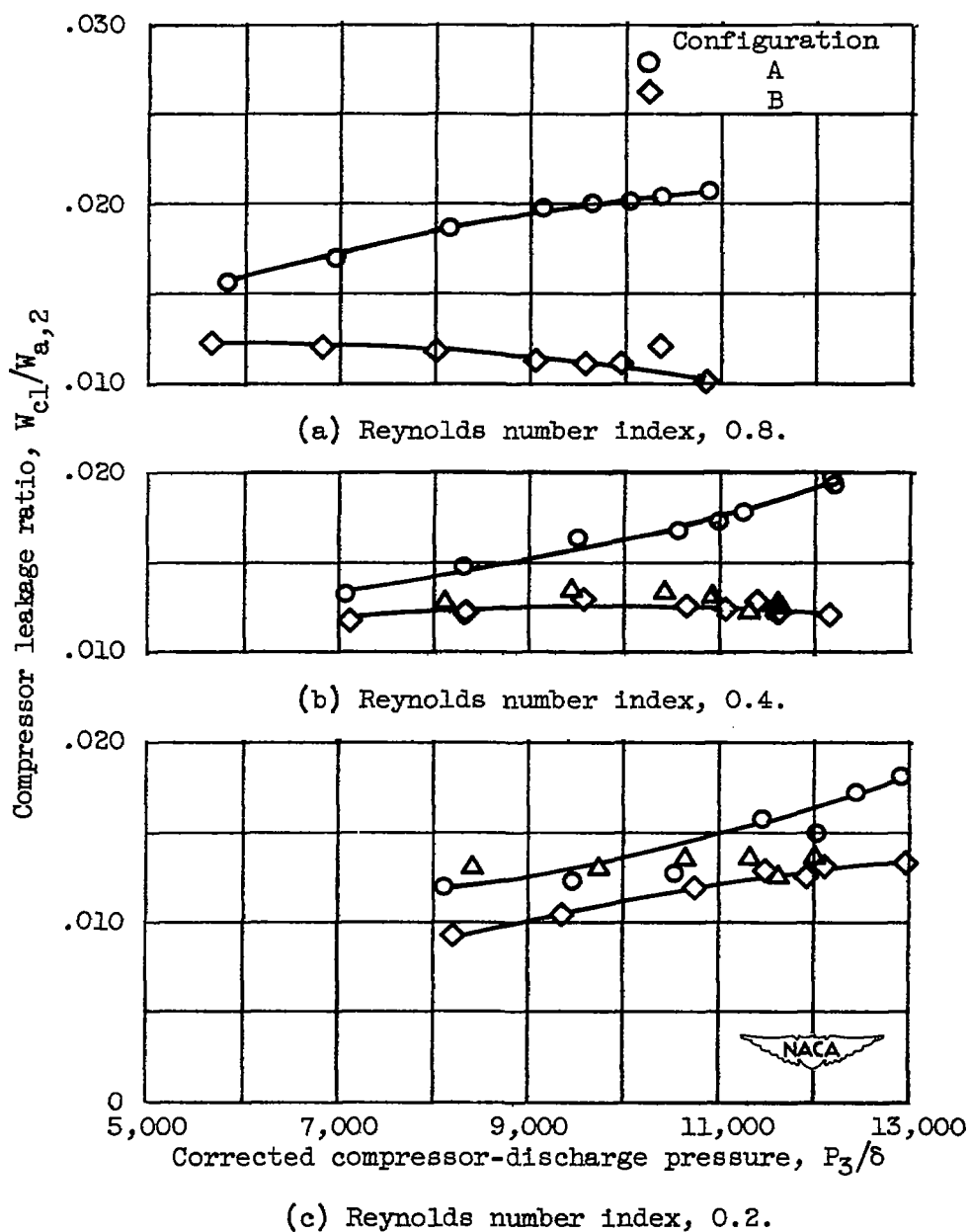
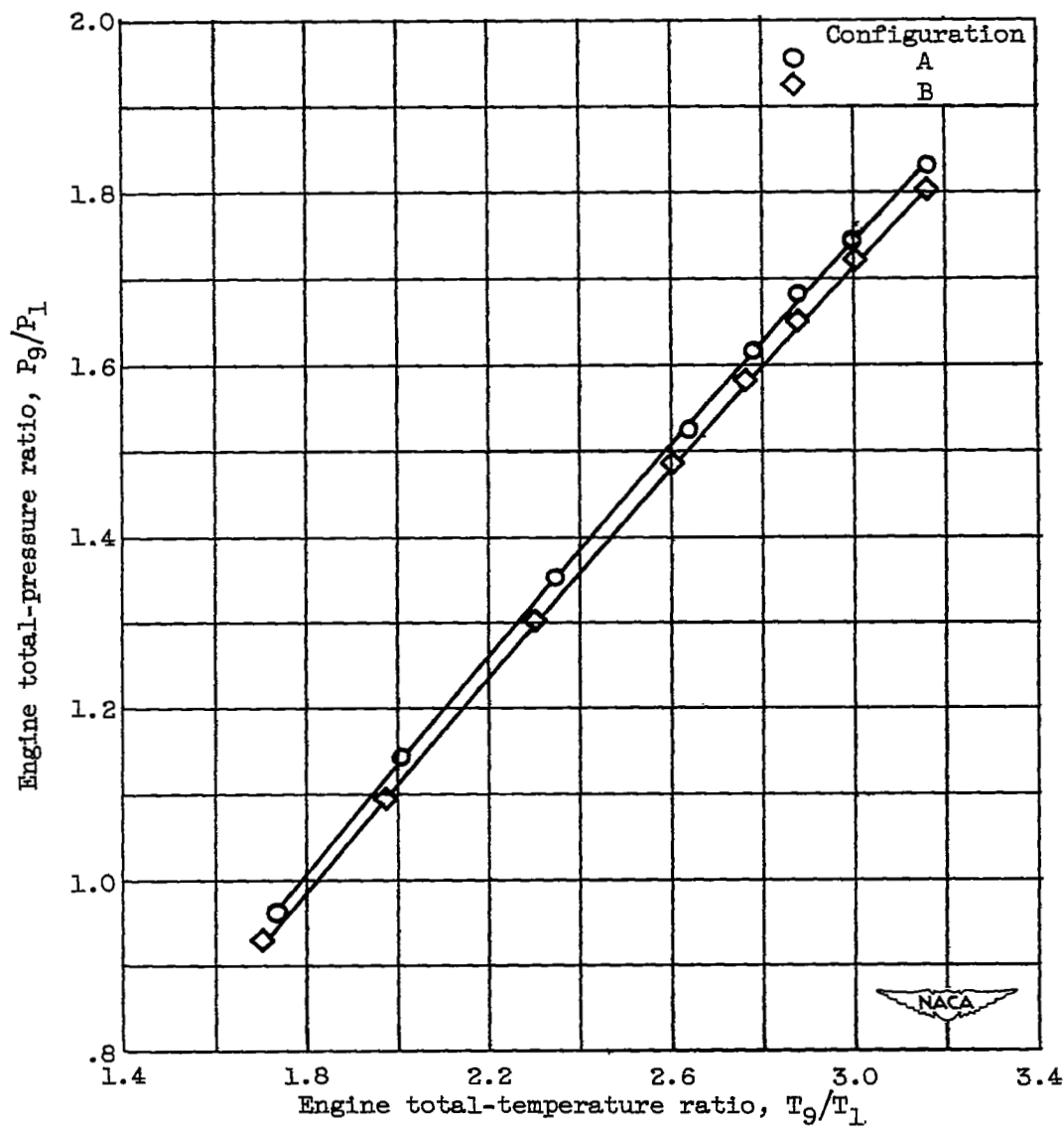
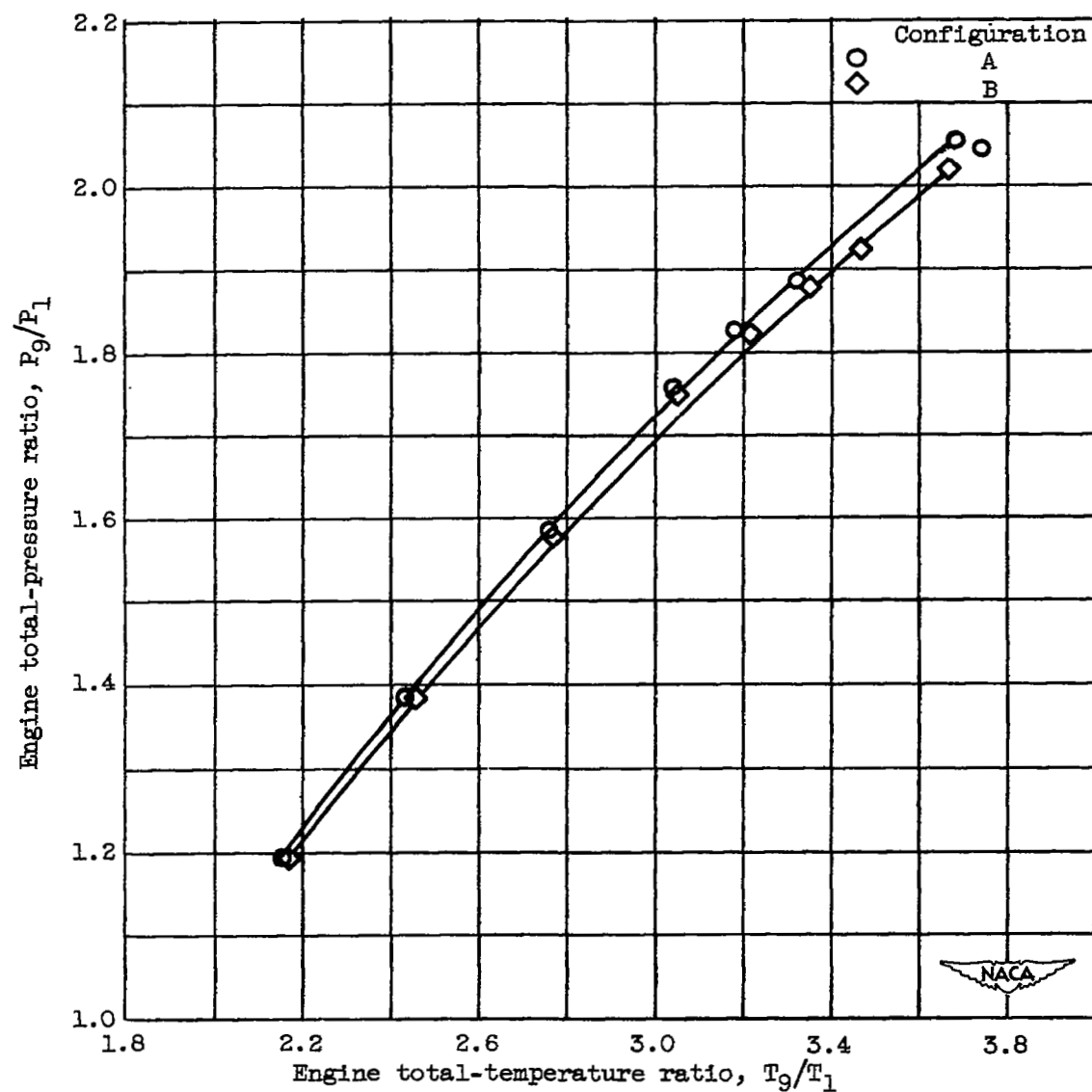


Figure 16. - Effect of improved twelfth-stage seal on compressor leakage air flow.



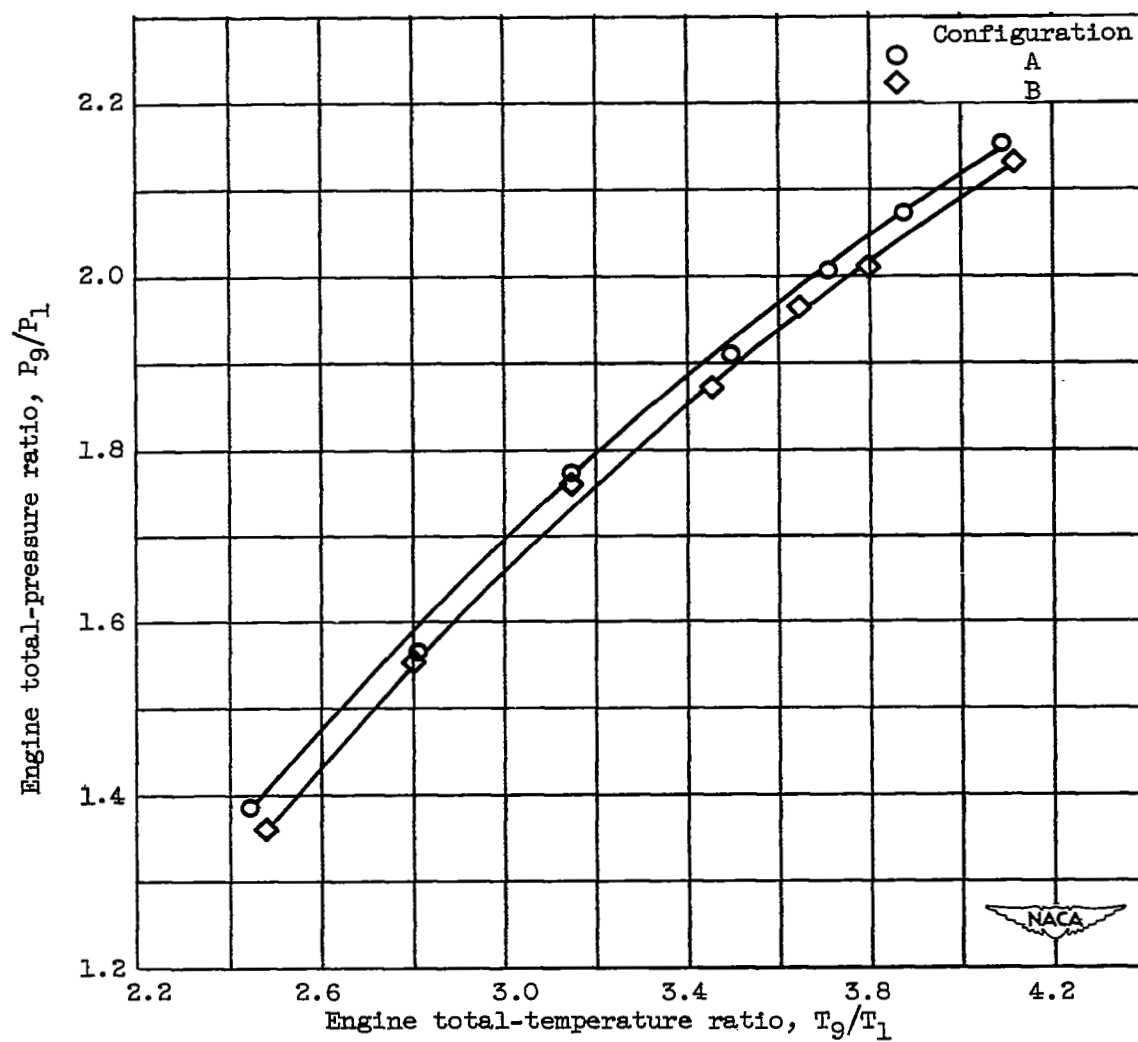
(a) Reynolds number index, 0.8.

Figure 17. - Effect of design modifications incorporated in configuration B on engine pumping characteristics.



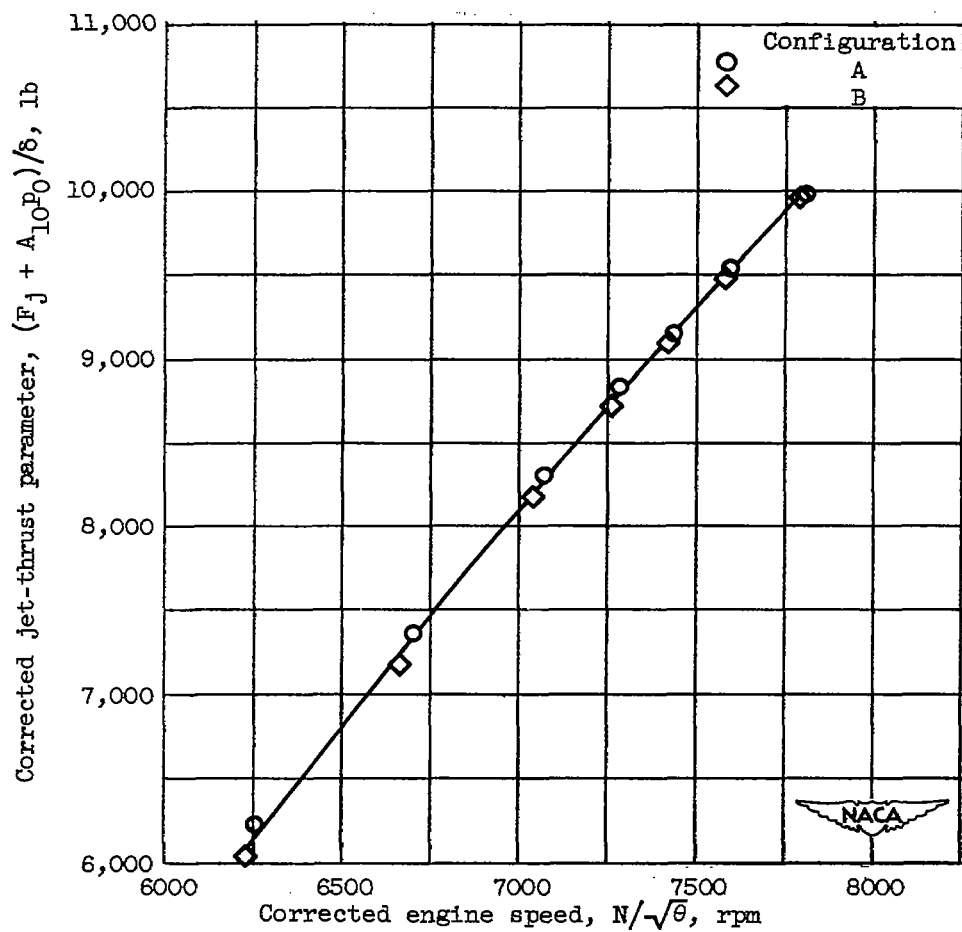
(b) Reynolds number index, 0.4.

Figure 17. - Continued. Effect of design modifications incorporated in configuration B on engine pumping characteristics.



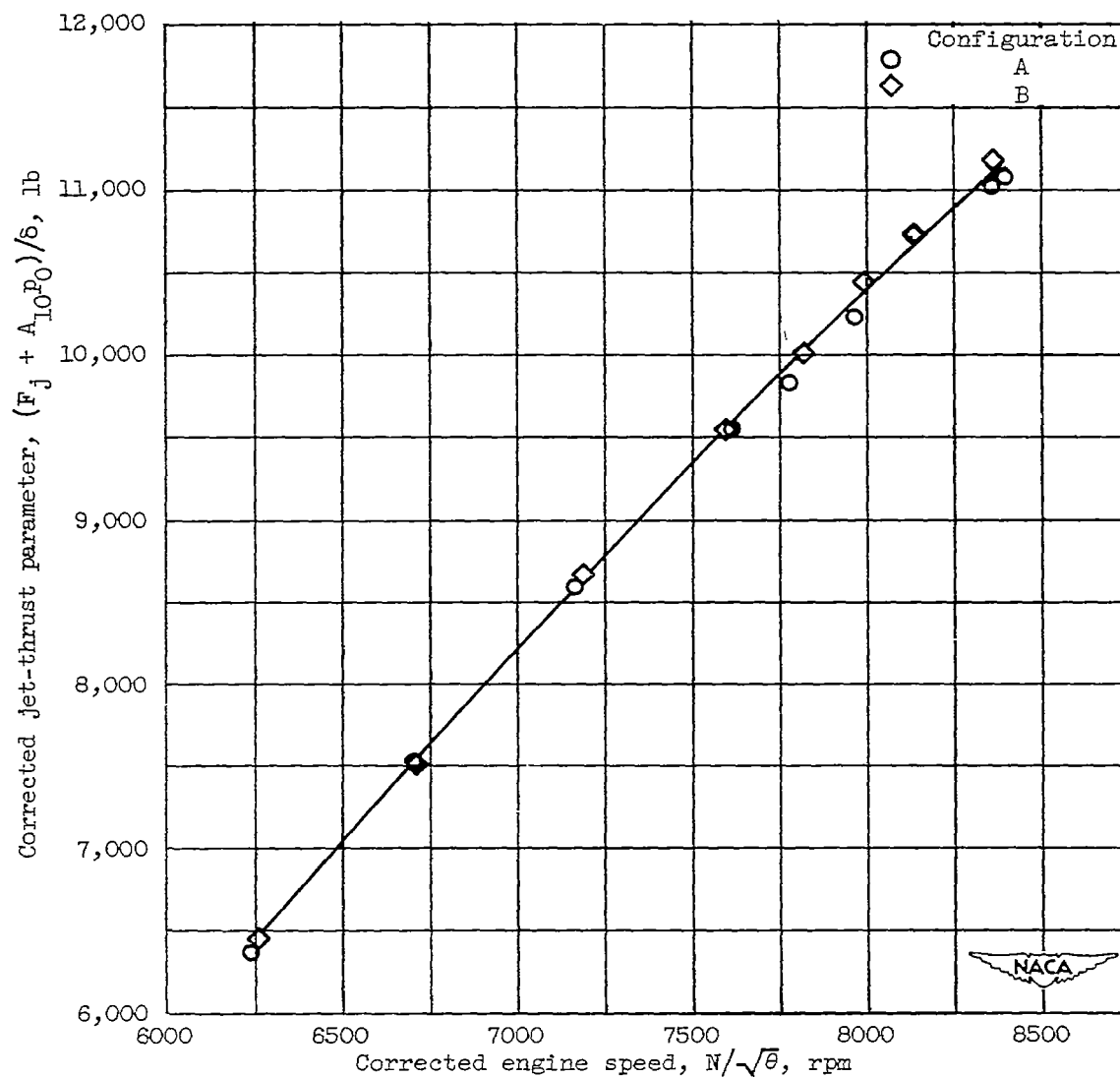
(c) Reynolds number index, 0.2.

Figure 17. - Concluded. Effect of design modifications incorporated in configuration B on engine pumping characteristics.



(a) Reynolds number index, 0.8.

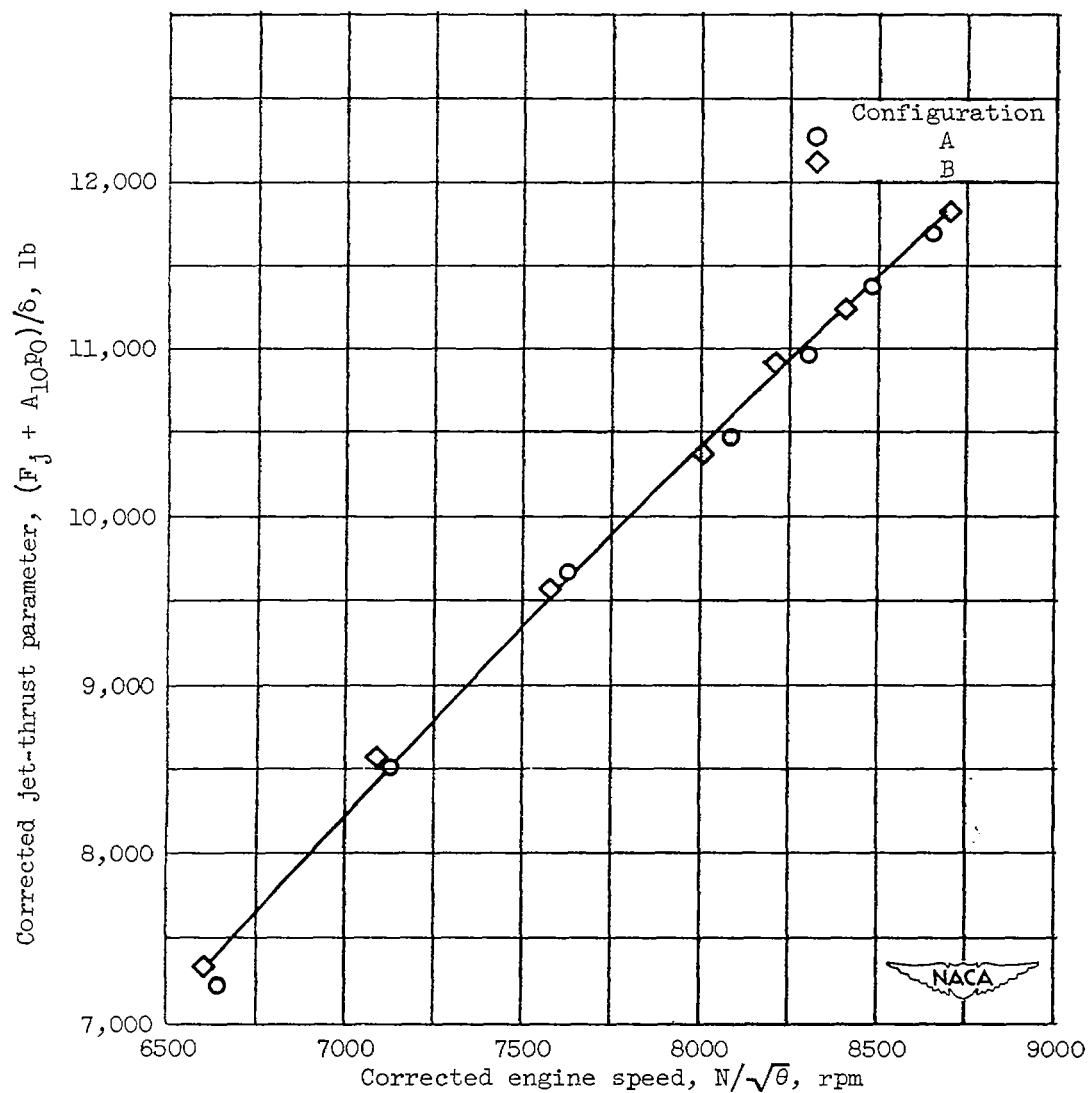
Figure 18. - Effect of design modifications incorporated in configuration B on jet-thrust parameter.



(b) Reynolds number index, 0.4.

Figure 18. - Continued. Effect of design modifications incorporated in configuration B on jet-thrust parameter.





(c) Reynolds number index, 0.2.

Figure 18. - Concluded. Effect of design modifications incorporated in configuration B on jet-thrust parameter.

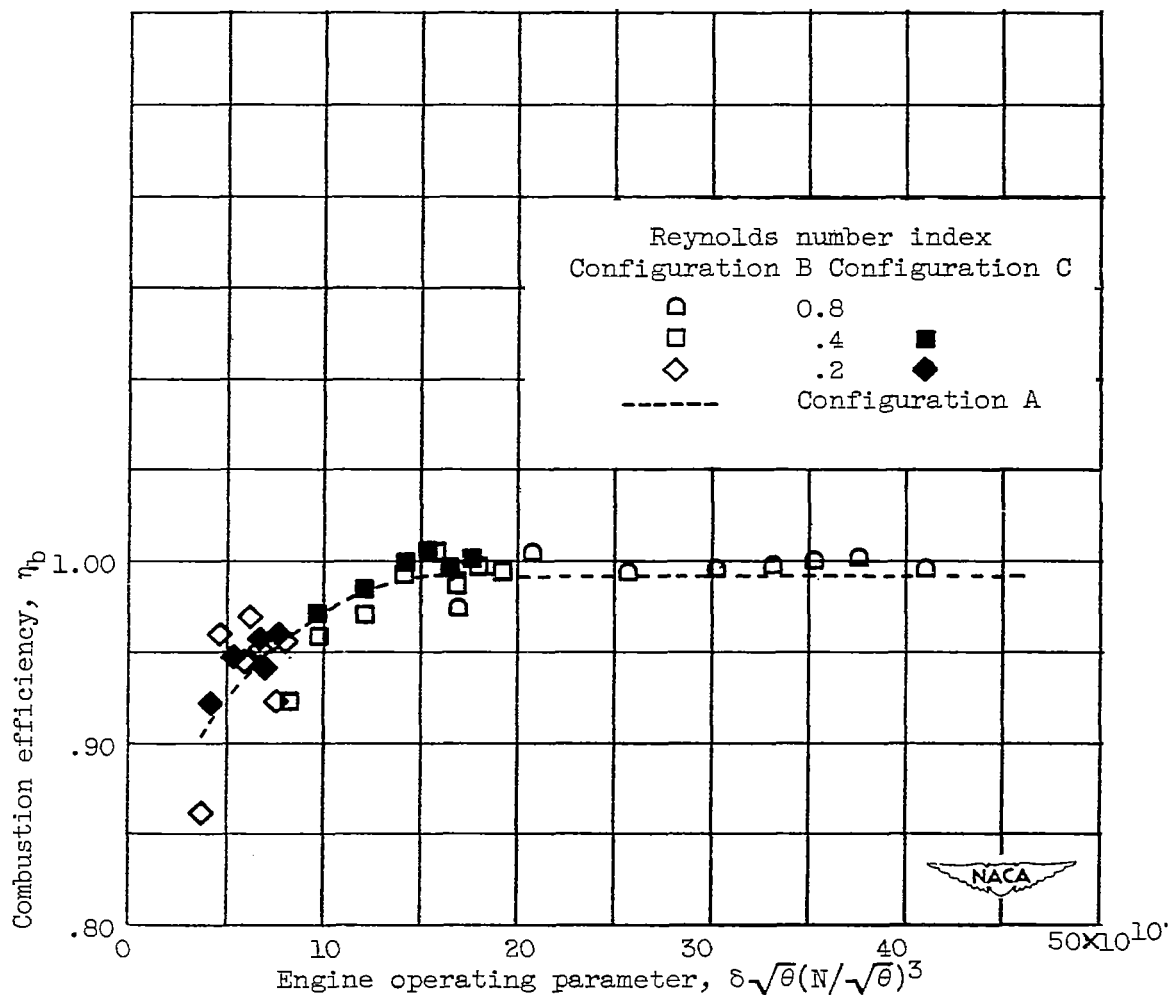


Figure 19. - Effect of design modifications incorporated in configurations B and C on combustion efficiency.

# SECURITY INFORMATION

[REDACTED]

NASA Technical Library



3 1176 01435 6621



[REDACTED]